Adoptive Therapy with T-cells Genetically Targeted to Tumor Associated Antigen through the Introduction of Chimeric Antigen Receptors (CARs)

Dissertation

zur

Erlangung der naturwissenschaftlichen Doktorwürde

(Dr. sc. nat.)

vorgelegt der

Mathematisch-naturwissenschaftlichen Fakultät

der

Universität Zürich

von

Pratiksha Gulati

aus Indien

Promotionskommission:

Prof. Dr. Christian Münz (Vorsitz)

Institute for Experimental Immunology, University of Zurich

PD. Dr. Ulf Petrausch

Institute for Experimental Immunology, University of Zurich

Department of Oncology, University Hospital Zurich

Prof. Dr. Christoph Renner

Department of Biomedicine, University Hospital Basel

Prof. Dr. Urs Greber

Institute of Molecular Life Sciences, University of Zurich

Zürich, 2017

Declaration

Herewith I declare that I have written this thesis myself and have only used the stated references.

Pratiksha Gulati

Zürich, Switzerland
06.07.2017

Publications arising from, or relating to, this thesis

Aberrant Lck signal via CD28 co-stimulation augments antigen-specific functionality and tumor control by redirected T-cells with PD-1 blockade in humanized mice. Gulati P, Rühl J, Kannan A, Pircher M, Schuberth P, Nytko K, Pruschy M, Sulser S, Haefner M, Jensen S, Soltermann A, Jungraithmayr W, Eisenring M, Winder T, Samaras P, Tabor A, Stenger R, Stupp R, Weder W, Renner C, Münz, Petrausch U. ***(submitted to Clinical Cancer Research, 2017)***

Treatment of malignant pleural mesothelioma by fibroblast activation protein-specific redirected T-cells. Schuberth PC, Hagedorn C, Jensen SM, Gulati P, van den Broek M, Mischo A, Soltermann A, Jüngel A, Marroquin Belaunzaran O, Stahel R, Renner C, Petrausch U. ***(J Transl Med, 2013)***

Abbreviations

ACT	Adoptive cell therapy
ALL	Acute lymphoblastic leukemia
APC	Antigen presenting cell
β_2m	β2 microglobulin
BTLA	B- and T-lymphocyte attenuator
CAR	Chimeric antigen receptor
CD	Cluster of differentiation
CEA	Carcinoembryonic antigen
CLIP	Class II associated Ii peptide
CLL	Chronic lymphocytic leukemia
cMet	Tyrosine-protein kinase Met
CR	Complete remission
CRAC	calcium release-activated Ca2+
CRS	Cytokine release syndrome
cTEC	Cortical thymic epithelial cells
CTL	Cytotoxic T lymphocyte
CTLA-4	Cytotoxic T-lymphocyte-associated protein-4
DAG	Diacylglycerol
DC	Dendritic cell
DMSO	Dimethylsulfoxide
DN	Double negative
DNA	Deoxyribonucleic acid
DNR	Dominant negative receptor
DP	Double positive
EDTA	Ethylenediaminetetraacetic acid
EGFR	Epidermal growth factor receptor
ELISA	Enzyme-linked immunosorbent assay
EpCAM	Epithelial cell adhesion molecule
ERAD	ER-associated protein degradation
FACS	Fluorescence activated cell sorting
FAP	Fibroblast activation protein

FBS	Fetal bovine serum
G-CSF	Granulocyte-colony stimulating factor
GD2	Disialoganglioside
GM-CSF	Granulocyte-macrophage colony stimulating factor
GPC3	Glypican 3
GvHD	Graft versus host disease
HCC	Hepatocellular carcinoma
HER2	Human epidermal growth factor receptor 2
HFL	Human fetal liver
HLA	Human leukocyte antigen
HSCs	Hematopoietic stem cells
HSP	Heat shock protein
huNSG	Humanized NSG
IDO	Indoleamine 2,3-dioxygenase
IFN	Interferon
IgG	Immunoglobulin G
IL	Interleukin
i.p.	Intraperitoneal
IP3	Inositol trisphosphate
IR	Inhibitory receptor
ITAM	Immunoreceptor tyrosine-based activation motif
ITIM	Immunoreceptor tyrosine based inhibitory motif
ITSM	Immunoreceptor tyrosine based switch motif
i.v.	Intravenous
LAG-3	Lymphocyte-activation gene-3
LCMV	Lymphocytic choriomeningitis virus
li	Invariant chain
MDSC	Myeloid derived suppressor cell
MHC	Major histocompatibility complex
MM	Multiple myeloma
MPM	Malignant pleural mesothelioma
MSLN	Mesothelin

MUC1	Mucin 1
NCI	National cancer institute
NHL	Non-hodgkin lymphoma
NIH	National Institute of Health
NK	Natural Killer
NO	Nitric oxide
NOG	NOD scid IL2Rγ deficient mice
NSCLC	Non small cell lung cancer
NSG	NOD scid gamma
PBMCs	Peripheral blood mononuclear cells
PBS	Phosphate buffered saline
PCR	Polymerase chain reaction
PD-1	Programmed cell death-1
PD-L1	Programmed cell death ligand-1
PIP2	phosphatidylinositol 4,5-bisphosphate
PL	Peritoneal Lavage
PLCγ1	phospholipase Cγ1
PRR	Pattern recognition receptor
PSCA	Prostate stem cell antigen
PSMA	Prostate specific membrane antigen
ROS	Reactive oxygen species
scFv	Single chain variable fragment
SLO	Secondary lymphoid organ
SP	Single positive
TAA	Tumor associated antigen
TAP	Transporter associated with antigen presentation
TCR	T-cell receptor
TCM	T-cell medium
T_{EM}	Effector memory T-cell
Tfh	Follicular helper T-cell
TGF	Tumor growth factor
Th1	T-helper 1

Th17	T-helper 17
Th2	T-helper 2
Th9	T-helper 9
TIGIT	T-cell immunoreceptor with Ig and ITIM domains
TIL	Tumor infiltrating lymphocyte
TIM-3	T-cell immunoglobulin and mucin-domain containing-3
TNF	Tumor necrosis factor
TRAIL	TNF-related apoptosis inducing ligand
Tregs	Regulatory T-cells
UCB	Umbilical cord blood
VEGF	Vascular endothelial growth factor
VEGFR	Vascular endothelial growth factor receptor
VISTA	V-domain Ig suppressor of T-cell activation
Zap-70	Zeta-chain associated protein kinase of 70 kDa

List of figures

List of Tables

Table of Contents

Chapter-1

Summary

1.1 Summary

The concept of immune-surveillance highlights the key role of the immune system in detecting and destroying transformed cells, thereby preventing development of cancers. However, cancer cells can develop mechanisms to escape immune-mediated destruction, some of which include; downregulating expression of surface antigens to avoid detection by immune cells, upregulating receptors that lead to immune cell exhaustion or inactivation and manipulating the surrounding microenvironment to release substances that suppress immune response. Immunotherapies are designed to overcome these challenges.

Adoptive cell therapy is one of the immunotherapeutic approaches which includes transferring T-cells with redirected specificity to recognize tumor associated antigens (TAAs) such as, through the introduction of chimeric antigen receptors (CARs). Chimeric antigen receptor (CARs) are recombinant receptors consisting of an antibody derived- antigen binding domain coupled to intracellular T-cell signalling domains. First generation CARs consist of intracellular CD3ζ signalling domain, while second generation CARs contain additional co-stimulatory domains such as, CD28 or 4-1BB.

Another immunotherapeutic approach involves blocking the activity of immune check-point proteins that acts as “brakes” for the immune system by sending inhibitory signals, such as, Programmed Death -1 (PD-1). Both CAR-T cells and PD-1 blockade therapy have generated clinical responses that are largely variable and limited to a certain patient population. In case of CAR-T cells an affirmative effect is seen in haematological malignancies, but rarely in solid cancers. To increase the clinical efficacy, a combination of two approaches is desired.

Fibroblast activation protein is an antigen expressed in stromal fibroblasts as well as cancer cells of different tumor types, including those of epithelial origin and mesotheliomas such as, malignant pleural mesothelioma (MPM). We have generated FAP-specific CAR-T cells harbouring distinct co-stimulatory domains. These redirected T-cells were analysed extensively *in vitro* and then tested *in vivo* in combination with PD-1 blockade. The *in vivo* studies were carried out in a humanized mouse model, aiming to allow interactions of redirected T-cells with human immune system components.

In this study, we identified a particular CAR with a mutated CD28 signalling domain that showed enhanced antigen-specific proliferation, T-cell metabolism and redirected T-cell mediated tumor control in combination with PD-1 blockade in humanized mice. In parallel, we used the herein and previously generated results to launch a phase I first-in-human clinical trial employing FAP-specific redirected T-cells in patients with MPM. As in humanized mice, we found persistence of FAP-specific CAR-T cells with mutated CD28 signalling domain in the MPM patient. These results identify characteristics of a functionally competent CAR, which balances anti-tumor reactivity with persistence *in vivo*. Our study shows the bench to bedside translation of FAP-specific redirected T-cells and lays the groundwork for further clinical testing of FAP-specific redirected T-cells.

1.2 Zusammenfassung

Eine der wichtigsten Aufgaben des Immunsystems ist es maligne Zellen zu erkennen und abzutöten, um somit die Entwicklung von malignen Tumoren zu verhindern. Während der malignen Entartung können Zellen allerdings Resistenzmechanismen gegen den immunologischen Angriff entwickeln. Hierzu gehören der Verlust der Expression von Oberflächenantigenen, die Expression von immunsuppressiven Rezeptoren, die zur Über- oder Inaktivierung der Immunzellen führen, sowie die Entstehung einer Umgebung im Tumor, die das Immunsystem unterdrückt. Tumorimmuntherapien sollen diese Resistenzmechanismen beeinflussen, so dass das Immunsystem wieder in der Lage ist, maligne Tumore zu bekämpfen.

Eine mögliche Immuntherapie ist der adoptive Transfer von genetisch veränderten T-Zellen. Diese T-Zellen tragen nach Gentransfer einen synthetischen, chimären Antigenrezeptor (chimeric antigen receptor (CAR), mit Hilfe dessen die T-Zellen tumor-assoziierte Antigene (TAA) erkennen können. CARs bestehen aus dem Antigen-erkennenden Teil eines Antikörpers und intrazellulären Signaldomänen, die zur T-Zell-aktivierung nötig sind. Die CARs der ersten Generation beinhalteten nur die CD3ζ Signaldomäne; weiterentwickelte CARs exprimieren zusätzlich co-stimulatorische CD28 oder 4-1BB Signaldomänen.

Eine andere immunologische Intervention gegen maligne Tumore ist die Blockade von immunologischen Checkpoints wie z.B. PD-1. Diese Checkpoints beinhalten Signalwege, die als „Bremsen“ auf das Immunsystem wirken. Therapien mit Checkpoint Blockaden haben bei Patienten ein klinisches Ansprechen der malignen Tumore induziert, der Erfolg der Therapien war jedoch sehr variabel und limitiert auf spezifische Patientengruppen. CAR-tragende T-Zellen konnten bis dato nur bei hämatologischen, malignen Erkrankungen erfolgreich eingesetzt werden und waren ineffektiv bei soliden Tumoren. Um die Behandlung von soliden, malignen Erkrankungen mit CAR-tragende T-Zellen klinisch nutzbar zu machen, wird die Kombination mit Checkpoint Inhibitoren als therapeutische Intervention vorgeschlagen.

Stromale Fibroblasten in verschiedenen malignen Tumoren mit epithelialem und mesothelialem Ursprung exprimieren das Fibroblast activation Protein (FAP). FAP wird auch im malignen Pleuramesotheliom exprimiert. Wir haben verschiedene FAP-spezifische, CAR-tragende T-Zellen generiert, welche unterschiedliche Signaldomänen tragen. Diese verschiedenen CAR-tragende T-Zellen wurden umfänglich *in vitro* analysiert und in der Kombination mit einer Checkpoint Blockade gegen PD-1 *in vivo* getestet. Um möglichst klinisch relevante *in vivo* Ergebnisse zu erarbeiten, wurde ein humanisiertes Mausmodell etabliert, das eine Interaktion der CAR-tragenden T-Zellen mit einem humanen Immunsystem in einem murinen Wirt ermöglicht. In dieser Arbeit haben wir einen bestimmten CAR identifizieren können, der eine mutierte CD28 Signaldomäne exprimiert. Dieser zeigte verstärkte antigen-spezifische Proliferation, Metabolismus der T-Zellen und Persistenz *in vivo*. Weiterhin führte er in Kombination mit PD-1 Blockade zu einer verbesserten Tumorkontrolle *in vivo*. Parallel konnten wir in einer ersten klinischen Studie in dem ersten Patient zeigen, dass die CAR-tragenden T-Zellen nach adoptiven Transfer im Patient überlebten. Diese translationale Arbeit legt die Basis für die weitere klinische Entwicklung von FAP-spezifischen, CAR-tragenden T-Zellen für weitere Tumore.

Chapter-2

Introduction

2.1 Cancer biology and pathogenesis

Cancer is the second-most leading cause of death worldwide after cardiovascular diseases [2]. Cancer was responsible for 8.8 million deaths in 2015 and nearly 1 in 6 deaths all over the world happen due to cancer [3]. Although, with the advancement in scientific tools and techniques, our knowledge of cancer has progressed, alongside the complexity of disease has increased. Thus, in spite of improved treatment strategies, incidences of cancer have been on an ascent [4]. Cancer can arise from several types of spontaneous or induced genetic mutations, for example, altered glycosylation, gain or loss of chromosomes and translocation [5]. Additionally, epigenetic changes such as DNA methylation can cause cancer progression by activating or suppressing the expression of crucial genes [6]. These mutations can affect a broad range of tissues and organs, causing distinct cancer types, such as breast cancer and prostate cancer. Apart from hereditary factors, environmental factors such as diet, exposure to certain chemicals (carcinogens) or radiation and lifestyle choices such as, smoking can contribute to cancer [2]. Tobacco use is the most important risk factor for cancer accounting for approximately 22% of cancer associated deaths [3]. Although the elemental cause of cancer can be due to inherited or acquired genetic mutations, the pathogenesis of cancer is diverse and depends on tissue or organ of origin and the molecular mechanisms involved [2]. Cancers are highly heterogenous, which means they consist of subpopulations of several clones of transformed cells with distinct genotypes, phenotypes, molecular mechanisms and biological behaviors [7]. This heterogenity is not only limited to tumors from different patients, but also occurs within a single tumor in an individual [7]. A recent study published in New England Journal of Medicine described the evolution and heterogeneity in Non small cell lung cancers and its relation to the clinical outcome [8]. The intratumoral and intrapatient heterogeneity present the greatest challenge in cancer treatment and is one of the most important determinant of treatment outcomes in cancer patients [9]. Overall, there is not a standard treatment prototype that applies to a certain form of cancer.

2.1.1 Hallmarks of Cancer

In 2000, Hanahan and Weinberg proposed six common traits shared by all cancer types, called hallmarks of cancer which are the underlying principles reflecting the complexity of cancer and are fundamental in transformation of normal cell to become a cancer cell [10].

Cancer cells are self-sufficient in their growth, resistant to anti-growth signals, insensitive to programmed cell death (apoptosis), possess a limitless replicative potential, can stimulate formation of own blood vessels to allow nutrient supply (angiogenesis) and can invade local tissue and spread to other sites (metastasis) [10]. In 2004, Schreiber and co-workers proposed evasion of immune-surveillance as another important trademark of cancer [11]. Later, in an update published in 2011, Weinberg and Hanahan proposed four added hallmarks of cancer, that is, reprogramming of metabolism, evasion of immune response, genomic instability and inflammation **(figure 2-1)** [12].

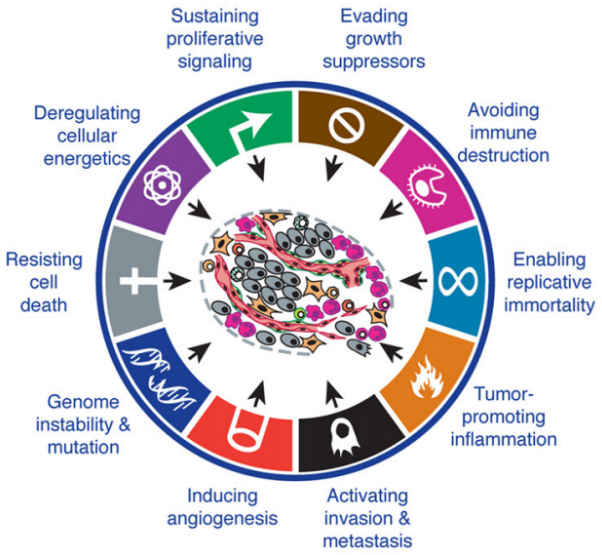

Figure 2-1. **The 10 updated hallmarks of cancer**, as proposed by Hanahan and Weinberg in 2011. *(Adapted from Hanahan D. et. al., Cell, 2011 [12]).*

2.1.2 Immune-surveillance and the process of cancer-immunoediting

The connection between immune system and cancer is known for over two centuries. In 1893, Willem Colley used live bacteria to treat cancer and showed modest clinical efficacy [13]. In 1909, Paul Ehrlich proposed the idea that transformed cells are continuously formed in our body, and that the immune system scans and eradicates them [14]. Further, in mid 20th century, failed attempts to transplant tumors in immune-competent animal models indicated that tumors could be suppressed by the immune system [15]. These findings formed the basis of immune-surveillance hypothesis which was first proposed by Burnet and Thomas in 1957 [14, 15]. The concept of immune-surveillance implied that the immune system identifies cancerous or pre-cancerous cells and destroy them before they can grow into established tumors [16].

The theory of immune-surveillance gained more attention in 1990, when using several types of knock-out animal models, the role of effector cells and cytokines such as, B cell, T cell, NK cells, IFN-γ and perforin in tumor progression was highlighted [11, 17]. For example, neutralization of IFN-γ resulted in increased tumor growth [18] and mice lacking IFN-γ responsiveness were shown to be more sensitive to tumor development than wild type mice [19]. Perforin was identified to have a key role in inhibition of tumors especially, B cell lymphomas [20, 21]. Furthermore, a series of publications showed that immune-deficient mice are more susceptible to spontaneous tumor development than wild type mice [22-26]. However, despite immune-surveillance, tumors still develop in the presence of a functioning immune system. By that time, it was also known that tumors which originated in immunocompetent mice, grew much easily than the ones which were developed in immunocompromised mice, when transplanted into syngeneic immunocompetent mice [23, 24, 27, 28]. This

observation indicated that the immune system not only provides protection against tumor development, but also shapes the tumor immune-environment. Thus, tumors which escape recognition by immune system are less immunogenic, which further support their growth [14]. Hence, the concept of "cancer immunoediting" came into light. Cancer-immunoediting first proposed by Schreiber and colleagues [11], consists of three phases; elimination, equilibrium and escape **(figure 2-2)** [29].

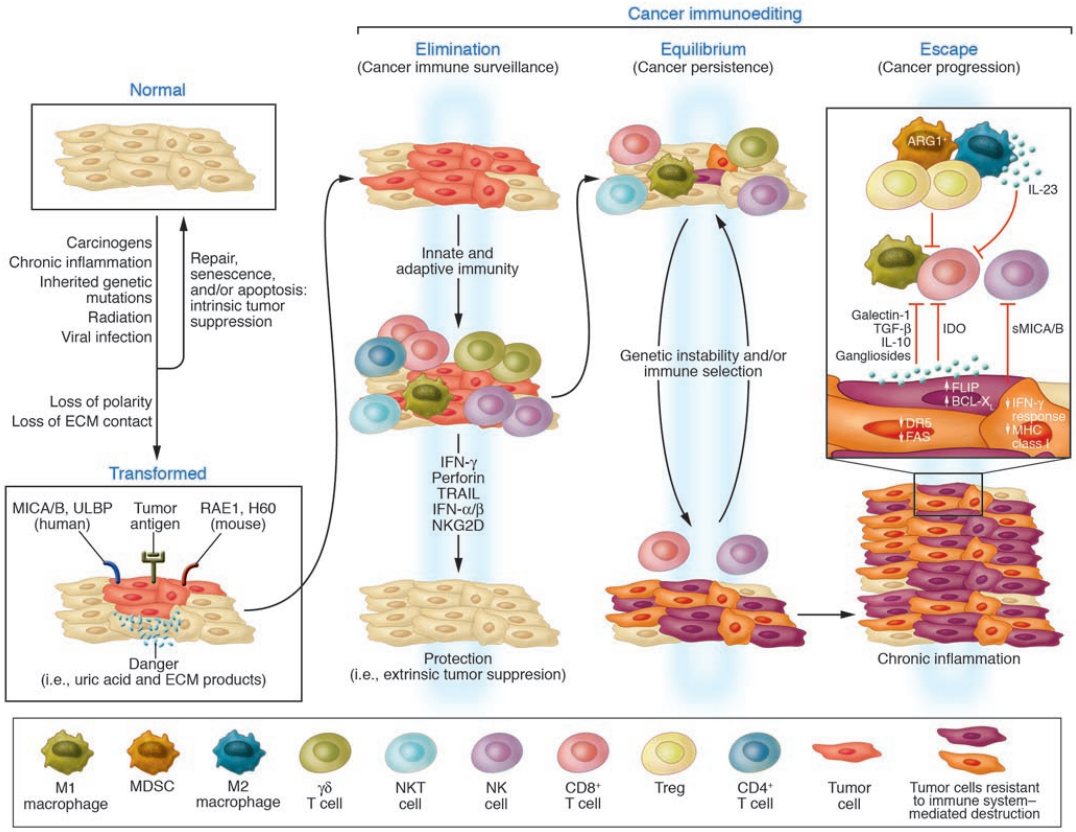

Figure 2-2. Process of cancer-immunoediting. Normal cells that get transformed and escape intrinsic control, are subjected to extrinsic tumor suppressor mechanisms mediated by the innate and adaptive immune components, which detect and eliminate developing tumors (Elimination phase). The tumor cells which escape destruction in elimination phase, enters a dynamic equilibrium with immune system, which keep tumor growth in check (equilibrium phase). The cells which manage to engage immune-suppressive mechanisms and display reduced immunogenicity, enters the escape phase and develop into progressively growing tumors (escape phase). *(Adapted from Smyth, M.J. et. al., Adv Immunol, 2006 [29]).*

The elimination phase is the same mechanism as described in the theory of immune-surveillance, whereby the immune-system recognize transformed cells and eradicate them before they can develop into tumor. The transformed altered cells upregulate several danger signals which activates both, innate and adaptive arms of the immune system. The elimination phase can be complete (when all the transformed cells are cleared) or incomplete (when some tumor cells persist). The cells that are not eradicated in the elimination phase, enters the equilibrium phase, where they either remain dormant or continue to evolve further changes (for example, accumulating DNA damage and other mutations). This can further inflect the stress-induced

antigens on their surface. As this process advances, the immune system exerts a selective pressure, and susceptible tumor clones are eliminated. If the pressure exerted by the immune system fails to completely eliminate tumor, then it leads to development of tumor cell variants, which are resistant to anti-tumor immune response and enters the escape phase. During the escape phase, the immune system is no longer able to suppress tumor growth, leading to establishment of a clinically detectable malignant tumor [29].

2.2 Immune system of the host

2.2.1 Components of the immune system

The immune system consists of a complex of cells and humoral factors which constitute the two interrelated arms of the immune system. The first arm is known as innate (natural) immunity, while the second is called adaptive (acquired) immunity and there is an extensive crosstalk between the two **(figure 2-3)** [30]**.** The components of the innate immune system form the first line of defence against infectious agents and initiate an early rapid pro-inflammatory response. The inflammation generated by innate immune components (granulocytes, macrophages, monocytes, mast cell, natural killer (NK) cells, and dendritic cells (DCs)) is important for initial containment of infection and for further direction and expansion of a more pronounced adaptive immune response. The adaptive arm of the immune system respond to the inflammatory signals from innate cells by expansion and differentiation of B and T lymphocytes which control a range of immunological responses specifically tailored to the infectious agent. Upon successful elimination of infection, adaptive immune system leaves behind a pool of memory cells that can last for many years and provide protection from re-infection with the same pathogen.

2.2.2 T-cell mediated immunity

T-cell mediated immunity is a part of the adaptive immune response which consists of developing antigen-specific T-cells to eliminate viral, bacterial and parasitic infections or malignant cells. The antigen specificity of T lymphocytes relies on recognition of unique MHC-bound antigenic peptides presented on antigen presenting cells (APCs), through T-cell receptor (TCR). T-cell mediated immunity consists of an initial recognition by naïve T-cells, effector response generated by activated T-cells and persistence of antigen-specific memory T-cells.

2.2.2.1 The Human Leukocyte Antigen (HLA) system

The genetic loci involved in rejection of allografts are known as major histocompatibility complex (MHC), and constitute the most polymorphic genetic system in humans [31]. The human MHC is also called the Human

Leukocyte Antigen (HLA) system, mainly because it was first identified and characterized using alloantibodies against leukocytes [32]. MHC molecules are membrane bound glycoproteins that play a role in the regulation of immune response by presenting processed antigenic peptides to T-cell receptor (TCR) on T-cells. The genetic polymorphism in MHC molecules result in variant amino acids in the antigen binding cleft which contributes to the diverse repertoire of peptides that can be bound and presented to T-cells [31]. MHC molecules are divided into two main classes; Class I and Class II **(figure 2-4)** [32].

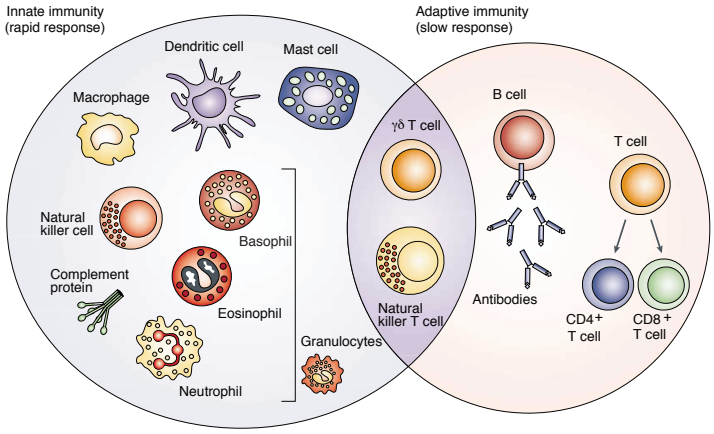

Figure 2-3. Components of the immune system. The innate immune response includes secretion of soluble factors such as complement proteins, and other cellular factors, including, dendritic cells (DCs), granulocytes, mast cells, macrophages and natural killer (NK) cells. Innate immunity provides the first line of defense against infections or pathogens by germ line encoded pattern-recognition receptors (PRRs) and other cell surface molecules, which can detect microbial constituents and trigger inflammatory reactions. In contrast to this, adaptive immunity, develops at a later stage of infection but manifests a high antigenic specificity and memory. It comprises of antibodies, B cells, CD4+ and CD8+ T-cells. NKT cells and γδ T cells are cytolytic T lymphocytes that function at the interface of innate and adaptive immunity. *(Modified from Dranoff G., Nat Rev Cancer, 2004 [30]).*

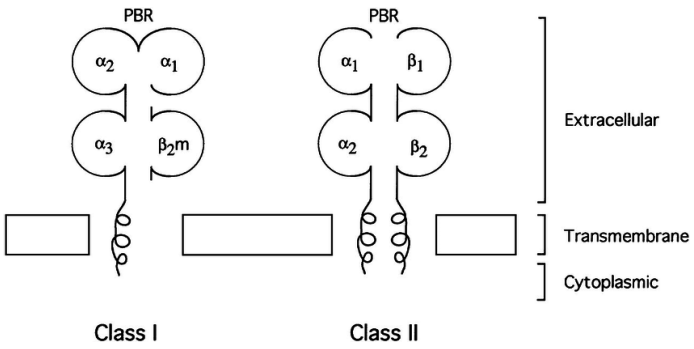

Figure 2-4. Schematic diagram of HLA class I and class II molecules. PBS is peptide binding site. *(Adapted from Choo, S.Y.., Med J, 2007 [32]).*

Class I MHC molecules occur on the surface of all nucleated cells and platelets. They present intracellular peptides from degraded cytosolic and nuclear proteins to CD8+ T-cells, thereby generating a cytotoxic T-cell response. The peptides presented by Class I molecules are usually 8-10 amino acid (a.a) in length. Structure of MHC class I consists of an alpha heavy chain non covalently bound to a β_2-microglobulin (β_2m) subunit [32]. Class-I MHC includes HLA-A, B and C genes.

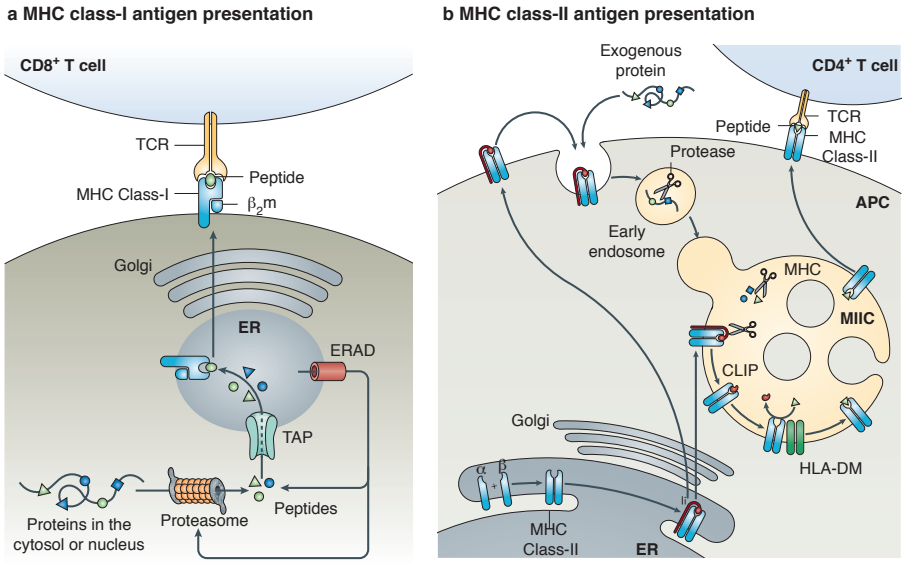

Figure 2-5. Antigen processing and presentation. a MHC class I molecules present intracellular antigenic peptides. Firstly, the antigen is degraded by proteasome. The resulting peptides are translocated into Endoplasmic Reticulum (ER) lumen via transporter associated with antigen presentation (TAP). In the ER, MHC class I molecules are assembled by non-covalent bonding of alpha heavy chain with β_2m. The peptide of approximately 8-9 a.a. inserts itself into peptide binding groove of MHC class I, which further stabilizes the whole complex. The completely assembled peptide–MHC class I complexes further leave the ER via Golgi for presentation on the cell surface. The MHC class I molecules which do not associate with peptides in the ER, are degraded in the cytosol. **b MHC class II** complex consisting of α and β chains form a complex with the invariant chain (Ii) in the ER. The Ii-MHC class II heterotrimer is transported via Golgi to MHC class II compartment (MIIC) where endocytosed proteins and Ii are degraded by proteases. The class II associated Ii peptide (CLIP) fragment of Ii remains in the peptide-binding groove of MHC class II and is further exchanged with antigenic peptide by the help of chaperone HLA-DM. Peptide loaded MHC class II molecules are transported to cell membrane for presentation to CD4+ T-cells. APC, antigen presenting cell; TCR, T-cell receptor; β_2m, β_2-microglobulin; ERAD, ER-associated protein degradation. *(Modified from Neefjes et. al., Nat Rev Immunol, 2011 [33]).*

MHC class II consists of polymorphic forms of genes HLA-DR, DP and DQ which hold peptides from extracellular proteins that have previously been engulfed and processed by an antigen presenting cell (APC). These peptides are generally 14 to 25 a.a. in length. Class II molecules are expressed on a restricted range of APCs including DCs, B cells, monocytes and macrophages. Other cells that can express MHC class II are activated T-cells and certain IFN-γ inducible cells, such as endothelial cells during inflammatory responses [31]. Class II molecules present peptides to CD4+ helper T-cells which lead to T-cell activation and cytokine production, driving both antigen specific T and B cell responses. Class II molecules are heterodimers of two non-covalently

associated glycosylated polypeptide chains; α and β [32]. The mechanism of antigen processing and presentation by MHC class I and class II is explained in **figure 2-5** [33].

2.2.2.2 T-cell development and acquisition of specificity in thymus

To recognize a wide variety of MHC bound antigenic peptides, mature T-cells develop a diverse TCR repertoire of varying specificities. T-cell receptor (TCR) is a heterodimer of α and β chains, each of which contains a constant (Cα, Cβ) and a variable (Vα, Vβ) domain [34]. Multiple variants of genes encoding α and β chains exist as a result of somatic rearrangements. The variable domains of the α and β chains form the antigen-binding site. Because of the presumptive nature of DNA recombination that dictates the assembly of gene segments forming domains of the TCR, a given TCR has no pre-determined specificity and can interact with a small spectrum of peptide-MHC complexes with different affinities [35]. The development of mature T-cells carrying a functional TCRs occurs in the thymus and involves a series of selection steps (**figure 2-6**) [36].

Lymphocytes originate from hematopoietic stem cells (HSCs) in the bone marrow. The process of T-cell development starts when the early T-cell precursor leaves the bone marrow and reach the thymus near cortico-medullary junction. Early T-cell precursors are CD44+ and negative for common T-cell lineage markers ($CD3^-CD4^-CD8^-CD25^-TCR^-$) and are called double negative 1 (DN1). Next, DN1 cells enter sub-capsular epithelium and start to express adhesion molecules CD44 and CD25 (IL-2 receptor α). At this stage the cells will initate TCR rearrangement (DN2). During the DN2 stage, T-cells loose CD117 expression and are fully committed T-cells. At DN3 stage ($CD4^-CD8^-CD24^+CD25^+CD44^{low}CD117^{low}$), T-cells are engaged in rearranging combinations for the β chains. Between the DN3a ($CD27^{low}$) and DN3b ($CD27^{high}$) phases, a very important checkpoint occurs, the β selection. If no functional β chain can be synthesized from TCR re-arrangements, the cell will not be able to produce a pre-T receptor and will die by apoptosis. At this stage TCR β re-arrangement occurs resulting in a unique β chain of TCR, and successful pairing with invariant surrogate pre-Tα and CD3 chains results in down-regulation of CD25 (DN4) ($CD4^-CD8^-CD24^+CD25^-CD44^-CD117^-$). The DN4 cells move to the medulla and upregulate both CD4 and CD8 and referred as double positive (DP) ($CD4^+CD8^+CD24^+CD25^-CD44^-CD117^-$). Next, rearrangements of TCR α chain occurs in a series of selection steps. Firstly, most double positive thymocytes which do not recognize self-antigens bound to self-MHC will die in a process called positive selection. Less than 5 % of thymocytes, with functional TCR that weakly recognize peptides in the context of self- MHC will survive [35]. Depending on the MHC molecule the TCR recognizes, the DP cell becomes single positive (SP); CD4+ is the TCR binds to MHC class II and CD8+ if TCR binds MHC class I. In the medulla, SP cells undergo negative selection where all self-reactive T-cells enter apoptosis. Overall the process consists of a series of successive selection steps which eliminates more than 90% of immature T-cells. The surviving selected cells are mature naïve T-cells that leave the thymus and further recirculate via lymph and blood continually re-entering lymphoid tissues, but not peripheral tissues. Antigen- inexperienced, naïve T-cells keep patrolling until they either encounter their cognate peptide:self-MHC complex or die [36].

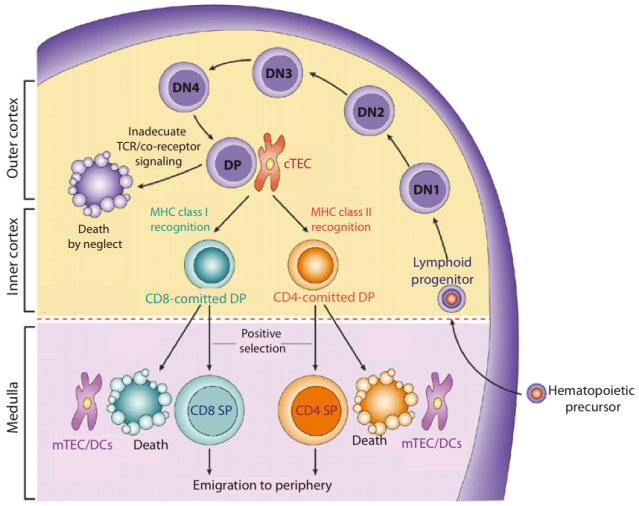

Figure 2-6. Development of T lymphocytes in thymus. Lymphoid progenitors lacking expression of T-cell receptor (TCR), CD4 and CD8, called as double negative (DN) cells migrate to the subcapsular epithelium in the thymus. The DN thymocytes pass through four stages of differentiation; DN1 ($CD44^+CD25^-$), DN2 ($CD44^+CD25^+$), DN3 ($CD44^-CD25^+$) and DN4 ($CD44^-CD25^-$) as they re-arrange TCR β chain. Further substantial proliferation of DN4 is accompanied by transition into a double positive (DP) thymocyte expressing CD4 and CD8 following re-arrangement of TCR-α chain and formation of a complete αβ TCR. The TCR+CD4+CD8+ thymocytes interact with cortical thymic epithelial cells (cTEC) expressing a high density of MHC class I and class II molecules associated with self-peptides. Inadequate signaling through TCR leads to apoptosis of majority of DP thymocytes (positive selection). Excessive TCR signalling from binding to self ligands in the thymic medulla promotes acute apoptosis (negative selection). Surviving thymocytes that express TCRs which bind peptide:MHC-class-I complexes become CD8+ T-cells, and those that express TCRs that bind peptide:MHC-class-II ligands become CD4+ T-cells. These cells then leave the thymus and migrate to peripheral lymphoid sites. DN double negative; DP double positive; SP single positive. *(Adapted from Germain R.N. et. al., Nat Rev Immunol, 2002 [36]).*

2.2.2.3 T-cell activation

TCRs detect antigens on the surface of APCs in the form of antigenic peptides bound to MHC molecules. TCR exist as a multimeric protein complex, composed of four distinct intracellular polypeptide chains; epsilon (ε), gamma (γ), delta (δ) and zeta (ζ), that assemble and function as three pairs of dimers (εγ, εδ, ζζ) and are collectively known as CD3. The α and β subunits of TCR contains the binding site to antigenic peptide and the co-receptor (CD4 or CD8) binds to the MHC molecule holding the peptide, thereby stabilizing the whole interaction (**figure 2-7**) [37].

Generated by recombination of DNA in the thymus, TCR provide a unique specificity to T-cell harbouring it. Mature T lymphocytes that migrate out of thymus and carry functional TCRs, are termed as naïve, since they have not yet encountered antigen and as a result have not been activated. Activation of naïve T-cells is needed to generate an immune response. Naïve T-cells undergo activation in the secondary lymphoid organs where they interact with antigen presenting cells, such as DCs, carrying antigenic-peptide bound to MHC class I or class II, in addition to other co-stimulatory receptors.

The process of positive selection which happens in the thymus results in TCRs which can weakly recognize self antigen-MHC complexes [35]. This chronic, weak interactions with self peptide-MHC molecules trigger "subliminal" signals and maintains T-cells in a state of heightened antigenic reactivity [35, 38]. As a result of this, the TCR is very sensitive to even minor traces of foreign peptides, such that even a single foreign peptide-MHC ligand at the T cell-APC contact surface, can result in full-fledged activation of T-cells.

Following recognition of MHC bound antigenic peptide by TCR, the T-cell and APC undergo actin mediated membrane reorganization, which allows grouping of TCRs on cell surface and formation of an immunological synapse [39]. Apart from TCR, other co-stimulatory and adhesion molecules are also recruited to the synapse site. This arrangement supports strong and prolonged intracellular interactions and appropriate spatial ordering of the TCR and other co-stimulatory receptors [40].

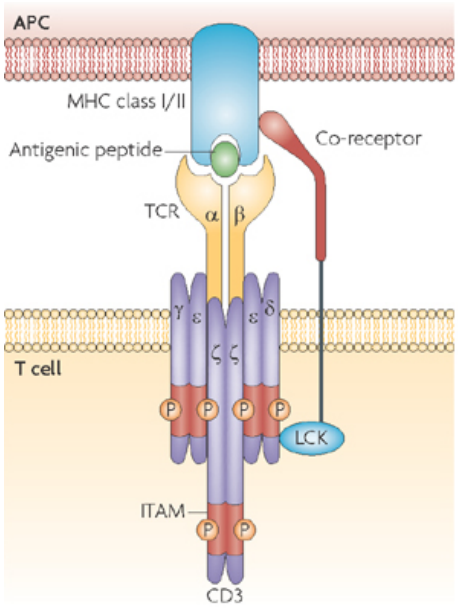

Figure 2-7. The T-cell receptor complex. TCR αβ heterodimers associate with the chains of the CD3 complex. This association is essential for expression of the TCR on the cell surface. The CD3 chains are also essential for signal transduction. The red regions represent immunoreceptor tyrosine-based activation motifs (ITAMs) which can be phosphorylated when the TCR recognizes a peptide presented by an MHC class I or class II molecule on antigen presenting cell (APC). *(Adapted from Gascoigne N.R. et. al., Nat Rev Immunol, 2008 [37]).*

Simply the recognition of antigen through TCR does not lead to activation of T-cells. Successful activation requires three important signals. First signal comes from recognition of the antigen through the TCR. Second is a co-stimulatory signal produced upon engagement of co-stimulatory molecules such as, CD80 (B7-1) and CD86 (B7-2) on APC with its respective ligand CD28 on T-cell. In the absence of co-stimulation, T-cells become anergic and undergo apoptosis [41]. Binding of CD28 to CD80/CD86 strengthens the formation of membrane microdomains and increases TCR proximity to CD3 complexes [41, 42]. The third signal is derived from binding of cytokines such as IL-2 and IFNα released from APCs, to their receptors on T-cells. Naïve T-cells which receive

these three signals (**figure 2-8**) [37] will undergo activation, expansion and generate a large antigen-specific effector T-cell population [43].

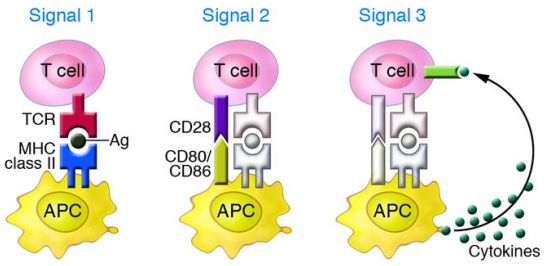

Figure 2-8. Antigen-specific T-cell activation requires three signals. Signal 1 constitutes the recognition of MHC bound antigenic peptide by TCR. Signal 2 involves binding of costimulatory molecules CD80/86 on APCs with their receptor CD28, on T-cells. Signal 3 comprises of cytokines released by APCs, that bind to cytokine receptors on T-cells and polarize them to an effector phenotype. Ag, antigen. *(Adapted from Gascoigne N.R. et. al., Nat Rev Immunol, 2008 [37]).*

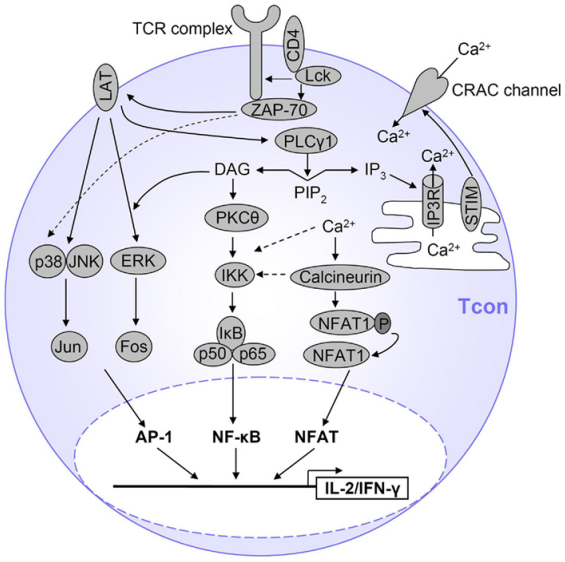

Figure 2-9. T-cell receptor activation induced intracellular signalling pathways. Activation through the T-Cell Receptor (TCR) intiates several signaling cascades which regulate cytokine production, cell survival, proliferation, and differentiation. One of the first events upon TCR activation is phosphorylation of immunoreceptor tyrosine-based activation motifs (ITAMs) on the intracellular domain of TCR/CD3 complex by lymphocyte protein tyrosine kinase Lck and Fyn. Zeta-chain associated protein kinase (Zap-70) is recruited to the TCR/CD3 complex where it gets activated, and promote recruitment and phosphorylation of adaptor protein LAT. LAT phosphorylates and activates phospholipase C γ1 (PLCγ1) causing hydrolysis of phosphatidylinositol 4,5-bisphosphate (PIP2) which produces second messengers diacylglycerol (DAG) and inositol trisphosphate (IP3). DAG activates PKCθ and the MAPK/Erk pathways, resulting in activation of transcription factor NF-κB and AP-1. IP3 triggers the release of Ca2+ from the ER and support the entry of extracellular Ca2+ into cells through calcium release-activated Ca2+ (CRAC) channels. Calcium-bound calmodulin activates the phosphatase calcineurin, which results in IL-2 gene transcription through the transcription factor NFAT. Feedback regulation at several steps within these pathways results in different outcomes. *(Adapted from Schmidt A. et. al., Front Immunol, 2012 [44]).*

In addition to this, extensive studies have revealed the role of interaction of TNF super family receptors; CD27, OX-40, 4-1BB and CD30 present on T-cells with appropriate ligands; CD70, OX-40L, 4-1BBL and CD30L on APCs to promote the survival of proliferating effector cells and differentiation into memory T-cells [45, 46].

Activation initiates a series of intracellular signalling cascades in T-cells. The cytosolic region of the CD3 complex is responsible for propagating these intracellular signals. Firstly, it leads to de-phosphorylation and activation of the tyrosine kinases FYN and Lck by CD45. FYN and Lck phosphorylate immunoreceptor tyrosine-based activation motifs (ITAMs) on the cytosolic CD3 complex, which further bind the ZAP-70 kinase. Activated ZAP-70 triggers a number of immune responses which involves protein-protein interactions, reversible modifications (phosphorylation and ubiquitination) and formation of intra-cellular messengers such as calcium and diacylglycerol [35]. These pathways collectively induces a transcriptional program resulting in robust IL-2 production, an autocrine and paracrine factor that stimulates T-cells to proliferate (**figure 2-9**) [44].

2.2.2.4 T-cell differentiation

T-cell mediated immune response can be divided into two broad categories. First is the helper CD4+ T-cell response, which generates cytokines and chemokines that activate neighbouring cells or recruits new immune cells to the site of infection. Second is the cytotoxic CD8+ T-cell response which directly kills the altered host cell by secreting cytotoxic molecules and cytokines. Depending upon the surrounding cytokine environment, a broad spectrum of specialized T-cell subtypes result from genetic programming of naïve T-cells.

2.2.2.4.1 Helper T-cell subsets

Helper T-cell responses consist of subsets; T-helper 1 (Th1), T-helper 2 (Th2), T-helper 17 (Th17), T-helper 9 (Th9), follicular helper (Tfh) and regulatory (Tregs) T-cells.

The release of cytokines IFNα/β and IL-12 in response to intracellular pathogens, stimulates the expression of transcription factor T-bet, which promotes differentiation into Th1 subset [47]. Th1 cells generates cytokines IFN-γ and TNF-α, which further activates neighbouring cells such as macrophages and enhances their phagocytic and antigen presenting function [48]. Activation of naïve T-cells by IL-4 induces differentiation to Th2 subset [49]. Th2 cells secrete IL-4, IL-5 and IL-13, which activates granulocytes such as eosinophils, mast cells and basophils, playing major role in elimination of parasites [50]. The cytokines generated by Th2 cells also stimulate B cells to produce IgE and IgA antibodies to neutralize mucosal surfaces of invading parasites [48]. Th9 cells produce IL-4, IL-13 and IL-9 in response to parasitic infections [51]. Upon stimulation with TGF-β and IL-6 produced as a result of infection with extracellular bacteria and fungi, T-cells differentiate into Th17 subtype [52]. Th17 cells upregulate transcription factor RORγT and secrete large amounts of IL-17 which activates neutrophils [52]. Overall, the differentiation into a specific T-cell subtype is influenced by the nature of the invading pathogen. Some T-cell differentiation is not specific to a certain pathogen, but supports immune

response common to majority of infections. For example, cytokines IL-21 and IL-27 induces transcription factor Bcl-6 and polarizes naïve T-cells to home to B-cell follicles in secondary lymphoid organs. This resultant T-cell subtype, called Tfh assist in generation of antibodies by B cells in the germinal centres [53].

A persistent, unchecked immune response can be harmful to the host. To prevent this, the immune system produces regulatory T-cells (Tregs), which can curb an immune response and keep inflammation in check. Tregs can be produced directly from thymic selection (natural Tregs) or as a result of differentiation in presence of cytokines such as TGF-β (inducible Tregs). Tregs mediated immune suppression involves activity of transcription factor FOXP3 which results in production of immune-suppressive cytokines IL-10, TGF-β and IL-35 [54]. These cytokines establish immune quiescence and maintain tolerance to self antigens.

2.2.2.4.2 Cytotoxic T-cells

Attributed to their capacity of cytolytic activity, CD8+ T-cells specialize in eradication of intracellular pathogens and cancer. When CD8+ T-cells recognize antigen in presence of IFNα/β and IL-12, they differentiate into cytotoxic T-cells, which secrete effector cytokines, IFN-γ and TNF-α. In addition to this, cytotoxic T-cells generate secretory vesicles containing granzyme and perforin, which can be released upon contact with infected cells leading to direct cell lysis (**figure 2-10**) [55].

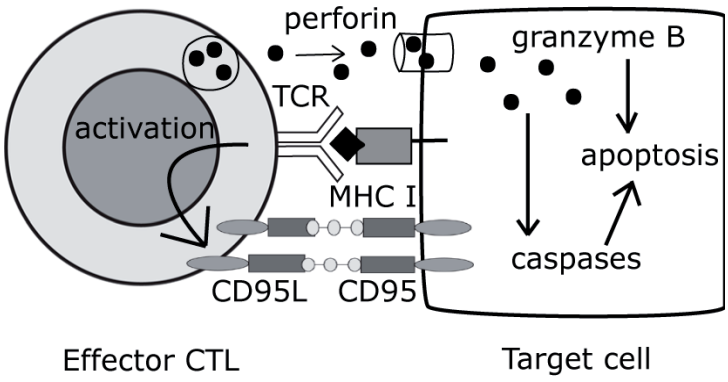

Figure 2-10. Cytotoxic T lymphocytes mediated cell killing. Cytotoxicity is mediated by two different pathways. First is by secretion of perforin and granzyme B. Perforin creates pores in the membrane of target cells, allowing granzyme B to enter the cell. Second is by interaction of CD95 (Fas) and CD95L (FasL). CD95 expression is upregulated on CTLs in response to T-cell activation. Both, granzyme B and interaction of CD95 with its ligand (CD95L), activates caspases leading to apoptosis of the target cell. *(Adapted from Femke B. et. al., Principles of Immunopharmacology, 2011 [55]).*

Since CD8+ T-cells recognize antigen presented with MHC class-I molecule, they can virtually interact with every cell in the body. In this way, cytotoxic T-cells can recognize altered cells expressing tumor associated antigens and lyse them.

2.2.2.5 Memory T-cells

The effector cells produced from activation and differentiation of naïve T-cells, proliferate enormously until the infectious agent is cleared. Once, the infection is terminated, there is a drastic decline in the effector T-cell population. Over 90 – 95% of antigen specific effector T-cells undergo apoptosis, leaving behind traces of "memory" cells which possess a range of phenotypes and functionalities.

Compared to naïve T-cells, memory cells have less stringent requirement for activation via antigenic and co-stimulatory receptors. Additionally, they possess increased proliferative potential and generate a more intense and rapid immune response upon re-infection. Memory cells can traffic through both, secondary lymphoid organs (SLOs) and peripheral tissues, allowing them to approach areas poorly accessed by naïve (peripheral) and effector (secondary lymphoid organs) T-cells.

Table 2-1. Phenotypic markers associated with naïve, effector and memory T-cells. *(Adapted from Femke B. et. al., Principles of Immunopharmacology, 2011 [55]).*

	naïve	effector	T_{EM}	T_{CM}
CCR7	+++	–	+/–	+++
CD62L	+++	–	+/–	+++
CD45RO	+	+++	+++	+
CD45RA	+++	–	+	++
CD95	+/–	+++	++	+/–
Granzyme B	–	+++	+/–	–
CD25	–	+	–	–
CD127	++	+/–	+	+++
CD28	++	–	+	++

There are two main subclasses of memory T-cells; central memory (T_{CM}) and effector memory (T_{EM}). These cells differ phenotypically in terms of cell surface markers, for example adhesion markers and homing receptors (**Table 2-1**) [55]. These phenotypic differences further translate to functional differences. T_{CM} cells have increased proliferation potential upon re-exposure to antigen. In contrast, T_{EM} cells possess rapid effector function (IFN-γ and granzyme B production), but a limited proliferative capacity. The high expression of CD62L and CCR7 allows homing of T_{CM} cells to SLOs, which constitutively express CCR7 ligands; CCL19 and CCL21. In SLO, T_{CM} cells are located to protect from a systemic infection and invade the peripheral tissues with new effector cells after stimulation. In contrast, lack of CCR7 and CD62L restricts T_{EM} cells to non lymphoid tissues. The trafficking location and high cytolytic capacity of T_{EM} cells, renders them as "first responders" in the peripheral site during re-infection [48]. Thus, T_{EM} cells control initial exposure to antigen, providing T_{CM} cells time to proliferate and produce new effectors. The presence of antigen, cytokines and the kind of inflammatory environment can influence key transcription factors which decide fate of T-cell differentiation into effector or

memory subtypes. Cytokines; IL-2 and IL-12 and transcription factors; Blimp-1 and T-bet drive the production of effector cells, while cytokine IL-21 and transcription factors; EOMES and Bcl-6 favour the development of long-lived memory T-cells.

2.3 Immune regulation in Cancer

2.3.1 Coordinated innate and adaptive immune response in cancer

Both innate and adaptive immune constituents are involved in recognition of cancer cells. The mechanism consisting of coordinated humoral and cellular reactions can be largely divided into two parts as illustrated in **figure 2-11 [30]**.

In the first part, components of innate immunity detect tumor cells by pattern recognition receptors (PRRs) and other cell surface molecules. For example, cancer cells regularly express stress related genes which can be recognized by NKG2D receptor expressed on NK cells, macrophages and some cytotoxic T-cells [56]. Following stimulation, NK cells can lyse tumors by secreting cytolytic molecules, perforin and granzyme or through apoptosis-inducing ligands such as tumor-necrosis factor (TNF)-related apoptosis inducing ligand (TRAIL) [57]. Additionally, NK cells secrete IFN-γ which enhances apoptosis and inhibits proliferation and angiogenesis in tumor cells [57]. Macrophages can lyse tumor cells by production of nitric oxide and other reactive oxygen species (ROS) [58]. The antigen presenting dendritic cells (DCs) can engulf and phagocytose dying tumour cells [59]. Heat-shock proteins that are released from necrotic cancer cells are complexed with tumour-derived peptides and after being ingested by DCs and macrophages can be presented for recognition and activation of adaptive immune response [59].

In the second part, the adaptive immune system employs an indirect pathway mediated by DCs, known as ”cross-priming” to recognize cancers [60]. Tumour cells mostly lack the expression of co-stimulatory molecules, which are necessary for activation of T-cells, and hence they cannot generate cellular responses by themselves [30]. The DCs which have phagocytosed dying tumor cells, migrate to the lymph nodes, process and load the tumor-derived material on to CD1D; for presentation to NKT cells and MHC class I and class II molecules for presentation to CD4+ and CD8+ T-cells [30]. Mature DCs upregulate expression of co-stimulatory molecules such as B7-1 and B7-2 to stimulate efficient T-cell activation. This pathway generates CD4+ and CD8+ T-cells specific to the MHC-bound tumour peptides derived from mutated proteins, aberrantly expressed gene products and normal differentiation antigens produced by the cancer cells [61]. Cytotoxic CD8+ T-cells causes tumor cell lysis through death ligands, such as TRAIL and perforin/granzyme pathway. CD4+ T-cells can differentiate into T helper 1 (Th1) cells which secrete IFN-γ and TNF-β or T helper 2 (Th2) cells which secrete interleukins such as IL-4, IL-5, IL-6, IL-12 and IL-13 and present tumor peptides to B cells [62]. These cytokines can enhance antibody production by B cells. Antibodies targeting cancer cell-surface molecules can inhibit key signalling pathways which support tumor survival. Additionally, antibodies can promote tumor antigen presentation by DCs by

forming immune complexes. Furthermore, they can stimulate tumor cell lysis by indirectly activating macrophages, granulocytes and NK cells through Fc receptor binding [30].

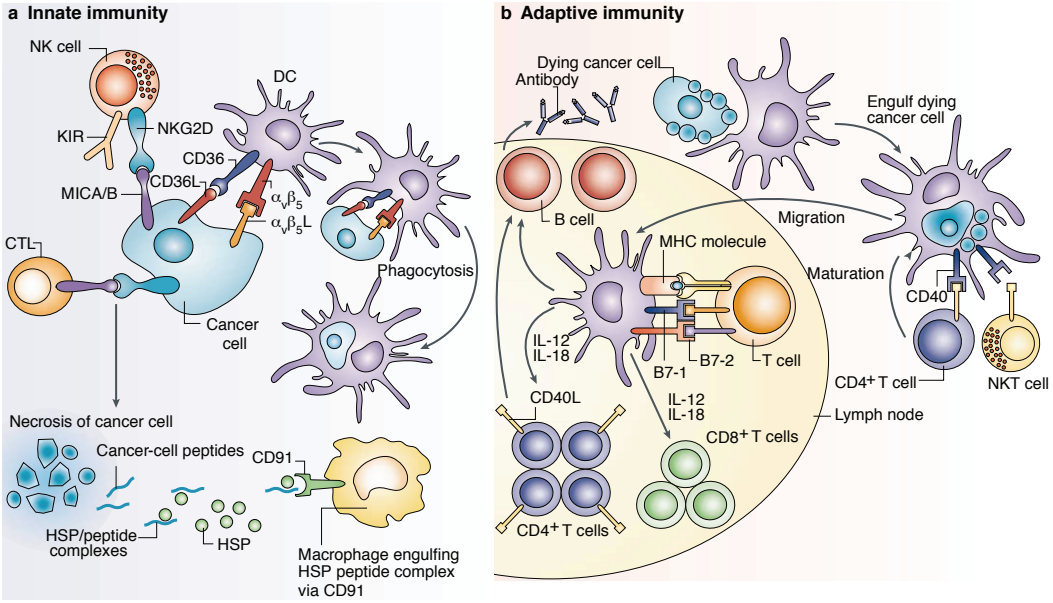

Figure 2-11. Immune pathways of cancer recognition. a. Innate immunity cells such as natural killer (NK) cells express pattern recognition receptor NKG2D which recognize stress induced genes such as MICA and MICB expressed by tumor cells. NK cells use a combination of inhibitory and activating receptors such as, killer cell immunoglobulin like receptors (KIRs) to detect the loss of major histocompatibility complex (MHC) class I expression on tumors. Dendritic cells (DCs) recognize apoptotic tumor cells through receptors CD36 and $\alpha_v\beta_5$ and uptake them for phagocytosis. Macrophages and DCs use scavenger receptor and CD91 to ingest heat-shock proteins (HSPs) containing peptides released from dying cancer cells. **b. Adaptive immunity** cells recognize cancer cells through cross-priming by DCs. DCs that have captured dying tumor cells or debris, migrate to regional lymph nodes and present the MHC-restricted tumor peptides to CD4+ and CD8+ T-cells. Mature DCs co-express co-stimulatory molecules B7-1 and B7-2 and secrete IL-12 and IL-18 to promote T helper 1 (T_H1) CD4+ response and cytotoxic CD8+ T-cell response. Activated CD4+ T-cells and NKT cells express CD40L which stimulate DC maturation. CD4+ T-cells and DCs can also trigger B cells to produce antibodies against tumor proteins. *(Modified from Dranoff G., Nat Rev Cancer, 2004 [30]).*

2.3.2 Immune-escape strategies in cancer

The immune system has the capacity to distinguish transformed cells from normal cells by identifying "non-self" antigens expressed on transformed cells. Tumor cells are also transformed cells, however they have the capacity to avoid immune detection since majority of tumor antigens are "self proteins". Tumors can modulate cell surface antigens. For example, they down-regulate MHC class I molecules, which prevents the cytolytic response from T-cells [63]. Certain tumor cells can release antigens into cytoplasm, thereby becoming immunologically invisible [64]. Alternatively, they can up-regulate inhibitory receptors which can curb activation of immune cells and avoid resultant lysis of tumor cells [65]. In addition, tumor cells can alter the expression of cell adhesion molecules and thereby obstruct contact with cytolytic cells [66]. Tumors can synthesize

immunosuppressive cytokines such as interleukin (IL)-10, Tumor growth factor (TGF-β) and vascular endothelial growth factor (VEGF) to induce tolerance [67]. Tumor cells can up-regulate the expression of ligands such as PD-L1, which upon recognition, induces exhaustion in cytotoxic T-cells. Further, they can also enhance secretion of anti-apoptotic molecules to escape cell death [67]. **Figure 2-12** summarizes tumor immune-escape strategies [68].

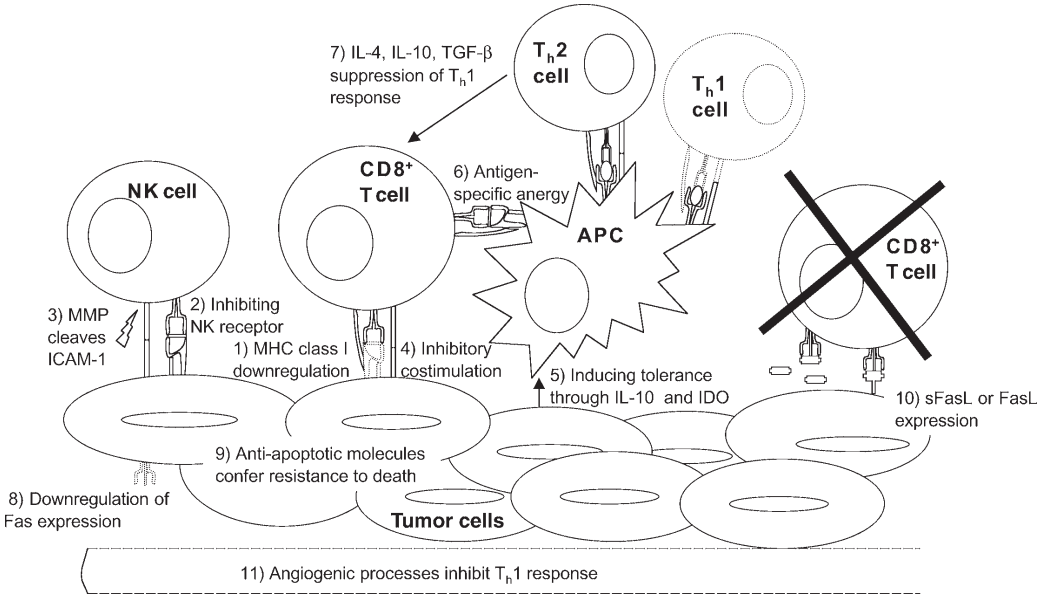

Figure 2-12. Tumor immune-escape strategies. Tumor cells can evade immune detection by (1) Down-regulating Major Histocompatibility complex (MHC) class I molecules, (2) inhibiting Natural Killer (NK) cell receptors, (3) obstructing cell to cell interactions, (4) up-regulating expression of inhibitory receptors which inhibit effector T-cell responses, (5) inducing tolerance in antigen presenting cells (APCs) by enhanced secretion of immune-suppressive cytokines such as interleukin (IL)-10 and indoleamine 2,3-dioxygenase (IDO), (6) inducing antigen-mediated anergy in T-cells, (7) leading to a type-2 response which suppresses T-helper (T_h) cell response, (8) down-regulating the expression of FAS, (9) enhanced secretion of anti-apoptotic molecules to escape death, (10) secreting soluble FAS (sFAS) thereby causing apoptosis of FAS-expressing T-cells and (11) forming blood vessels for nutrient supply (angiogenesis) and as a result, indirectly inhibiting T_h1 response. *(Adapted from Yi Ting Koh. et.al., Cancer drug resistance [68]).*

2.3.2.1 T-cell exhaustion

T-cell exhaustion refers to functional silencing of effector T-cells due to continuous TCR stimulation from persistent antigen [69]. Exhaustion of T-cells differs from other dysfunctions such as anergy and senescence. T-cell anergy is induced during priming due to lack of co-stimulatory receptors and senescence refers to growth arrest after extensive proliferation.

T-cell exhaustion was intially documented in mice infected with lymphocytic choriomeningitis virus (LCMV), where a chronic viral infection resulted in impaired function of virus specific cytotoxic T-cells, which was later demonstrated to be reversible [70, 71]. Mice with exhausted T-cells develop severe spontaneous auto-immune diseases [72, 73]. Besides that, presence of exhausted T-cells in patients with auto-immune diseases indicates favourable prognosis [74]. Aside from a favourable position in auto-immunity, T-cell exhaustion is

detrimental to anti-tumor immune responses and is one of the predominant immune-escape mechanisms adopted by tumor cells [75-79].

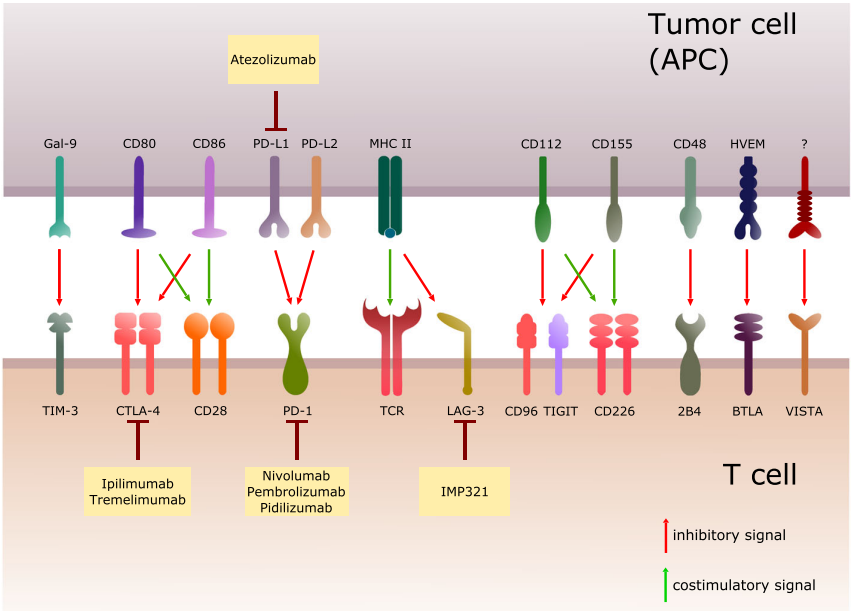

Figure 2-13. Inhibitory receptors on exhausted T-cells and their corresponding ligands. Blocking antibodies against the inhibitory receptors and their ligands in clinical trials are mentioned with the aim of reversing T-cell exhaustion. *(Adapted from Catakovic, K., et al., Cell Com Signal, 2017 [80]).*

Characteristics of T-cell exhaustion are continuous increase in T-cell dysfunction due to persistent exposure to antigen, up-regulation of multiple inhibitory receptors (IR), loss of effector cytokines; IL-2, IFN-γ and TNF-α, altered cell metabolism and a distinct transcriptional profile [80]. Exhausted T-cells express a range of inhibitory receptors, namely, programmed cell death-1 (PD-1), Cytotoxic T-lymphocyte-associated protein-4 (CTLA-4), T-cell immunoglobulin and mucin-domain containing-3 (TIM-3), Lymphocyte-activation gene-3 (LAG-3), CD96, T-cell immunoreceptor with Ig and ITIM domains (TIGIT), 2B4 (CD244), B- and T-lymphocyte attenuator (BTLA) and V-domain Ig suppressor of T-cell activation (VISTA) as shown in **figure 2-13** [80]. Blocking interaction of these receptors with their respective ligands (also known as immune-checkpoint inhibition), is routinely used to reverse T-cell exhaustion and regain anti-cancer immunity. The most therapeutically exploited exhaustion markers are PD-1/PD-L1 axis and CTLA-4.

2.3.2.2 Programmed cell death 1 (PD-1)

Transient PD-1 expression is seen upon T-cell activation, but sustained expression is a marker of T-cell exhaustion [81]. The intracellular domain of PD-1 consists of an immunoreceptor tyrosine based inhibitory motif (ITIM) and an immunoreceptor tyrosine based switch motif (ITSM). Binding of PD-1 to its ligand (PD-L1 or PD-L2) leads to phosphorylation of ITIM/ ITSM and further recruitment of the phosphatases SHP1/ SHP2, which

negatively impact Pi3K and RAS signalling pathways [82-84]. Tregs have been shown to express PD-1 in addition to CTLA-4 [85].

In a chronic infection model of LCMV, two major subsets of PD-1+ T-cells were identified based on intensity of PD-1 expression and transcriptional profile [86]. The first subset with phenotype T-bet^{hi}PD-1^{int}, showed limited proliferation and residual IFN-γ and TNF-α secretion. Second subset, identified with high levels of Eomesodermin (Eomes) and PD-1 (Eomes^{hi}PD-1^{hi}) showed higher Blimp-1 and granzyme B production. Additionally, co-expression of other inhibitory receptors (CD160, Lag-3, 2B4 and Tim-3) in Eomes^{hi}PD-1^{hi} cells, induced a severe state of exhaustion, despite a higher cytotoxic activity compared to T-bet^{hi}PD-1^{int} cells. Furthermore, it was shown that the first subset of cells (T-bet^{hi}PD-1^{int}) gave rise to second (Eomes^{hi}PD-1^{hi}) in an antigen dependant manner [86]. The authors showed that blocking PD-1 interaction with its ligand, induced an anti-viral state in the LCMV model. Eomes^{hi}PD-1^{hi} T-cells showed a poor response to PD-1 pathway blockade, but T-bet^{hi}PD-1^{int} cells efficiently reversed exhaustion and induced protective immunity against LCMV infection [87]. These findings suggest that blocking PD-1 signalling might reverse exhaustion in only a limited fraction of T-cells.

2.3.2.3 Checkpoint blockade in clinical trials and standard of care

Checkpoint inhibition is a new, recently accepted and attractive option as a single therapeutic or a combination partner with other standard therapies for cancer. Blocking antibodies against PD-1, PD-L1 and CTLA-4 have shown clinical success and are continuously being put to test in further clinical trials [80]. The expression of these inhibitory receptors is not just restricted to exhausted cytotoxic CD8+ T-cells, but also found on T helper, Tregs and APCs [80]. Thus, the outcome of these therapeutic antibodies cannot be narrowed down to one specific immune cell population. CTLA-4 and PD-1/PD-L1 blocking antibodies differ in their mode of action. While CTLA-4 antibodies reduce the threshold for T-cell activation, PD-1/PD-L1 blocking antibodies aim at regulating effector T-cell activity (**figure 2-14**) [88-90].

2.3.2.3.1 PD-1 blockade

PD-1 blockade has become standard treatment in lung, kidney, bladder, and head and neck cancer [91]. Also it is used to treat Hodgkin`s lymphoma and melanoma and most recently has been approved for the treatment of micro-satellite instable cancer of any entity [91]. In regards to clinical testing, Nivolumab and Pembrolizumab have been used in malignant melanoma and NSCLC. Nivolumab showed significant improvement in overall survival and progression free survival in previously untreated melanoma patients without BRAF mutation [92]. In NSCLC patients, both nivolumab and pembrolizumab showed improved survival rates [93-96]. Pidilizumab, another PD-1 inhibitor, was used in relapsed follicular lymphoma and diffuse large B cell lymphoma and showed overall response rates of 66% and 51%, respectively [97, 98]. Several clinical trials

have also tested a combination of PD-1 and CTLA-4 blockade. In a study by Postow et.al., using PD-1 blockade (nivolumab) and CTLA-4 blockade (ipilimumab) showed significant improvement in progression free survival over PD-1 blockade (nivolumab) alone or placebo control [99].

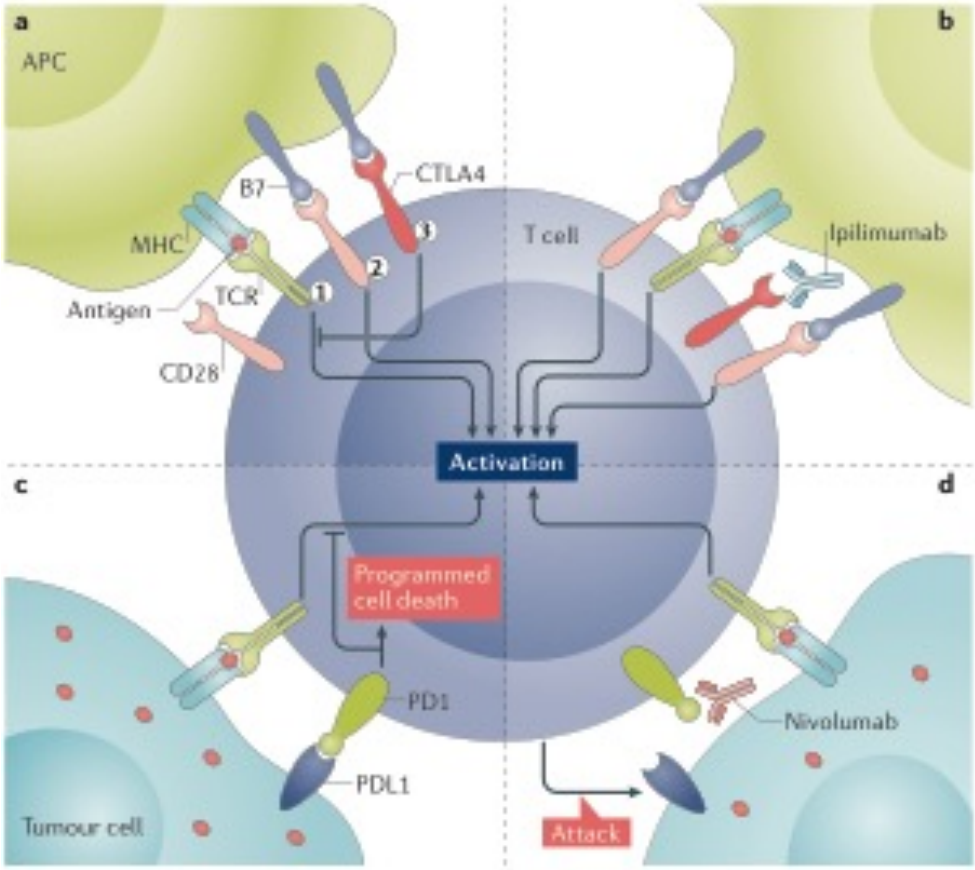

Figure 2-14. Mechanism of action of CTLA-4 and PD-1/PD-L1 axis checkpoint therapy. a The first and second (2) signal in T-cell activation are provided by binding of TCR to MHC bound antigenic peptide (1) and co-stimulatory receptor; CD28 to its ligand B7 (2) on APC. Cytotoxic T-lymphocyte antigen 4 (CTLA-4) receptor expressed by T-cell binds to B7 ligand (3) and competes with CD28 to negate the second co-stimulatory signal needed for T-cell activation. **b** CTLA-4 blocking antibodies, for example, ipilimumab blocks the binding of CTLA-4 to B7 and indirectly increases T-cell activation. **c** Tumor cells up-regulate PD-L1 as a mechanism of immune evasion, whereby PD-1/PD-L1 interaction results in T-cell exhaustion. **d** PD-1 blocking antibodies, such as nivolumab, increases the sensitivity of T-cells towards generating an anti-tumor response. *(Adapted from Byun, D., et al., Nat Rev Endocrinol, 2017 [90]).*

Further, in a phase-III trial using ipilimumab pre-treated advanced melanoma patients, nivolumab demonstrated higher objective response rate than chemotherapy as the second line of treatment [100]. When compared to ipilimumab, pembrolizumab showed prolonged progression free survival in melanoma [101].

All the checkpoint inhibitor antibodies showed similar immune-related adverse events in these clinical trials. The adverse events affected gastrointestinal tract, skin and liver function. Diarrhoea and colitis was observed in almost all the trials [80]. Compared to standard chemotherapy, the adverse events generated from check point inhibitors were easy to manage and tolerable.

2.4 Adoptive cell therapy (ACT) in cancer

Adoptive cell therapy is a personalized immunotherapeutic approach to treat cancer. It involves, administration of *ex vivo* modified or expanded tumor-reactive lymphocytes into cancer bearing host. ACT relies on the principle that lymphocytes can be expanded *in vitro*, as well as tested and selected based on their high avidity and effector functions against tumor. The success of ACT relies on one prime factor, which is the reactivity of adoptively transferred lymphocytes to target antigens expressed on cancer and not on other normal tissues. ACT employs either natural host derived lymphocytes that exhibit anti-tumor reactivity or host lymphocytes that are genetically engineered to re-direct their specificity to tumor antigens.

2.4.1 Tumor infiltrating lymphocytes (TILs)

The first evidence of T-cells leading to allograft rejection in animals was established in 1960 [102]. Later, attempts to treat transplanted tumors in mice showed modest efficacy due to limited ability to expand and manipulate T-cells *in vitro* [103, 104]. In 1976, IL-2 was identified as T-cell growth factor and provided a way to expand T-cells *ex vivo* without loss of effector functions [105]. High doses of IL-2 could inhibit tumor growth in mice [106] and infusion of IL-2 expanded lymphocytes could treat lymphoma [107].

Tumor-infiltrating lymphocytes (TILs) isolated from the tumors or tumor-draining lymph nodes were used as a concentrated source for adoptive transfer. In 1988, the first adoptive transfer was performed at the Surgery Branch of the National Institutes of Health (NIH), where TILs transplanted into patients with metastatic melanoma showed objective regression in tumors [108, 109]. However, initial responses were short term and transferred cells could barely be detected in circulation. A major improvement in the therapeutic efficacy was observed in patients who received lymphodepletion using non-myeloablative chemotherapy, before adoptive transfer [110]. In some lymphodepleted patients, infused cells represented up to 80% of CD8+ T-cells in circulation several months after infusion. Lymphodepletion reduced inhibitory factors, allowed infused cells to proliferate and avoided competition for growth factors, such as, IL-2 and other important cytokines [111].

Adoptive transfer of TILs showed clinical success in melanoma by demonstrating tumor regression in 20 to 25% of patient population [112, 113]. This effect was most probably governed by T-cells that targeted mutant peptides which are generated by de novo somatic mutations, and known as neoepitopes. Recently, a study used T-cells targeting the driver of mutations in cancer; “KRAS” oncogene, that is known to carry “hot spot” mutations in several forms of cancer, contributing to their progression [114]. The authors used cytotoxic T-cells targeting the most frequent mutation in the KRAS (KRAS G12D) that was identified in almost 45% of pancreatic cancers and 13% of colorectal cancers. In a 50 year old patient with metastatic colorectal cancer, the authors reported objective regression of all seven lung metastases after infusion of four different clonotypes of T-cells that were isolated from the TILs of the patient and specifically targeted KRAS G12D [114].

There are several limitations associated with the TILs approach. Firstly, not every tumor is resectable. Secondly, of the resectable tumors, not all show good number of TILs that can be isolated. Thirdly, it is not sure if isolated TILs are efficacious enough to recognize tumor or if they can be expanded *in vitro* [102]. In the TILs approach, T-cells are expanded in high doses of IL-2 and IL-2 is administered further into the patients receiving adoptive transfer, with severe toxicities consequently. After isolation, TILs are tested for reactivity against tumor in an IFN-γ assay. Only reactive cells are expanded and infused into the patient, although there has not been a clear correlation between the IFN-γ secretion and clinical response [115]. Since it is not always possible to regulate the quality and quantity of TILs that can be isolated, new approaches have been developed involving genetic engineering of T-cells to express anti-tumor receptors, such as recombinant T-cell receptor (TCR) or Chimeric Antigen Receptor (CAR).

2.4.2 Genetically engineered T-cells

Genetic modification allows to manipulate antigenic specificity of T-cells, thereby re-directing them to specifically target tumor associated antigens (TAAs). T-cells of any specificity can be isolated from peripheral blood, and engineered to express a recombinant T-cell receptor (TCR) or a chimeric antigen receptor (CAR) which redirect their specificity to target tumor cells.

2.4.2.1 TCR transduced T-cells

The tumour-specific TCR α and β chains are identified, isolated and cloned into vectors and transduction of T-cells is performed to generate tumour-reactive T-cells. To generate a recombinant TCR, an appropriate target antigen sequence needs to be identified. This can be isolated from a rare tumor-reactive T-cell or, otherwise alternative techniques can be employed to generate highly active anti-tumor T-cells. One method is to immunise transgenic mice that co-express the human leukocyte antigen (HLA) system with human tumour proteins to generate human T-cells expressing TCRs against tumor antigens [116]. Another approach is called allogeneic TCR gene transfer, in which tumour-specific T-cells are isolated from patient experiencing remission and the isolated TCR sequences are transferred to T-cells from another patient who shares the disease but is non-responsive [117, 118]. Finally, *in vitro* manipulation can be done to alter TCR sequence, enhancing their anti-tumor activity by increasing the strength of the interaction (avidity).

The first successful clinical trial using recombinant TCR was performed in 2006, where TCR transgenic T-cells targeting MART-1 demonstrated significant tumor regression [119]. Because the recombinant TCR is restricted to a certain HLA allele, this limits the therapy to only certain HLA-matched patients. On the other hand, one benefit of TCR gene therapy is that it can be used to also target intracellular antigens presented by HLA molecules.

2.4.2.2 Chimeric Antigen Receptor (CAR) transduced T-cells – "Redirected T-cells"

CARs are recombinant receptors that combine antigen recognition of an antibody with T-cell activating function [120]. The structure of CAR consists of three moieties; an extracellular domain derived from single-chain variable fragment (scFv) of the antibody which binds to a specific tumor antigen, a transmembrane domain and an intracellular signalling domain comprising of the signal-transduction component of the T-cell receptor (e.g., CD3ζ or FcεRIγ) and a costimulatory receptor (e.g., 4-1BB, CD28, or OX40) [121]. Signal transduction through the intracellular domain of the CAR induces persistence, trafficking and effector functions in transduced T-cells. Unlike TCR, CAR can recognize antigen independent of MHC. Thus, CARs can be generated against a wide range of cell surface targets including, proteins, carbohydrates, and glycolipids [122]. The first generation CARs include T-cell activation domain CD3ζ or FcRγ in intracellular motif, thus inducing only transient T-cell activation [123, 124]. Although the first generation CARs showed anti-tumour responses, they failed to expand *in vivo* because of lack of co-stimulation [123]. Thus, the second and third generation CARs were developed which include one or more costimulatory domains (CD28, 4-1BB, or OX40) in addition to a T-cell activation domain (**figure 2-15**) [125].

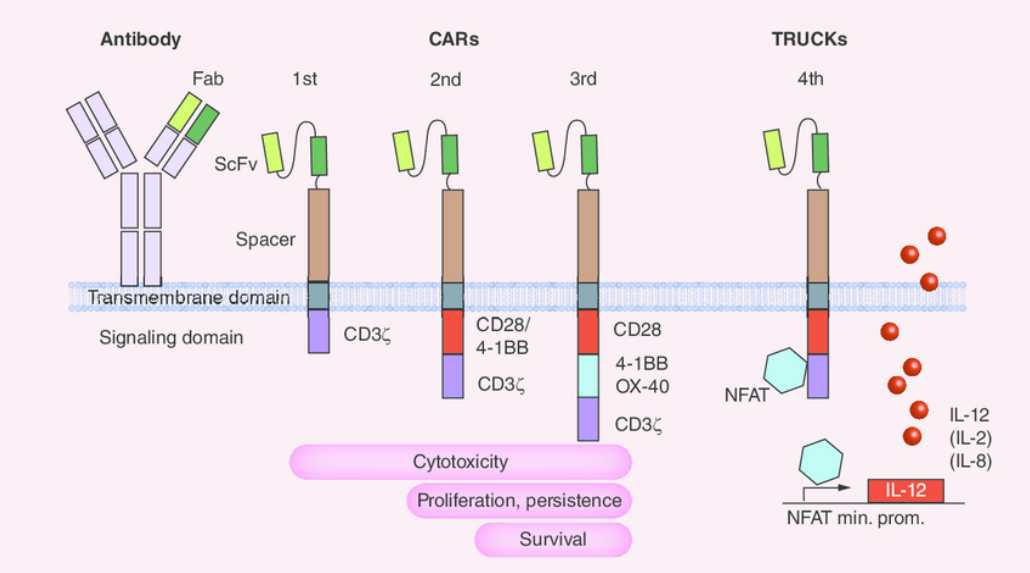

Figure 2-15. Different generations of Chimeric antigen receptor (CAR) constructs. First-generation CARs contain solely the T-cell activation domain (CD3ζ or FcRγ). Second-and third-generation CARs consist of one or two additional costimulatory signaling domains (CD28, CD27, OX40, 4-1BB), respectively. Co-stimulation enhances the overall survival, proliferation and cytotoxicity of activated T-cells. Fourth generation CARs, also known as TRUCKs are genetically modified to express CARs along with an inducible cytokine gene cassette driven by an NFAT sensitive promoter. Consequently, immune stimulatory cytokines such as IL-12 are secreted upon CAR engagement. *(Adapted from Kalaitsidou, M., et al., Immunotherapy, 2015 [125]).*

The addition of co-stimulatory signal contributed to enhanced expansion, antitumor activity, and cytokine secretion (such as IL-2, TNF-α, and IFN-γ) by CAR-T cells [126]. Besides this, recently fourth generation CARs, also

known as “TRUCK” T-cells have been introduced by some studies [127]. The fourth generation CARs have additional genetic modification and contain inducible expression of genes such as proinflammatory cytokines (IL-12) or T-cell co-stimulatory ligands (4-1BB-L). Binding of CAR to its target antigen, can release these transgenic proteins which further aid to the T-cell response generated. Cytokines like IL-12 can further increase activation level of CAR-T cells and activate other innate immune cells. The transgenic cytokine is produced only when signal through CAR-T cells is induced. Compared to the first three generations, the ‘TRUCK’ T-cells provided more advantages on affecting local suppressive cells and were able to cause more anti-tumour destruction [121].

The CAR constructs are transfected into T-cells using recombinant plasmids or viral vectors, which directs specificity of T-cells towards the target antigen recognized by CAR. Thus, CAR harbouring T-cells are termed as “redirected” T-cells. CARs have also been constructed to target specific peptides bound to HLA molecules, thereby allowing targeting of intracellular molecules [121]. Antigen recognition and activation through the CAR, initiates redirected T-cell mediated cytotoxicity through methods described above.

2.4.2.2.1 CAR-T cells in clinical trials

For translating CAR therapy in clinics, it is important to have a potent CAR and a suitable target antigen expressed selectively on tumor cells and absent from other vital cells. In clinical trials, CD19 has been the most widely exploited target tumour antigen in haematological cancers. CD19 was considered as an ideal target in B-cell malignancies based on its high and uniform expression on B cells in most lymphomas and leukemias and its established role in signalling tumor cells [128-130]. Furthermore, CD19 is not shed into circulation, which prevents off-target adverse effects [131]. The first *in vivo* study in 2003, using CD19 CARs demonstrated complete eradication of systemic lymphoma in immunodeficient mice following a single infusion of CAR-T cells [132]. This study provided the foundation and rationale for further clinical studies.

CD19 CAR cells have been exploited in several clinical trials [133]. As expected, most of these trials using CD19 CARs induced B cell aplasia [134-138], however this condition is clinically manageable. Remarkably, this condition could in fact benefit the therapy in a way that B cell elimination would prevent the emergence of anti-CAR antibodies [139], which were reported in other CAR-T cell trials [140, 141]. Using CD19 CAR-T cells in clinical trials, several groups have reported promising results in different B cell malignancies including, diffuse large B cell lymphoma [134], non-Hodgkin lymphoma (NHL) [142], multiple myeloma (MM) [143], chronic lymphocytic leukemia (CLL) [144] and acute lymphoblastic leukemia (ALL) [145]. These studies focussed on relapsed, chemotherapy refractory patients, and employed predominantly CD28 and 4-1BB CARs. Despite of variation in disease condition, ScFv, transduction methods, manufacturing processes, all studies reported high rates of overall and complete response, especially in ALL, where complete remission (CR) rates of >90% are observed [131, 139]. CR rates range from 23% to 50% in CLL and 47% to 100% in NHL [131]. Apart from CD19, other targets have been investigated in haematological malignancies, such as, CD20, CD33, B-cell maturation antigen. **Table 2-2** illustrates completed clinical trial using CAR-T cells in haematological malignancies [1]. Most of the CAR-T

cell trials have employed autologous T-cells derived from the patient. However, recently, allogeneic anti-CD19 CAR-T cells were investigated in ALL, CLL and NHL patients [146]. Of the 20 patients treated with allogeneic CAR-T cells, 40% achieved CR or partial response.

2.4.2.2.2 Toxicities reported in clinical trials

Lymphodepleting conditioning regimens and total body irradiation, are often administered before the infusion of CAR-T cells, allowing for greater T-cell expansion [131]. The major toxicity associated with CAR-T cell infusions is cytokine release syndrome (CRS), a potentially lethal systemic inflammatory adversity [147]. CRS is a result of intense tumor killing response generated by high number of activated lymphocytes, including, B cells, T cells and NK cells. It happens when adoptive transfer of CAR-T cells result in secretion of cytokines to a level which is several hundred times higher than baseline levels. CRS is typically characterized by high fever hypotension and neurological changes, and when uncontrolled, can lead to organ failure [148]. Some studies have used a fractionated CAR-T cell dose to minimize CRS mediated toxicity [131]. The second major toxicity is "on target, off tumor" effect which is observed when the target antigen (for CAR) is expressed on normal tissues [121]. For example, a clinical trial using CAR-T cells targeting human epidermal growth factor receptor 2 (HER2), also known as ERBB2 was put to halt after death of the first patient [149]. Within 15 minutes after administration of 10^{10} HER2 specific CAR-T cells, the patient experienced respiratory distress, and showed a dramatic pulmonary infiltrate. The patient died after 5 days and her serum samples showed marked increase in cytokine levels, such as, IFN-γ, granulocyte-macrophage colony stimulating factor (GM-CSF), TNF-α, IL-6 and IL-10, correlating to a cytokine storm. The investigators also concluded that the high dose of CAR-T cells localized to lung after administration and triggered cytokine release by recognition of low levels of HER2 expressed on lung epithelial cells [149].

Apart from this, CAR-T cells can also lead to tumor lysis syndrome [122] which involves similar symptoms as CRS. The quick onset and progression of such adversities require rapid detection and further interventions to reduce treatment related mortality. Other toxicities of CAR T-cell therapy include, neutropenia, infection, neurotoxicity, diarrhoea and nausea [120].

2.4.2.2.3 CAR-T cells in solid tumors

CAR-T cells against several target antigens in solid tumor are being tested in clinical trials (**Table 2-3**). Until now, most positive trials reported have used anti-IL-13Rα2 CARs in glioblastoma (1 patient with tumor regression) [150], anti-CEA CARs in liver metastases (1 patient with stable disease) [151], anti-GD2 CARs to target neuroblastoma (3 out of 11 patients with complete remissions) [152] and anti-HER2 CARs for sarcoma (4 out of 17 patients showed stable disease) [153]. There are several barriers that limits the success of this therapy in solid tumors. Firstly, it is difficult to find antigens that are specifically and uniformly expressed on tumor. Unlike

in hematologic malignancies, CAR-T cells must be able to traffic from circulation into solid tumor sites despite defective chemokine signals. They must then efficiently infiltrate the tumor stroma to generate tumor antigen specific cytotoxicity, regardless of heterogeneity. Even after successfully reaching tumor, T-cells can become dysfunctional due to unfavourable tumor microenvironment characterized by nutritional depletion, acidic pH, oxidative stress and hypoxia; presence of inhibitory molecules and cytokines; immune suppressive cells, such as Tregs, myeloid derived suppressor cells (MDSCs) and tumor associated macrophages; and other negative regulatory mechanisms, such as upregulation of cytoplasmic and surface inhibitory receptors [154].

2.4.2.2.4 Combinatorial approach: checkpoint blockade with CAR-T cells

The first proof of concept showing improved anti-tumor efficacy of CAR-T cells when combined with PD-1 blockade was established in 2013. In a study by John et. al. using Her2+ tumor bearing mice, it was shown that CAR-T cells with anti-PD-1 blockade showed significantly improved anti-tumor activity [155]. The remarkable tumor regression in this model was followed by reduced infiltration of myeloid derived suppressor cells (MDSCs) in the tumor microenvironment. Another study conducted by Moon and colleagues, showed augmented expression of PD-1 on CAR TILs which corresponded to reduced function in a mesothelioma model [156]. Further, blocking PD-1 could restore mesothelin-directed CAR-T cell cytotoxicity *in vitro*.

Aside from monoclonal antibodies, some studies involved genetic engineering strategies to block PD-1. One approach is the generation of CARs incorporating cell-surface dominant negative receptors (DNRs) which can override the inactivating signals in the tumor microenvironment. DNRs consist of extracellular region of a membrane receptor and generally contain a mutation in the intracellular chain, resulting in an absence of downstream signal transduction and subsequent loss of function [157]. In this way, DNRs are mostly able to compete with their endogenous receptors for binding to target ligands. Cherkassky et al showed that combining CAR T-cells with the expression of a dominant negative form of PD-1 led to increased persistence, higher antitumor effects and prolonged survival in a mesothelioma xenograft model [158]. Further, it was shown that CAR T-cells with 4-IBB costimulatory domain could function at lower doses compared to CAR-T cells with CD28 signaling domains, and 4-1BB CARs were more resistant to PD-1 mediated exhaustion.

Another approach to circumvent checkpoint inhibition is by generating switch receptor. Switch receptors contain the extracellular portion of an antibody specific for an inhibitory receptor, such as PD-1, fused to an intracellular signalling molecule, such as CD28, which reinforces the effector function of the cell [159, 160]. The resulting CAR construct function as “dominant negative” by competing with endogenous PD1. Additionally, it provides an active signalling through the cytoplasmic domain after PD-L1 binding. Liu et. al. inserted the PD-1-CD28 switch-receptor into CAR vectors [160]. This receptor was introduced by Prosser and colleagues [161] and contains the extracellular domain of PD-1 fused to the transmembrane and signalling domains of CD28 co-receptor. The PD-1-CD28 CAR T-cells were tested in xenograft models of established mesothelioma and prostate cancer. The authors reported a significant increase in the frequency of CAR-T cells

infiltrating tumors and peripheral blood, a higher *ex vivo* anti-tumor function, and pronounced cytokine secretion. Interestingly, they also observed reduced levels of other checkpoint inhibitors; LAG3, TIM-3 and CEACAM1 expression and an increase in IL-2 signalling. Remarkably, the replacement of the switch-receptor with a mutant signaling domain abrogated these results, suggesting a central role for the CD28 costimulatory domain in the fusion construct.

Another recent study generated CAR-T cells capable of secreting anti-PD-L1 antibodies [162]. Using a humanized renal cell carcinoma mouse model, the authors showed that secretion of anti-PD-L1 antibodies from CAR-T cells significantly reduced tumor growth and increased migration of adoptively transferred human NK cells into the tumor. These NK cells demonstrated an anti-tumor activity through ADCC and by providing IFN-γ stimulation to $CD8^+$ T-cells. Lately, CRISPR/Cas9 mediated gene editing was used to disrupt PD-1 in CD19 targeting CAR-T cells. These PD-1 lacking CAR-T cells demonstrated enhanced anti-tumor activity *in vitro* and *in vivo* [163].

Overall, these research evidences indicate that checkpoint blockade holds promise to alleviate the effects of immunosuppression in the tumor microenvironment and can boost the cytotoxic function of CAR-T cells.

2.5 Humanized mice

Preclinical testing in cancer research involves transplanting human xenografts into murine hosts to investigate tumor development and efficacy of anti-cancer therapeutics [164]. Co-transplantation of human immune elements allow to study interaction of immune system and its effect on tumor development. To achieve this, immune-compromised NOD/SCID/IL2Rγnull (NSG) mice are routinely used due to their ability to take up human xenografts, including cancer cells. NSG mice carry mutations which are characterized by impaired B cell, T cell, NK cell and lymph node development [165].

Despite large efforts to reduce variability, 80% of the drug candidates that show promising results in animal models, fail to demonstrate efficacy when tested in humans [166]. This is predominantly due to differences between humans and mice in terms of organ physiology, cellular dynamics and regulatory proteins [167, 168]. Thus, one of the prime interest in translational studies is to make the model organism more human like, such as humanization of the mouse model [169]. A humanized mouse is a murine host containing human components to an extent that a graft versus host disease (GvHD) is not triggered when transplanting human xenografts [164]. The two predominant approaches to generating humanized mice are; incorporating human transgenes through genetic engineering or transplantation of functional human immune cells, tissues and organs in mice [170].

NSG mice show multi-lineage hematopoietic cell engraftment after transplantation of human hematopoietic stem cells [171]. One method is to transplant human PBMCs. This method leads to stable engraftment of activated T-cell populations. However, the engrafted mice usually develop xenogenic GvHD after a few weeks and this effect is enhanced when mice are irradiated prior to engraftment [172]. A more

sophisticated method is transplantation of human hematopoietic stem cells (HSCs) in mice. HSCs can be obtained from cord blood, fetal liver, bone marrow or peripheral blood [173]. After three months of transplantation, almost 60% of the PBMCs in mouse blood appear to be of human origin. Further, B and T cells make up to 45% each, of the peripheral PBMCs, with the majority of T-cells being $CD4^+$, NK cells frequency is around 5% and the rest of the immune compartment is composed of monocytes (3%) and DCs (2%) [174].

The technological approaches are diverse and the efficiency of engraftment in mice depends on source of HSCs, isolation conditions, culture conditions, engraftment route etc [175-177]. For example, cord blood derived HSCs showed higher engraftment potential in NSG mice, compared to adult bone marrow derived cells irrespective of the route of engraftment; intrafemoral, intravenous or intrahepatic [175]. Often, neonatal mice are used and intrahepatic route of administration is recommended [177], since liver is the main hematopoietic organ at birth [178].

In a more complex approach, genes for human HLA antigens or human cytokines that are necessary for optimal function and maintenance of human immune cells, such as; GM-CSF, IL-2, IL-7, SCF, are incorporated into the mouse genome [164]. Another popular method is knock out of genes that encode for murine MHC class I or class II [164]. These techniques are aimed to enhance the human innate and adaptive immunity in the murine host, reduce the risk of GvHD and support the development of human HLA-restricted T-cells [179]. A third more advanced method is the bone-liver thymus (BLT) model. In this approach, fetal liver and thymus tissue are implanted under the kidney capsule and autologous HSCs are co-transplanted in mice [180, 181]. The fetal tissues develop a functional humanized organoid. MHC molecules expressed by the implanted human tissues allows for selection process of human lymphocytes. This results in the development of human T-cells that can generate an antigen-specific immune response. Studies using BLT model, reported a higher engraftment rate of human immune cells in the peripheral blood than in any other model [180, 181].

Despite several advantages, there are certain limitations of the humanized mouse models which limits their applicability. Firstly, the percentage distribution of reconstituted human B and T cells and myeloid cells in humanized mice is very different than what is found in humans. The reconstituted human immune cells in the blood of humanized mice are predominantly B cells with only a very little proportion of myeloid cells, while in humans, myeloid cells form the highest fraction in blood [182]. Secondly, the established adaptive immune system is naïve and an appropriate antigen-mediated T-cell response is not possible since human T-cells cannot be educated by HLA restriction in mouse thymus [182]. Thirdly, the B cells that develop in murine host are immature and do not undergo isotype switching from IgM to IgG after immunization or infection [183]. Lastly, there is a risk of GvHD caused by de novo generated T-cells [164].

Overall, humanized mice provide a preclinical platform that is more close to humans and continue to improve our understanding of relevant biological processes that can be exploited further by anti-cancer therapeutics.

2.6 Aims and outline of this thesis

Recently, monoclonal antibodies targeting negative immune regulators (immune checkpoint molecules), such as PD-1, have demonstrated significant success in treating a variety of malignancies. However, only 20-40% of the patients achieve clinical response to checkpoint inhibitors, indicating that the non-responding patients may not have the cellular repertoire to fight cancer. A potential solution to this problem can be co-infusion of T-cells specifically targeting tumor associated antigens. In this study, we sought to examine whether a combined immunotherapeutic approach involving blockade of PD-1 signalling along with infusion of tumor specific CAR-T cells could provide enhanced anti-tumor benefit.

As outlined in the introduction above, CAR-T cells have shown remarkable clinical success, especially in CD19 clinical trials. These trials employed CARs which varied not only in specificity, but also in the co-stimulation that was conferred upon antigen binding. Co-stimulation can have a tremendous impact on the survival of CAR-T cells, for example, CAR-T cells with CD28 co-stimulation showed survival of 1 to 3 months [184] , while CARs with 4-1BB co-stimulation showed prolonged survival which exceeded to 4 years in some patients [185]. However, these are findings from different trials performed under different settings. Till date, it remains unclear as to if a particular co-stimulatory signal is better over the other, with respect to performance of redirected T-cells. The long term success of this therapy lies in generating redirected T-cells that can efficiently expand, persist and specifically target tumor cells without generating toxic effects in the host. There is currently little understanding of if and how CAR structure can influence these properties.

So far, immune-compromised mice have been predominantly exploited in redirected T-cells studies. Such a model can only give a superficial view on performance of redirected T-cells, since these mice lack other human immune cells, which provide important immune interactive signals that can have consequences on long-term immunological control of cancer. A humanized mouse model, which provide in part a human immune environment, can provide a better understanding of interplay between redirected T-cells and other human immune cells. It also mimics the human situation more closely. Thus, the aims of this thesis are:

1. To establish a humanized mouse model for studying autologous CAR redirected T-cells.
2. To study the effect of different co-stimulation on the phenotype, proliferation and anti-tumor efficacy of redirected T-cells.
3. To test survival and anti-tumor efficacy mediated by redirected T-cells in synergy with PD-1 blockade in a humanized mouse host.

We have designed CARs comprising of either CD28, Δ-CD28 (lacks Lck signaling through CAR) and 4-1BB co-stimulation and compared their proliferation, survival and anti-tumor efficacy *in vitro* and in humanized mouse model in combination with PD-1 blockade.

Table 2-2. Summary of reported CAR-T cell trials in haematological malignancies *(Adapted from Kenderian S. et. al. Biol. Blood Marrow Transplant, 2017 [1])*

Malignancy	Center	Target	No.	CAR	Vector	Disease	Results	Role of HCT	Chemotherapy	Notes
CLL	FHCRC [41, 42]	CD19	6	41BB-ζ	LV	CLL	CR, 3/6 (50%); PR, 1/6 (17%)	N/A	Two cohorts: Cy and Flu/Cy	FLU/CY improved persistence and CR
	MDACC [28]	CD19	2	28-ζ	SB	CLL	Responses not reported for each disease type	N/A	N/A	
	NCI [17]	CD19	4	28-ζ	RV	CLL	CR, 3/4 (75%); PR, 1/4 (25%)	None	Flu/Cy	
	NCI [62,81]	CD19	5	28-ζ	RV	CLL post–allo-HCT	CR, 1/5; PR, 1/5	Allo-CART cells to treat relapse post- HCT	None	No GVHD
	UPenn [14]	CD19	14	41BB-ζ	LV	CLL	CR, 4/14 (28.5%); PR, 4/14 (28.5%)	No relapse if patient achieves CR	Flu/Cy (n = 3); pento/CY (n = 5); Benda (n = 6)	Two developed CD19 negative Richter
ALL	China (multicenter) [18]	CD19	50	28-41BB-27-ζ		ALL	CR, 94.3% when blasts <50%; 66.7% when blasts >50%	N/A	Variable	
	MDACC [28]	CD19	42	28-ζ	SB	Adjuvant post–allo-HCT (10); relapse (8)	Adjuvant trial: CR, 3/10 (30%); relapse trial: CR, 3/13 (23%, for all diseases)	N/A	N/A	
	MSKCC [57]	CD19	46	28-ζ	RV	Adult ALL	83% CR rate	12 patients underwent HCT	Cy	No differences in outcomes whether or not HCT was done
	NCI [82]	CD19	21	28-ζ	RV	Children and young adult ALL	CR (ITT): 61%; OS, 51% at 6 mo; DFS, 78.8% at 6 mo CR: 13/16 (81%) in low burden (<25% blasts); 10/22 (46%) in high burden	17/20 patients with MRD-negative disease went to HCT	Flu/Cy	No relapses after HCT; 2/3 patients with no HCT relapsed with CD19-negative disease
	NCI [62,81]	CD19	5	28-ζ	RV	ALL relapse post-HCT	4/5 patients with MRD-negative CR	Allogeneic CARTs to treat relapses post- HCT	None	No GVHD
	Swedish (2-center) [100]	CD19	2	28-41BB-ζ	RV	ALL	CR, 6/11 (55%, for all diseases)	N/A	Flu/Cy	One patient developed CD19-negative relapse
	UPenn/CHOP [58]	CD19	53	41BB-ζ	LV	Children and young adults ALL	CR, 50/53 (94%); EFS, 70% at 6 mo and 45% at 12 mo; OS, 78% at 12 mo; 20 relapsed, 13/20 (65%) with CD19-negative disease. CART persisted for 3-39 mo	6/29 patients in CR received HCT	Flu/Cy	Of the 20 relapsed patients, 3 had HCT after CART19
NHL	NCI [50]	CD22	6	41BB-ζ	LV	R/R ALL, children and young adults	MRD-negative CR: 1/6 (33%); SD, 2/6 (67%)	N/A	Flu/Cy	5 patients had a CD19 negative relapse at enrollment
	City of Hope [43,65]	CD19	16	NHL1: ζ NHL2: 28-ζ	LV	NHL (adjuvant after HCT)	NHL1: CR, 5/8 (63%); PFS, 50% at 2 yr NHL2: CR, 8/8 (100%); PFS: 100% at 6 mo	CART cells given after auto-HCT	High-dose chemotherapy and HCT	NHL1: $CD8^+$ Tcm NHL2: Tcm (CD4 and CD8)
	FHCRC [41,42]	CD19	28	41BB-ζ	LV	NHL	CY cohort: CR, 1/12 (8%); PR, 5/12 (42%) FLU/CY cohort: CR, 5/12 (42%); PR, 3/12 (25%)	N/A	Two cohorts: Cy and Flu/Cy	FLU/CY improved persistence and CR
	MDACC [28]	CD19	17	28-ζ	SB	17 NHL	Adjuvant trial, CR, 4/5 (80%); relapse trials, CR, 3/13 (23%, for all diseases)	Allogeneic CARTs to treat relapse post HCT	N/A	No GVHD
	MSKCC [66]	CD19	8	28-ζ	RV	NHL after HCT	CR, 5/8; PD, 2/8; NRM, 1/8	CARTs were given after auto-HCT	High-dose chemotherapy and HCT	
	NCI [17]	CD19	15	28-ζ	RV	Lymphoma, adults	85.6% CR in DLBCL, 100% in indolent lymphoma	None	Flu/Cy	
	NCI [62,81]	CD19	10	28-ζ	RV	5 MCL, 5 DLBCL	MCL: PR, 1/5; DLBCL: CR, 1/5	Allogeneic CARTs to treat relapses post HCT	None	No GVHD

Table 2-2. Continued

Malignancy	Center	Target	No.	CAR	Vector	Disease	Results	Role of HCT	Chemotherapy	Notes
	Swedish (2-center) [100]	CD19	9	28-41BB-ζ	RV	Lymphoma	CR, 6/11 (55%, for all diseases)	N/A	Flu/Cy	One patient developed CD19 negative relapse
	UPenn [64]	CD19	38	41BB-ζ	LV	Adult NHL (19 DLBCL, 8 FL, 2 MCL)	CR: 54% in DLBCL, 100% in FL, 50% in MCL; PFS: 62% at 10 mo (DLBCL, 54%; FL, 100%)	N/A	Benda (6), Cy (11), Flu/Cy (1), EPOCH (3), radiation/Cy (3)	
	FHCRC [49]	CD20	4	28-41BB-ζ	LV	NHL	PR, 1/4 (25%); 2/4 (50%) remained in remission	N/A	Cy	CART20 was used in consolidation or treat residual disease
MM	UPenn [67]	CD19	1	41BB-ζ	LV	MM	Stringent CR	CARTs were given after auto-HCT	High-dose chemotherapy and HCT	Rationale is to target myeloma stem cell
	NCI [51]	BCMA	11	28-ζ	RV	R/R MM (median regimens, 7)	1/6 on dose level 2 VGPR, 2/6 on dose level 2 SD; 1/2 highest-dose CR	N/A	Flu/Cy	Improved responses in higher-dose cohort
AML	Peter MacCallum Cancer Centre [101]	LeY	4	28-ζ	RV	R/R AML	Transient cytogenetic CR, 1/5 (20%); transient reduction in blasts, 1/5 (20%); SD, 2/5 (40%)	None	Flu/Cy	CARTs were detected in sites of extramedullary disease
	PLA general hospital [53]	CD33	1	41BB-ζ	RV	R/R AML	Transient reduction in blasts	None	None	Patient developed CRS and transient hyperbilirubinemia
	Zhejiang University [54]	CD123	1	28-41BB-27-ζ	LV	R/R AML	Transient reduction in blasts	None	Cy	Patient developed CRS
HL	Baylor [52]	CD30	9	28-ζ	RV	7 HL, 2 ALCL	CR, 1/9 (11%); PR, 1/9 (11%), SD, 4/9 (44%); PD, 3/9 (33%)	N/A	None	None

FHCRC indicates Fred Hutchinson Cancer Research Center; MDACC, M.D. Anderson Cancer Center; MSKCC, Memorial Sloan Kettering Cancer Center; NCI, National Cancer Institute; UPenn, University of Pennsylvania; CHOP, The Children's Hospital of Philadelphia; LV, lentiviral; RV, retroviral; SB, Sleeping Beauty; CLL, chronic lymphocytic leukemia; ALL, acute lymphoblastic leukemia; NHL, non-Hodgkin lymphoma; DLBCL, diffuse large B cell lymphoma; MCL, mantle cell lymphoma; FL, follicular lymphoma; AML, acute myelogenous leukemia; HL, Hodgkin lymphoma; MM, multiple myeloma; ALCL, anaplastic T cell lymphoma; R/R, relapsed refractory; CR, complete response; PR, partial response; SD, stable disease; PD, progressive disease; VGPR, very good partial response; EFS, event free survival; PFS, progression-free survival; DFS, disease-free survival; MRD, minimal residual disease; OS, overall survival; CART, chimeric antigen receptor T cells; HCT, hematopoietic cell transplantation; Flu, fludarabine; Cy, cyclophosphamide; NRM, nonrelapse mortality; Tcm, central memory T cells; GVHD, graft-versus-host disease; CRS, cytokine release syndrome.

Table 2-3. Completed and ongoing clinical trials with CAR-T cells in solid tumors. ***(Data compiled from www.clinicaltrials.gov)***

Target	Trial and phase	Status	Age	No of patients	Institution	Disease	Outcomes
CD133	NCT02541370 Phase I	Recruiting			Chinese PLA General Hospital, China	CD133 positive malignancies	
CD133	NCT02541370 Phase I	Recruiting	18 - 70	20	Chinese PLA General Hospital, China	Refractory advanced malignancies	
CD171	NCT02311621 Phase I	Recruiting	≤ 18	80	Seattle Children's Hospital, USA	Neuroblastoma	
CD70	NCT02830724 Phase I/II	Not yet open	18 - 70	113	National Cancer Institute (NCI), USA	CD70+ cancers	
CEA	NCT01373047 Phase I	Completed	≥ 18	6	Roger Williams Medical Center, USA	Liver metastases	Safe and feasible. No grade 3 or 4 adverse events, 1 patient with stable disease 23 months post infusion and 5 patients died due to progressive disease, increased liver metastasis in 4 out of 6 patients
CEA	NCT02349724 Phase I	Recruiting	18 - 80	75	Southwest Hospital China	Lung, colorectal, gastric, breast, pancreatic cancer	

Target	Trial and phase	Status	Age	No of patients	Institution	Disease	Outcomes
CEA	NCT02416466 Phase I	Ongoing	≥ 18	8	Roger Williams Medical Center, USA	Liver metastases	
CEA	NCT02850536 Phase I	Not yet open	≥ 18	5	Roger Williams Medical Center, USA	Liver metastases	
cMet	NCT01837602 Phase I	ongoing	all	15	Abramson Cancer Center of the University of Pennsylvania, USA	Triple negative breast cancer, metastatic breast cancer	
EGFR	NCT02873390 Phase I/II	Recruiting	18 - 65	20	Ningbo Cancer Hospital, China	EGFR positive solid tumor	
EGFR	NCT02862028 Phase I/II	Recruiting	18 - 65	20	Shanghai International Medical Center, China	EGFR positive solid tumor	
EGFR	NCT02331693 phase I	Recruiting	18 - 70	10	Renji Hospital, China	Glioma	
EGFR	NCT01869166 Phase I/II	Recruiting	18 - 80	60	Chinese PLA General Hospital	NSCLC	
EGFRvIII	NCT02844062 phase I	Recruiting	18 - 70	20	Beijing Sanbo Brain Hospital	Glioma	
EGFRvIII	NCT01454596 Phase I/II	Recruiting	18 - 70	107	National Cancer Institute (NCI)	Glioma	
EGFRvIII	NCT02209376 Phase I	Active, not recruiting	≥ 18	12	University of Pennsylvania/ University of California	Glioma	
EGFRvIII	NCT02664363 Phase I	Recruiting	18 - 80	48	Duke University Medical Center	Glioma	
EpCAM	NCT02915445 Phase I	Recruiting	18 - 65	30	Sichuan University, China	Nasopharyngeal carcinoma and breast cancer	

Target	Trial and phase	Status	Age	No of patients	Institution	Disease	Outcomes
EpCAM	NCT02725125 Phase I/II	Recruiting	≤ 75	19	Sinobioway Cell Therapy Co., Ltd., China	Stomach neoplasms	
EpCAM	NCT02729493 Phase I/II	Recruiting	≤ 75	25	Sinobioway Cell Therapy Co., Ltd., China	Liver neoplasms	
EphA2	NCT02575261 Phase I/II	Recruiting	18 - 80	60	Fuda Cancer Hospital, Guangzhou, China	EphA2+ malignant glioma	
FAP	NCT01722149 Phase I	Recruiting	18 - 75	6	University of Zurich	Malignant pleural mesothelioma	
GD2	NCT00085930 Phase I	Completed		11	Baylor College of Medicine	Neuroblastoma	Safe and feasible, 3 out of 11 patients in CR
GD2	NCT02439788 Phase I	Not yet open	1 - 18	18	Baylor College of Medicine	Neuroblastoma	
GD2	NCT01822652 Phase I	Ongoing	all	11	Baylor College of Medicine	Neuroblastoma	
GD2	NCT02765243 Phase II	Recruiting	1 - 14	30	Zhujiang Hospital, China	Relapsed or refractory neuroblastoma	
GD2	NCT01953900 Phase I	Recruiting	1	26	Baylor College of Medicine	GD2+ Sarcoma	
GD2	NCT02761915 Phase I	Recruiting	≥ 1	27	Cancer Research UK	Relapsed or refractory neuroblastoma	
GD2	NCT02919046 Phase I/II	Recruiting	1 - 14	22	Sinobioway Cell Therapy Co., Ltd., China	Relapsed or refractory neuroblastoma	
GD2	NCT02107963 Phase I	Recruiting	1 - 35	72	National Cancer Institute (NCI)	Sarcoma, osteosarcoma, neuroblastoma, melanoma	

Target	Trial and phase	Status	Age	No of patients	Institution	Disease	Outcomes
GPC3	NCT02395250 Phase I	Recruiting	18 - 70	20	RenJi Hospital, China	Advanced HCC	
GPC3	NCT02715362 Phase I/II	Recruiting	18 - 69	30	Shanghai GeneChem Co., Ltd., China	Advanced HCC	
GPC3	NCT02723942 Phase I/II	Recruiting	18 - 70	60	Fuda Cancer Hospital, Guangzhou, China	GPC3+ HCC	
GPC3	NCT02905188 Phase I	Not yet open	≥ 18	14	Baylor College of Medicine	HCC	
GPC3	NCT02876978 Phase I	Recruiting	18 - 70	20	Carsgen Therapeutics, Ltd., China	Recurrent or refractory lung squamous cell carcinoma	
HER2	NCT02713984 Phase I/II	Recruiting	18 - 80	60	Southwest Hospital, China	HER2 positive cancer	
HER2	NCT01935843 Phase I/II	Recruiting	18 - 80	10	Chinese PLA General Hospital	HER2 positive cancer	
HER2	NCT02547961 Phase I/II	Recruiting	18 - 80	60	Fuda Cancer Hospital Guangzhou	Breast cancer	
HER2	NCT02442297 Phase I	Recruiting	≥ 18	14	Baylor College of Medicine	Glioma	
HER2	NCT01109095 Phase I	Active, not recruiting	all	16	Baylor College of Medicine	Glioma	
HER2	NCT00889954 Phase I	Active, not recruiting	≥ 3	19	Baylor College of Medicine	HER2 positive cancer	
HER2	NCT00924287 Phase I/II	Completed	≥ 18	1	National Cancer Institute (NCI)	HER2 positive sarcoma	Trial terminated after death of first patient due to cytokine storm

Target	Trial and phase	Status	Age	No of patients	Institution	Disease	Outcomes
HER2	NCT00902044 Phase I/II	Recruiting	all	19	Baylor College of Medicine	HER2 positive sarcoma	No toxicities, 4 patients with stable disease from 12 weeks to 14 months
IL-13Rα2	NCT02208362 Phase I	Recruiting	18 - 75	total 100, 1 patient reported so far	City of Hope Medical Center	Glioblastoma	Fractionate -d dose of CAR-T cells, no toxic effects ≥ grade 3, regression in tumor observed
MSLN	NCT02930993 Phase I	Recruiting	18 - 70	20	China Meitan General Hospital	Mesothelin positive tumors	
MSLN	NCT02706782 Phase I	Recruiting	18 - 69	30	Shanghai Renji Hospital	pancreatic cancer	
MSLN	NCT02159716 Phase I	Active, not recruiting	≥ 18	21	University of Pennsylvania	Mesothelin positive tumors	
MSLN	NCT02792114 Phase I	Recruiting	≥ 18	24	Memorial Sloan Kettering Cancer Center	Mesothelin positive breast cancer	
MSLN	NCT02465983 Phase I	Active, not recruiting	≥ 18	12	University of Pennsylvania	pancreatic cancer	
MSLN	NCT02959151 Phase I/II	Recruiting	18 - 69	20	Shanghai Tumor Hospital	pancreatic cancer	
MSLN	NCT01355965 Phase I	Active, not recruiting	≥ 18	18	University of Pennsylvania	pleural mesothelioma	
MSLN	NCT02414269 Phase I	Recruiting	≥ 18	24	Memorial Sloan Kettering Cancer Center	Malignant pleural disease	

Target	Trial and phase	Status	Age	No of patients	Institution	Disease	Outcomes
MSLN	NCT01583686 Phase I/II	Recruiting	18 - 70	15	National Cancer Institute (NCI)	Mesothelin positive tumors	
MSLN	NCT02580747 Phase I	Recruiting	18 - 70	20	Chinese PLA General Hospital	Mesothelin positive tumors	
MSLN	NCT01897415 Phase I	Active, not recruiting	≥ 18	16	University of Pennsylvania	Pancreatic ductal adenocarcinoma	
MUC1	NCT02617134 Phase I/II	Recruiting	18 - 80	20	PersonGen BioTherapeutics (Suzhou) Co., Ltd., China	MUC1+ solid tumor	
MUC1	NCT02587689 Phase I/II	Recruiting	18 - 70	20	PersonGen BioTherapeutics (Suzhou) Co., Ltd., China	MUC1+ advanced refractory solid tumor	
MUC1	NCT02839954 Phase I/II	Recruiting	≥ 18	10	PersonGen BioTherapeutics (Suzhou) Co., Ltd., China	MUC1+ relapsed or refractory solid tumor	
PSMA	NCT01140373 Phase I	Recruiting	≥ 18	18	Memorial Sloan Kettering Cancer Center, USA	Prostate cancer	
PSCA	NCT02744287 Phase I	Not yet open	≥ 18	30	Bellicum Pharmaceuticals, USA	Non-resectable pancreatic cancer	
ROR1	NCT02706392 Phase I	Participation by invitation	≥ 18	60	Fred Hutchinson Cancer Research Center, USA	ROR1+ malignancies	
T1E28z	NCT01818323 Phase I	Recruiting	≥ 18	30	King's College London, UK	Head and neck cancer	

Target	Trial and phase	Status	Age	No of patients	Institution	Disease	Outcomes
VEGFR2	NCT01218867 Phase I/II	Completed	18 - 70	24	NCI, USA	Metastatic cancer	

NCI – National cancer institute; CEA – Carcinoembryonic antigen; cMet – Tyrosine-protein kinase Met; EGFR – Epidermal growth factor receptor; EpCAM – Epithelial cell adhesion molecule; EphA2 – Ephrin type-A receptor 2; GD2 – Disialoganglioside; GPC3 – Glypican 3; HCC – Hepatocellular carcinoma; MSLN – Mesothelin; MUC1 – Mucin 1; PSMA – Prostate specific membrane antigen; PSCA – Prostate stem cell antigen; VEGFR – Vascular endothelial growth factor receptor; CR – Complete remission

Chapter-3

Generation of humanized mouse model

Comparison of Human Fetal Liver and Adult Blood derived Hematopoietic Stem Cell Engraftment in NOD-*scid*/$\gamma c^{-/-}$ Immunodeficient Mice

3.1 Abstract

Humanized mice provide a powerful tool to study interactions between human immune cells and human cancers. In this study, we have compared two different sources of hematopoietic stem cells (HSCs); one obtained from second trimester human fetal liver (HFL) tissue, and the other from granulocyte colony stimulating factor (G-CSF) mobilized adult blood (also termed as leukapheresis harvests), for generating a human immune compartment in NOD-*scid*/$\gamma c^{-/-}$ (NSG) mouse host. Our data indicates that stem cells from leukapheresis harvests lack multi-potency as indicated by significantly high frequency of cells co-expressing CD38, a marker for differentiated stem cells. Further, when injected into irradiated neonates from NSG mice, leukapheresis derived HSCs showed a poor human immune reconstitution which was significantly lesser than HFL derived HSCs. Thus, HFL provided a better source to achieve humanization and present a powerful model system to study, apart from other diseases, cancer immunotherapeutic approaches.

3.2 Introduction

Pre-clinical evaluation of anti-cancer therapeutics predominantly employs cell culture techniques and animal models aiming to examine preliminary efficacy and toxicity before putting the drugs into humans. Nearly 85% of novel drug candidates that show promising results in preclinical testings, fail in clinical trials [186]. A major obstacle to adequate understanding of the mechanism and efficacy of anti-cancer drugs, is the limitations in currently available animal model systems.

Pre-clinical mouse models have co-evolved with developments in cancer therapeutics. The earliest animal studies used immunocompetent mouse models. However, these mice served as hosts for transplanting murine tumors only and could not accept human xenografts due to allogenecity of the human cells towards murine immune compartment, which led to rejection of transplants [187]. Thus, immunodeficient mice were established [188]. Firstly, nude mice were developed which lacked T-cells, and so were incompetent in mounting an immune response against implanted human tissues. Next, the NOD strain was developed that lacked innate immune components. Subsequently, SCID mice were identified, which lacked both B and T cells and could be successfully engrafted with not only human tissues but also human hematopoietic cells. However, their applicability was still restricted due to the presence of NK cells and a leaky expression of B and T cells as the mouse aged. This leakiness was further eradicated in RAG-1 and RAG-2 mice strains, however, NK cells persisted. Lastly, the NSG (NOD-*scid*/$\gamma c^{-/-}$) mouse strain was developed by mutation of the common cytokine receptor γ-chain locus in a formerly bred NOD/SCID strain. NSG mice lacks murine T cells, B cells, macrophages, NK cells and NKT cells and have become the most increasingly used model system for studying human cancers [189]. These mice readily accept xenografts of human origin.

Inspite of the advancements, these animal models although serve as accessible hosts, are restricted in their ability to mimic the extremely complex process of human physiology and carcinogenesis. Xenograft tumors transplanted into these mice grow in an environment exceedingly divergent from their origin, usually resulting in encouraging results that are most often clinically incompetent. The NSG model systems cannot completely propogate the conditions as in human host since they lack a human immune environment that is known to shape up anti-cancer immunity and has a huge impact on the outcome of anti-cancer therapeutics.

It is well established that the immune system can have paradoxical roles in cancer development [190]. On one hand, the process of immune surveillance can sometimes lead to complete eradication of newly arising malignant cells, while on the other hand, a chronic activation of various type of innate immune cells near pre-malignant tissues can actually provide an environment that is conducive to tumor growth [190]. Thus, it is critical to consider the key interactions between the immune system and cancer cells and how it can aid or impede the response to an anti-cancer therapy.

To bridge this gap, humanized mice were developed by engrafting human immune system components in immunodeficient mice. These mice provide a robust tool for examining immune-mediated pathogenesis in various human diseases [181, 188]. Using humanized mice, response to anti-cancer therapies can be studies in

the context of a functional human immune system and resultant tumor microenvironment. Recent studies have highlighted the increased similarities of humanized mouse host to cancer patients in terms of the structure of implanted tumor, metastasis, and signalling [189].

The concept of humanized mice was first introduced in 1988, using C.B-17-*scid* mice as recipients for human hematopoietic tissues including fetal liver, bone marrow and thymus derived from second trimester human foetuses [191-193]. In this model, the transplanted human hematopoietic tissues led to reconstitution of low levels of human T and B cells that further showed primary antibody responses when autologous fetal skin (source of dendritic cells) was co-implanted with thymus, bone marrow and lymph node [194]. Adoptive transfer of human peripheral blood mononuclear cells (PBMCs) in the same mouse strain showed development of human B, T and dendritic cells [195]. Additionally, an impaired innate immune system because of either a beige mutation in C.B-17-*scid* or by mating C.B-17-*scid* with the NOD strain, permitted the recipients to acquire higher levels of mature human T and B cells [196, 197]. Next, an enhanced immunodeficiency by additional knock down of common cytokine receptor gamma chain ($\gamma c^{-/-}$) resulted in further profound engraftment of human B, T and dendritic cells [198].

Currently, humanized mice are increasingly produced by engrafting human HSCs into mice of NOD-*scid*/$\gamma c^{-/-}$ [199] or Balb/c-*Rag1*$^{-/-}$/$\gamma c^{-/-}$ [200] strain. Although, these mice develop human B, T ,NK cells as well as cells on myeloid lineage, the overall human immune system function is incomplete [201]. Furthermore, the engraftment levels varies and are dependent on several factors including, genetic background and the age of mouse, route of injection, pre-conditioning regime and source of HSCs [171]. Nevertheless, humanized mice provide a promising tool to study human diseases and are clinically more relevant and close to humans.

We were interested in comparing the human HSCs isolated from either granulocyte colony stimulating factor (G-CSF) mobilized adult blood (leukapheresis harvests of cancer patients) or human fetal liver (HFL), for preparing humanized mice to be used in our ongoing studies with redirected T-cells. Thus, we performed a side-by-side comparison of the frequencies of reconstituted human immune populations following intra-hepatic neonatal transplantation in NSG mice that received HSCs from either of the sources. Additionally, we also compared the differentiation phenotype of HSCs derived from the two sources. Our data indicate that HSCs isolated from human fetal liver (HFL) are less differentiated and provide better reconstitution in NSG mice. Thus, HFL derived humanized mice were subsequently used for all experiments employing adoptive transfer of redirected T-cells.

3.3 Results

We aimed to develop a humanized mouse model to study the survival of redirected T-cells and later *in vivo* anti-tumor efficacy of redirected T-cells. To this end, we first were interested in identifying a good source of hematopoietic stem cells (HSCs) that could provide a robust human immune reconstitution in humanized mice. Thus, we produced and compared humanized mice using HSCs derived from human fetal liver (HFL) or granulocyte colony stimulating factor (G-CSF) mobilized adult blood (Leukapheresis; Leuk). Leukapheresis harvests were left overs from cancer patients that were initially allocated autologous $CD34^+$ stem cell transplantation but did not need further treatment.

We injected HSCs from the two sources (HFL or Leuk), intra-hepatically into sub-lethally irradiated (1 gray) neonates (2-5 days old) from NSG mice and analyzed human immune reconstitution in the blood post three months of injection **(figure 3-1)**.

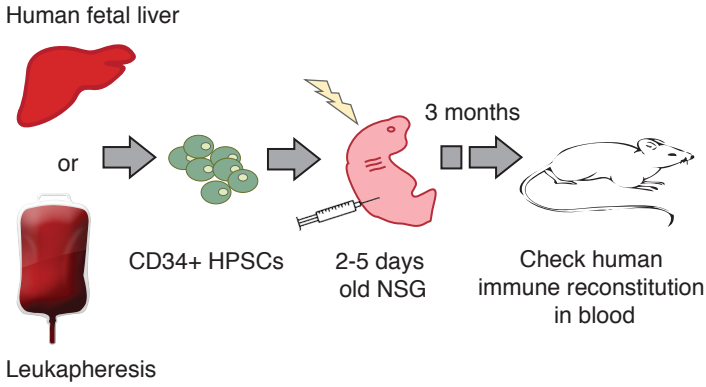

Figure 3-1. Layout of production of humanized mice. CD34+ Hemaopoietic stem cells (HSCs) were isolated from Leukapheresis (adult blood) or second trimester Human Fetal Liver (HFL) and injected intra-hepatically into sub-lethally radiated (radiation dose = 1gray) 2-5 days old NSG mice. After 3 months, reconstitution of human immune compartment in the blood was determined by flow cytometry.

Before injecting mice, purity of the HSCs isolated was confirmed by staining for CD34 and we could achieve >90% purity. We further looked into CD38 expression on CD34+ HSCs. It is known that hematopoietic stem cells which have multi-lineage potential and can generate colonies consisting of both lymphoid and myeloid compartments, express low to almost no CD38 [202]. Additionally, B-cell and T-cell generation potential resides in the more primitive $CD34^+CD38^{-/lo}$ cells [203]. We found that a significantly higher frequency (~90%) of $CD34^+$ HSCs derived from leukapheresis (Leuk) co-expressed CD38, compared to HFL derived CD34+ cells (30 – 40% cells co-expressed CD38) **(figure 3-2)**. CD38 is a marker for more differentiated progenitor cells.

Next, we compared the frequencies of human immune populations in humanized mice reconstituted with HSCs derived from HFL or leukapheresis (Leuk). NSG mice engrafted with HFL derived HSCs showed significantly higher frequencies of human CD45+, CD3+, CD8+ and CD19+ cells **(figure 3-3)**.

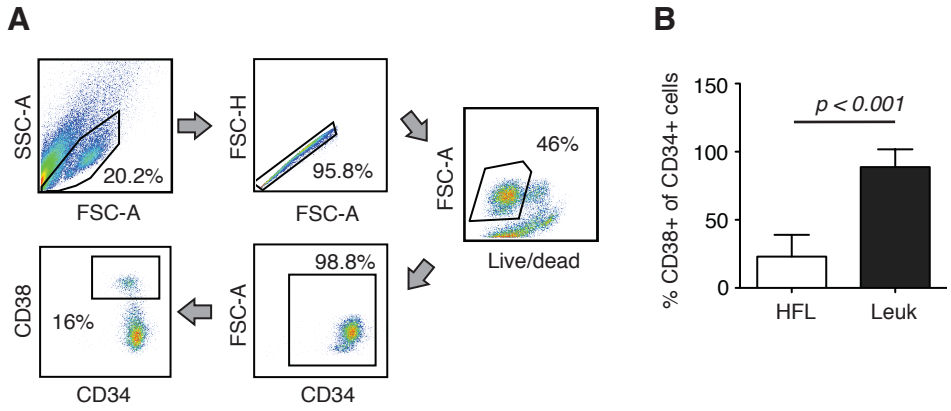

Figure 3-2. Leukapheresis derived hematopoietic stem cells (HSCs) showed higher frequency of CD34+ cells that co-expressed CD38. Hemaopoietic stem cells (HSCs) isolated from Leukapheresis (Leuk) or Human Fetal Liver (HFL) were stained for CD34 and CD38 markers and analyzed by flow cytometry. **A** Representative gating strategy is shown. To determine the purity of CD34+ cell isolation and the frequency of CD34+ cells co-expressing CD38; we first gated on cells based on forward scatter (FSC-A) and side scatter (SSC-A), followed by doublet exclusion and further selecting living cells only. This was followed by gating on CD34+ cells and further gating on CD38+ cells. **B** Graph showing frequency of CD38+ cells of CD34+ cells isolated form HFL or Leuk (number of donors (n) HFL =13 and Leuk =12). Statistics is done using unpaired t-test.

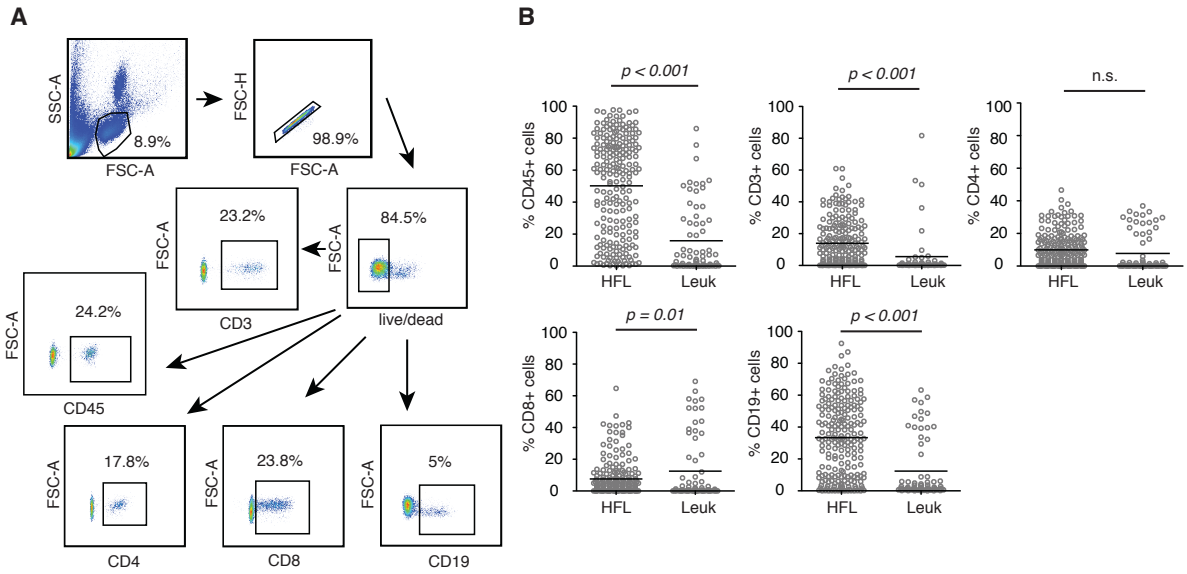

Figure 3-3. HFL derived hematopoietic stem cells (HSCs) provide better human immune reconstitution in humanized NSG mice. A Gating strategy from one representative mouse is shown. Blood isolated from humanized mice was stained for human markers CD45, CD3, CD4, CD8 and CD19 and acquired on a flow cytometer. For analysis, we first gated on lymphocytes fraction based on forward scatter (FSC-A) and sideward scatter (SSC-A). This was followed by doublet exclusion and further selecting living cells only. The living cells were subgated to identify populations for each of the human markers; CD45, CD4, CD3, CD8 and CD19. **B** Graphs representing frequencies (%) of CD45+, CD3+, CD4+, CD8+ and CD19+ cells of living cells in blood of reconstituted mice that received CD34+ from HFL or Leukapheresis (Leuk). HFL; n=165 and Leuk; n=67. Statistics is performed using unpaired t-test.

The substandard immune reconstitution in leukapheresis derived humanized mice indicated poor multi-potency of leukapheresis derived HSCs and correlated to our previous observation of a highly differentiated phenotype (increased CD38 expression). Parallel to this observation, we also noticed that almost 5% of leukapheresis derived humanized mice showed reconstitution of either CD19+ cells or CD3+ cells in the blood. This suggests that the HSCs from leukapheresis are highly differentiated and more committed to develop into only one of the either B cell or T cell lineages. Thus, we further employed HFL reconstituted mice as a model to study redirected T-cells.

3.4 Discussion

In this study, we compared the human immune reconstitution efficiency of HFL or leukapheresis derived HSCs in NOD-scid/$\gamma c^{-/-}$ (NSG) mice. Some parameters were kept consistent, for example, the mouse strain, age and irradiation regime prior to intra-hepatic injection of HSCs. However, due to poor reconstitution efficacy of leukapheresis derived HSCs observed in the beginning and also reported before [201, 204]; for this comparison, we started with a dose of leukapheresis derived HSCs (2 $X10^6$ cells per mouse) that is 10 times higher than HFL derived HSCs (0.2 X 10^6 cells per mouse). Even after injecting a 10 times higher dose, we could not achieve more or atleast equivalent human immune reconstitution efficacy as HFL.

There are several reports which indicate that the background strain of mouse can have consequences on engraftment efficiencies. A study by Lepus et. al. compared three different mouse strains; NOD-scid/$\gamma c^{-/-}$, Balb/c-*Rag1*$^{-/-}\gamma c^{-/-}$ and C.B-17-*scid/bg* as recipients of HSCs obtained from either of the three different sources; human fetal liver (HFL), umbilical cord blood (UCB) or adult blood, for generating humanized mice [201]. The authors reported that mice of NOD-scid/$\gamma c^{-/-}$ strain were most receptive for all HSC sources. Both HFL and UCB were identified as better sources over adult blood, generating highest number of human immune cells. Furthermore, NSG mice showed relatively higher levels of human T-cells in blood compared to Balb/c-*Rag1*$^{-/-}\gamma c^{-/-}$ or C.B-17-*scid/bg* mice and proved to be a better competent host for producing humanized mice. The authors also tested functionality of reconstituted human immune system and concluded that the NSG mice engrafted with HFL CD34+ HSCs showed a competent and functional human immune repertoire as indicated by proliferation of splenocytes upon stimulation with PHA, secondary lymphoid or white pulp expansion, secretion of human immunoglobulins IgM and low levels of IgG after immunization with T-dependent antigens and recruitment of human macrophages and lymphocytes in response to delayed type hypersensitivity (DTH).

Another study comparing mice with different backgrounds, namely, NOD, Balb/c or C.B-17 showed that polymporphism in a single gene (Sirpa) in mice with NOD background, but not Balb/c or C.B-17 background can lead to increased survival and resulting reconstitution by HSCs in NSG mice [205]. NOD/Sirpa receptor on mouse macrophages showed enhanced binding to CD47 on HSCs, thereby preventing phagocytosis of HSCs by mouse macrophages. In contrast Balb/c Sirpa receptor showed weak engagement with CD47, ultimately leading to lower levels of reconstitution in Balb/c-*Rag1*$^{-/-}\gamma c^{-/-}$ mice, attributed to moderate HSCs survival.

Based on the insights from these studies, we used NSG mice as host to achieve humanization. In their study, Lepus et.al. used 0.5 – 1 $X10^6$ adult blood derived HSCs that did not show an adequate reconstitution. We have used a two times higher dose in our study (2 X 10^6 cells), however, it still failed to provide an optimum human immune reconstitution and did not match up with HFL derived humanized NSGs.

There are several evidences of engraftment in NSG mice using HFL, UCB or adult blood derived HSCs. Predominantly, UCB and HFL supported engraftment of both B cell and T cell compartments in NSG mice [198, 199, 206]. In contrast, injection of HFL or UCB HSCs into Balb/c-*Rag1*$^{-/-}\gamma c^{-/-}$ indicated trivial numbers of T cells,

but primarily generating B cells and DCs [201, 207]. Another study using adult blood derived HSCs showed engraftment of only B cells in NSG mice [204].

There are reports that describe several routes of administration of HSCs, including facial vein [199], intra-peritoneal [207] or intra-hepatic [200, 201]. We adopted the intra-hepatic route of engraftment which is technically easier than facial vein injection method in our hands and has been proven before to lead to consistent engraftment frequencies [201]. Furthermore, injecting the hematopoietic progenitors directly into the liver can be advantageous, since a higher fraction of cells can home in the liver, whereas by intraperitoneal route, the cells would need to travel to the liver, which is the primary site for haematopoiesis. Considering that haematopoiesis occurs during the first few weeks of mouse postnatal development, a targeted delivery directly into the site of haematopoiesis could provide utmost engraftment and would may be even need lower cell numbers to achieve optimum levels of reconstitution.

Using Balb/c-*Rag1*$^{-/-}\gamma c^{-/-}$ mouse strain, Gimeno et. al. have shown that engraftment efficiency can depend on the age of the mice, where young neonates (1 day old) showed increased engraftment than older ones (1-2 weeks old) [207]. Based on these observations, we used young cohort of mice; 2-5 days old, for HSCs engraftment. Our data indicates mean reconstitution frequencies of 50% CD45+, 15% CD3+ and 35% CD19+ cells, in HFL derived and 18% CD45+, 5% CD3+ and 11% CD19+ cells in leukapheresis derived humanized mice.

Using HFL derived HSCs also provides an opportunity to co-engraft autologous thymic tissue, which has been shown to aid in education of developing T-cell through autologous human HLA expressing thymic stromal cells and positive selection in human thymus [181]. The resulting T-cells acquire a specificity through thymic education and are capable of generating response to immunizations *in vivo* [181, 208]. Our model does not include co-engraftment of human thymus which could have provided more potent T-cell responses. However, considering the aims of our studies, we inject T-cells that have been *in vitro* redirected to achieve a certain specificity against target antigen. Thus, our humanized model system act as a support system to the adoptively transferred population through an existing active human immune environment. In our hands, HFL reconstituted mice provided a more uniform development of T-cells, unlike leukapheresis derived mice, where often either B cell or T cell reconstitution was observed correlating to poor multi-potency of the HSC population. Thus, HFL derived humanized mice can serve as donors for autologous T cells, which can be used to produce redirected T-cells for testing in our model. Transfer of such autologous T cells would also prevent development of GvHD and rejection due to allogenecity.

Overall, we have demonstrated that HFL provides a better to source to reconstitute NSG mice and shows successful development of different immune lineages. HFL reconstituted mice will be used for adoptive transfer experiments employing redirected T-cells.

3.5 References

1. Mak, I.W., N. Evaniew, and M. Ghert, *Lost in translation: animal models and clinical trials in cancer treatment.* Am J Transl Res, 2014. **6**(2): p. 114-8.
2. Day, C.P., G. Merlino, and T. Van Dyke, *Preclinical mouse cancer models: a maze of opportunities and challenges.* Cell, 2015. **163**(1): p. 39-53.
3. Shultz, L.D., F. Ishikawa, and D.L. Greiner, *Humanized mice in translational biomedical research.* Nat Rev Immunol, 2007. **7**(2): p. 118-30.
4. Morton, J.J., et al., *Humanized Mouse Xenograft Models: Narrowing the Tumor-Microenvironment Gap.* Cancer Res, 2016. **76**(21): p. 6153-6158.
5. de Visser, K.E., A. Eichten, and L.M. Coussens, *Paradoxical roles of the immune system during cancer development.* Nat Rev Cancer, 2006. **6**(1): p. 24-37.
6. Melkus, M.W., et al., *Humanized mice mount specific adaptive and innate immune responses to EBV and TSST-1.* Nat Med, 2006. **12**(11): p. 1316-22.
7. McCune, J.M., et al., *The SCID-hu mouse: murine model for the analysis of human hematolymphoid differentiation and function.* Science, 1988. **241**(4873): p. 1632-9.
8. Namikawa, R., et al., *Long-term human hematopoiesis in the SCID-hu mouse.* J Exp Med, 1990. **172**(4): p. 1055-63.
9. Kyoizumi, S., et al., *Implantation and maintenance of functional human bone marrow in SCID-hu mice.* Blood, 1992. **79**(7): p. 1704-11.
10. Carballido, J.M., et al., *Generation of primary antigen-specific human T- and B-cell responses in immunocompetent SCID-hu mice.* Nat Med, 2000. **6**(1): p. 103-6.
11. Mosier, D.E., et al., *Transfer of a functional human immune system to mice with severe combined immunodeficiency.* Nature, 1988. **335**(6187): p. 256-9.
12. Hesselton, R.M., et al., *High levels of human peripheral blood mononuclear cell engraftment and enhanced susceptibility to human immunodeficiency virus type 1 infection in NOD/LtSz-scid/scid mice.* J Infect Dis, 1995. **172**(4): p. 974-82.
13. Tereb, D.A., et al., *Human T cells infiltrate and injure pig coronary artery grafts with activated but not quiescent endothelium in immunodeficient mouse hosts.* Transplantation, 2001. **71**(11): p. 1622-30.
14. Ito, M., et al., *NOD/SCID/gamma(c)(null) mouse: an excellent recipient mouse model for engraftment of human cells.* Blood, 2002. **100**(9): p. 3175-82.
15. Ishikawa, F., et al., *Development of functional human blood and immune systems in NOD/SCID/IL2 receptor {gamma} chain(null) mice.* Blood, 2005. **106**(5): p. 1565-73.
16. Traggiai, E., et al., *Development of a human adaptive immune system in cord blood cell-transplanted mice.* Science, 2004. **304**(5667): p. 104-7.
17. Lepus, C.M., et al., *Comparison of human fetal liver, umbilical cord blood, and adult blood hematopoietic stem cell engraftment in NOD-scid/gammac-/-, Balb/c-Rag1-/-gammac-/-, and C.B-17-scid/bg immunodeficient mice.* Hum Immunol, 2009. **70**(10): p. 790-802.
18. Shultz, L.D., et al., *Humanized mice for immune system investigation: progress, promise and challenges.* Nat Rev Immunol, 2012. **12**(11): p. 786-98.
19. Miller, J.S., et al., *Single adult human CD34(+)/Lin-/CD38(-) progenitors give rise to natural killer cells, B-lineage cells, dendritic cells, and myeloid cells.* Blood, 1999. **93**(1): p. 96-106.
20. Huang, S. and L.W. Terstappen, *Lymphoid and myeloid differentiation of single human CD34+, HLA-DR+, CD38- hematopoietic stem cells.* Blood, 1994. **83**(6): p. 1515-26.
21. Shultz, L.D., et al., *Human lymphoid and myeloid cell development in NOD/LtSz-scid IL2R gamma null mice engrafted with mobilized human hemopoietic stem cells.* J Immunol, 2005. **174**(10): p. 6477-89.
22. Takenaka, K., et al., *Polymorphism in Sirpa modulates engraftment of human hematopoietic stem cells.* Nat Immunol, 2007. **8**(12): p. 1313-23.
23. Yahata, T., et al., *Functional human T lymphocyte development from cord blood CD34+ cells in nonobese diabetic/Shi-scid, IL-2 receptor gamma null mice.* J Immunol, 2002. **169**(1): p. 204-9.
24. Gimeno, R., et al., *Monitoring the effect of gene silencing by RNA interference in human CD34+ cells injected into newborn RAG2-/- gammac-/- mice: functional inactivation of p53 in developing T cells.* Blood, 2004. **104**(13): p. 3886-93.

25. Tonomura, N., et al., *Antigen-specific human T-cell responses and T cell-dependent production of human antibodies in a humanized mouse model.* Blood, 2008. **111**(8): p. 4293-6.

Chapter-4

Optimized CAR co-receptor with PD-1 blockade

Aberrant Lck signal via CD28 costimulation augments antigen-specific functionality and tumor control by redirected T-cells with PD-1 blockade in humanized mice

Pratiksha Gulati (1,2), Julia Rühl (2), Abhilash Kannan (3), Magdalena Pircher (1), Petra Schuberth (1), Katarzyna J Nytko (4), Martin Pruschy (4), Simon Sulser (5), Mark Haefner (6), Shawn Jensen (7), Alex Soltermann (8), Wolfgang Jungraithmayr (9,14), Maya Eisenring (10), Thomas Winder (1), Panagiotis Samaras (1), Annett Tabor (11), Rene Stenger (12), Roger Stupp (1), Walter Weder (9), Christoph Renner (13), Christian Münz* (2) & Ulf Petrausch* (1,2)

Short title: **Optimized CAR co-receptor with PD-1 blockade**

(1) Department of Oncology, University Hospital Zurich, Rämistrasse 100, 8091 Zürich, Switzerland

(2) Institute for Experimental Immunology, University of Zurich, Winterthurerstrasse 190, 8057 Zürich, Switzerland

(3) Institute of Molecular Life Sciences, University of Zurich, Winterthurerstrasse 190, 8057 Zürich, Switzerland

(4) Department of Radiation Oncology, University Hospital Zurich, Rämistrasse 100, 8091 Zürich, Switzerland

(5) Institute of Anesthesiology, University Hospital Zurich, Rämistrasse 100, 8091 Zürich, Switzerland

(6) Oncology Bülach, Bannhaldenstrasse 7, 8180 Bülach, Switzerland

(7) Laboratory of Molecular and Tumor Immunology, Earle A. Chiles Research Institute, Providence Cancer Center and Providence Portland Medical Center, 4805 NE Glisan St., Portland, OR 97213, USA

(8) Institute of Pathology and Molecular Pathology, University Hospital Zurich, Schmelzbergstrasse 12, 8091 Zurich, Switzerland

(9) Department of Thoracic Surgery, University Hospital Zurich, Rämistrasse 100, 8091 Zürich, Switzerland

(10) Department of Immunology, University Hospital Zurich, Rämistrasse 100, 8091 Zürich, Switzerland

(11) European Institute for Research and Development of Transplantation Strategies GmbH (EUFETS), Vollmersbachstrasse 66, 55743 Idar-Oberstein, Germany

(12) Swiss Center for Regenerative Medicine, Wyss Institute, University of Zurich, Moussonstrasse 13, 8044 Zurich, Switzerland

(13) Department of Biomedicine, University Hospital Basel, Hebelstrasse 20, 4031 Basel, Switzerland

(14) Department of Thoracic Surgery, Campus Ruppiner Kliniken, Fehrbellinerstrasse 38, 16816 Neuruppin, Medical University Brandenburg, Germany

Corresponding author: Ulf Petrausch, Institute for Experimental Immunology, University of Zurich, Winterthurerstrasse 190, 8057 Zürich, Phone: +41 44 635 37 01, FAX: +41 44 635 68 83, email: ulf.petrausch@uzh.ch

* These authors contributed equally

Conflict of Interest: The authors have declared that no conflict of interest exists

4.1 Abstract

Combination therapy of adoptively transferred redirected T-cells and checkpoint inhibitors aims for higher response rates in tumors poorly responsive to immunotherapy like malignant pleural mesothelioma (MPM). So far, neither the composition of an optimally active chimeric antigen receptor (CAR) nor the synergy with checkpoint inhibitors has been characterized. Fibroblast Activation Protein (FAP)-specific CARs with different co-stimulatory domains including CD28, Δ-CD28 (lacking lck) or 4-1BB were established. CAR-T cells in combination with PD-1 blockade were analyzed *in vivo* in a humanized mouse model. Finally, the Δ-CD28 CAR was tested clinically in a MPM patient. All the three CARs demonstrated FAP-specific functionality *in vitro*. Gene expression data indicated a distinct activity profile for the Δ-CD28 CAR including higher expression of genes involved in cell division, glycolysis, fatty acid oxidation and oxidative phosphorylation. *In vivo,* only T-cells expressing the Δ-CD28 CAR in combination with PD-1 blockade controlled tumor growth. When injected into the pleural effusion of a MPM patient, the Δ-CD28 CAR could be detected for up to 21 days and showed functionality. Overall, anti-FAP-Δ-CD28/CD3ζ CAR-T cells revealed superior *in vitro* functionality, synergy with PD-1 blockade and persistence in a MPM patient. Therefore, further clinical investigation of this optimized CAR is warranted.

4.2 Introduction

Redirected T-cells express a chimeric antigen receptor (CAR) specific for a target antigen on the surface of tumor cells. CARs are composed of an antibody derived, target antigen specific single-chain variable fragment (scFv) which is linked to T-cell co-stimulatory domains such as CD28, 4-1BB, CD137, or OX40 in addition to a T-cell signaling domain, CD3ζ [209]. The most advanced clinical response employing redirected T-cells has been shown using anti-CD19-CARs. Early clinical trials using CD19 CAR-T cells, demonstrated the eradication of malignant B cells expressing CD19 [210]. Additionally, in a trial using CD19-specific 4-1BB CAR, it was shown that redirected T-cells expanded after transfer and converted into T-cells with memory-like phenotypes [144]. Encouragingly, some patients who achieved a clinical remission, remained in remission for up to 4 years after the treatment [185]. With CARs targeting CD19, responses in clinical trials could be seen in lymphoma, myeloma and most impressively in acute lymphoblastic leukemia [211]. Based on these promising clinical findings the therapeutic strategy of transferring redirected T-cells needs further evaluation, beyond CD19 expressing diseases, to allow clinical benefit in other malignant diseases and tumors with different target antigens.

Redirected T-cells must be analyzed extensively *in vitro* and *In vivo* before clinical application. For *in* vivo testing of redirected T-cells, we employed a previously developed humanized mouse model. Humanized mice provide the opportunity to study human redirected T-cells in a partly developed human immune environment. Therefore, these models are potentially capable to uncover immunological phenomena by blocking or boosting anti-cancer immune reactions induced by redirected human T-cells otherwise not detectable in immune compromised mice.

Malignant pleural mesothelioma (MPM) is a disease which can not be cured even at early stages [212]. Recently, encouraging data using PD-1 blocking antibodies indicated that the immune system can attack MPM and result in clinical responses [213, 214]. However, only a minority of patients responded to PD-1 blockade. One possible explanation could be the absence of a T-cell repertoire that can be activated and unleashed by PD-1 blockade to form a therapeutic immune response. A potential strategy to overcome this limitation is the combination therapy of PD-1 blockade and adoptive transfer of redirected T-cells against antigens expressed by MPM. However, up to now no pre-clinical data indicates the optimal combination of redirected T-cell and PD-1 blockade.

Fibroblast Activation Protein (FAP) is expressed in MPM and is therefore a potential target antigen for immune therapy using FAP targeted redirected T-cells [215]. We developed and functionally tested a CAR recognizing FAP (scFv F19) composed of a co-stimulatory CD28 moiety lacking the lck signal (Δ-CD28) linked to a CD3ζ T-cell activation domain [216]. The motivation to delete the lck binding domain was to potentially augment *in vivo* anti-tumor activity of the CAR due to expected reduced regulatory T-cell infiltration because of decreased IL-2 production upon activation [217].

We were interested to investigate the FAP-specific redirected T-cells in combination with PD-1 blockade. Additionally, we were keen on understanding the impact of different co-stimulations on the survival and efficacy

of the FAP specific CAR-T cells. Therefore, we constructed and tested anti-FAP CAR constructs with different co-stimulatory moieties, CD28, Δ-CD28 and 4-1BB *in vitro* and *in vivo,* using a humanized mouse model. We believe that the humanized mouse model, due to its partly developed human immune compartment, can provide a better estimate of the clinical response of FAP-specific redirected T-cells with PD-1 blockade.

This study provides the rationale for the combination of FAP-specific redirected T-cells and PD-1 blockade in patients with MPM and other malignant tumors expressing FAP.

4.3 Results

4.3.1 Stimulation of T-cells using anti-CD3/CD28 coated beads results in enhanced activation and shows reduced expression of senescence marker.

The ability to expand tumor-specific Tcells without impairing their functional capacity is crucial for the success of adoptive immunotherapies in cancer. We investigated the consequences of high or low degree of CD3/28 stimulation on the phenotype of T-cells and their ability to get transduced to express CARs. It is known that immobilization of CD3 and CD28 specific antibodies on a surface such as beads (CD3/28 beads) can deliver a stronger proliferative signal and are more efficient in expanding T-cells compared to soluble CD3 and CD28 specific antibodies (CD3/28 ab) [218].

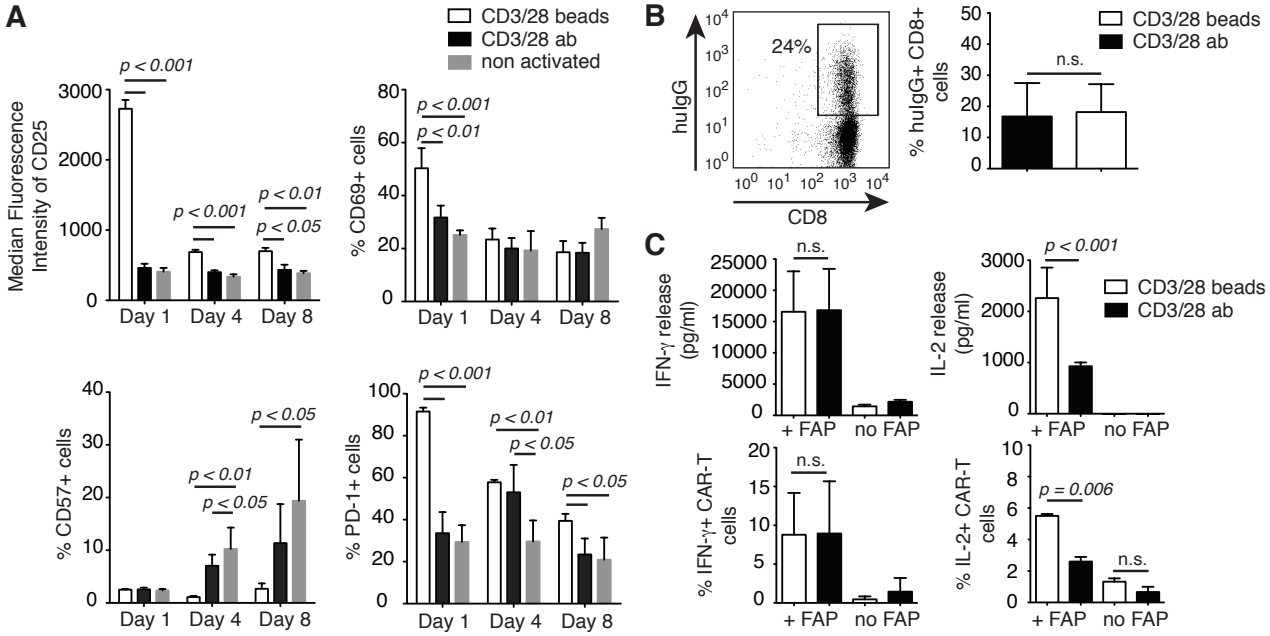

Figure 4-1. Phenotypic profiling of T-cells activated with CD3/28 beads or CD3/28 ab and comparison of transduction efficacies. $CD3^+$ T-cells isolated from buffy donors are incubated with anti-CD3 and anti-CD28 coated beads (CD3/28 beads) or soluble anti-CD3 and anti-CD28 antibodies (CD3/28 ab) **A** Median surface expression of CD25, % $CD69^+$ cells (top panel) and % $CD57^+$ cells, % $PD\text{-}1^+$ cells (bottom panel) are compared at day 1, day 4 and day 8 after removal of CD3/28 stimulus in CD3/28 beads or CD3/28 ab or non-activated T-cells. Representative plots from one experiment with two buffy donors is shown (n=2). P values are calculated using one way ANOVA with tukey's post test for multiple comparisons. **B** CD3/28 ab or CD3/28 beads stimulated cells are transduced to express CD28-CD3ζ or Δ-CD28/CD3ζ CARs. Left Panel shows representative staining for redirected T-cells post transduction. CAR transduced T-cells are detected by FACS using anti human IgG antibody to stain for CAR receptor; gated $huIgG^+CD8^+$ (24%) and transduction efficacies after CD3/28 beads or CD3/28 ab activation are compared (right panel) (n=4). **C** $CD8^+$ cells activated with CD3/28 beads or CD3/28 ab are transduced to express F19-CD28/CD3ζ CAR. IFN-γ and IL-2 release is measured by ELISA (top panel) and % IFN-γ and IL-2 secreting cells are identified by Intra-cellular staining (ICS) and compared in response to antigen-specific (+FAP) stimulation or no stimulation (no FAP). Representative data from one experiment with two buffy donors is shown (n=2). Statistics is done using unpaired t-test. Data is presented as mean ± S.D.

Our data indicate increased T-cell activation upon CD3/28 bead stimulation compared to CD3/28 antibodies as indicated by significantly higher median expression of the CD25 T-cell activation marker (**figure 4-1 A, top panel**) and higher frequencies of PD-1^{+} cells (**figure 4-1 A, bottom panel**). PD-1 is known to be augmented in activated T-cells [219]. We observed significant higher frequency of CD69^{+} cells only during the early phase (day 1) in CD3/28 beads stimulated cells (**figure 4-1 A, top panel**). Frequency of CD57^{+} cells was significantly increased in CD3/28 antibody activated compared to CD3/28 beads activated cells (**figure 4-1 A, bottom panel**). CD57 is a general marker of replicative senescence and proliferation incompetence in T-cells [220]. Besides this, there was no difference in the ability of CD3/28 antibody or CD3/28 beads activated T-cells to get transduced and express CARs (**figure 4-1 B**). Furthermore, CAR-T cells activated with CD3/28 beads produced significantly higher levels of IL-2 upon antigen-specific stimulation. Nonetheless, antigen-specific IFN-γ secretion remained unaffected (**figure 4-1 C**). These findings indicate possible early senescence attributed to increased CD57^{+} cells and reduced proliferation or expansion potential due to low levels of IL-2 production in CAR-T cells generated by CD3/28 antibody stimulus compared to CD3/28 beads. Thus, we used CD3/28 beads to produce redirected T-cells for further *in vitro* experiments and the subsequent clinical trial.

4.3.2 Deletion of Lck binding moiety in CD28 co-stimulatory domain provides a highly proliferating, increasingly metabolizing, activated cell-like gene expression profile in redirected T-cells.

We intended to investigate the effect of different co-stimulations through the CAR to identify differences, which could endow CAR-T cells with precise tumor targeting properties, ideal survival and efficacy. We designed and compared CAR constructs with three different co-stimulatory moieties; CD28, Δ-CD28 (CD28 lacking Lck binding domain) & 4-1BB (**figure S4-1**).

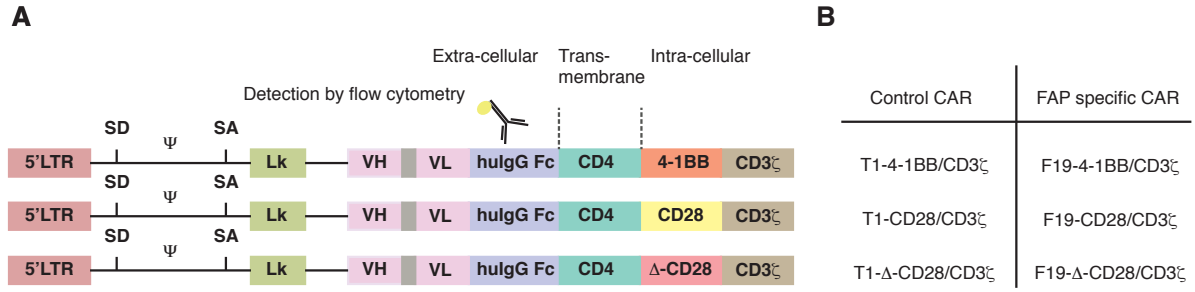

Figure S4-1. Schematic diagram of the CAR receptors. A. Chimeric antigen receptor (CAR) constructs consist of Lk leader sequence, variable heavy (VH) and light (VL) chains of the antigen binding domain of antibody, human CH2/3 immunoglobulin domain (huIgG Fc), CD4 transmembrane domain (CD4) linked to either of the co-stimulatory signalling domains 4-1BB (top) or CD28 (middle) or Δ-CD28 (bottom) and a CD3ζ T-cell signalling domain. The human IgG domain provides for detection of CAR-transduced T cells by flow cytometry using an anti-human IgG antibody. **B.** The nomenclature of control CAR (T1; target antigen is NY-ESO-1) or antigen-specific CAR (F19; target antigen is FAP) corresponding to its architecture.

Redirected T-cells with distinct co-stimulatory domains were stimulated with FAP and the fold change (Log_2FC) of differentially regulated genes was compared in antigen stimulated CAR-T cells over control CAR-T cells; F19-CD28/CD3ζ over T1-CD28/CD3ζ, F19-Δ-CD28/CD3ζ over T1-Δ-CD28/CD3ζ and F19-4-1BB/CD3ζ over T1-4-1BB/CD3ζ (**figure S4-2**).

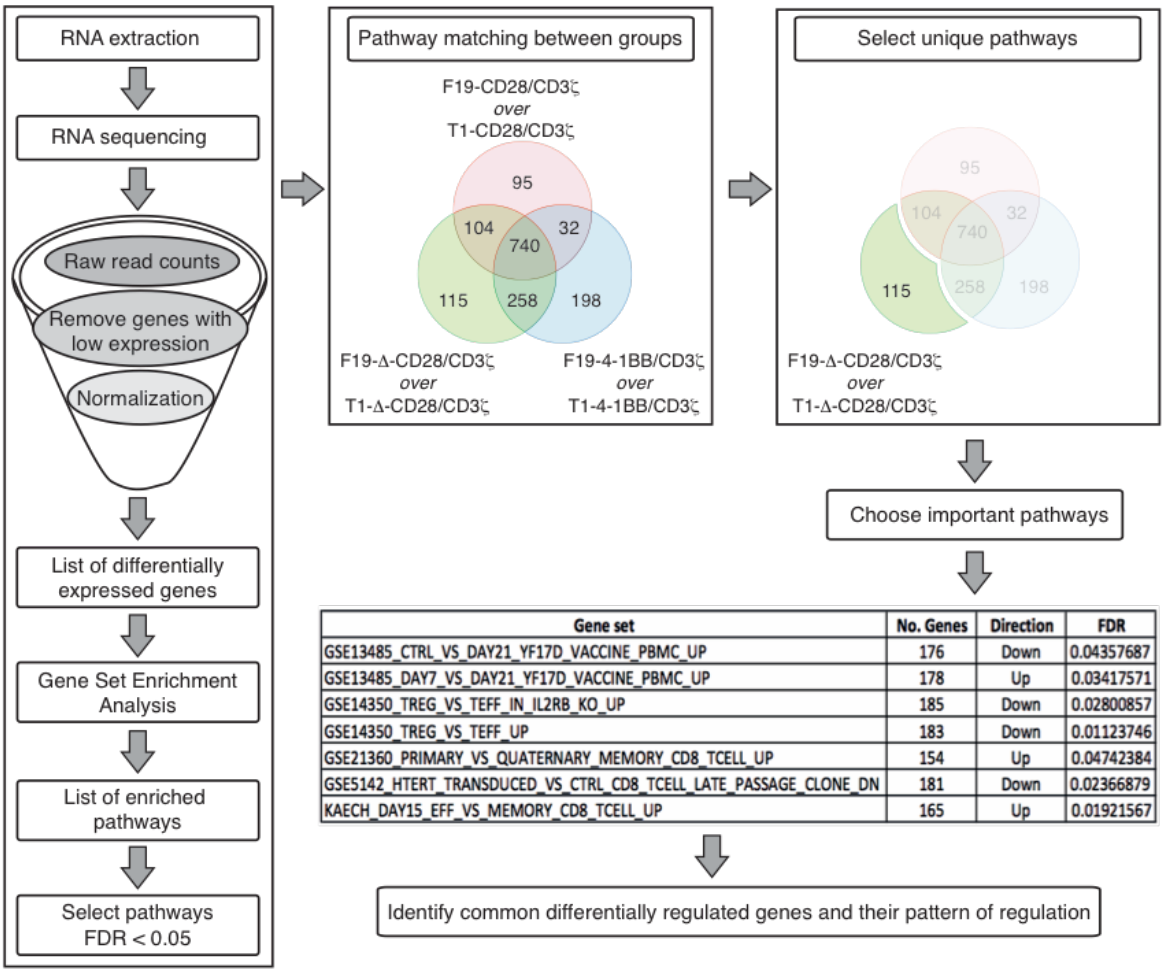

Figure S4-2. Flow chart of transcriptome profiling after antigen-specific stimulation of redirected T-cells with different co-stimulations. RNA was extracted and sequenced from FAP-specific; F19-CD28/CD3ζ, F19-Δ-CD28/CD3ζ, F19-4-1BB/CD3ζ and control; T1-CD28/CD3ζ, T1-Δ-CD28/CD3ζ, T1-4-1BB/CD3ζ redirected $CD8^+$ T cells, after stimulation with FAP. The raw read counts obtained from sequencer were further filtered to remove genes with low expression and normalized for RNA compositional bias. Differential gene expression analysis was performed to identify fold change in gene levels (Log_2FC values) in FAP-specific CAR-T cells over control CAR-T cells for each of the co-stimulation; CD28 specific (F19-CD28/CD3ζ over T1-CD28/CD3ζ), Δ-CD28 specific (F19-Δ-CD28/CD3ζ over T1-Δ-CD28/CD3ζ) and 4-1BB specific (F19-4-1BB/CD3ζ over T1-4-1BB/CD3ζ). A list of differentially expressed genes containing the Log fold change values (Log_2FC) and False Discovery Rate (FDR) values was generated and genes with FDR < 0.05 were chosen and further subjected to Gene Set Enrichment Analysis (GSEA). GSEA analysis provided a list of enriched pathways and pathways with FDR < 0.05 were selected. This was followed by matching the list of pathways between the three groups; CD28 specific, Δ-CD28 specific and 4-1BB-specific, as indicated by Venn diagram. The numbers in each intersection of the Venn diagram represents the number of pathways common for those particular conditions. Next, we enlisted the pathways that were unique to Δ-CD28 specific co-stimulation and chose relevant immune linked pathways from that list. For each of the selected pathways, we constructed heatmaps to identify genes that are most commonly occurring within different pathways and their specific patterns of regulation, to further find correlations.

Using Gene Set Enrichment Analysis (GSEA), we observed a unique transcriptome profile for redirected T-cells that received stimulation through the Δ-CD28/CD3ζ CAR. Stimulation through the Δ-CD28/CD3ζ CAR showed highest expression of cell cycle genes; indicating enhanced proliferation in an antigen-specific manner (**figure 4-2 A, genes listed in table S4-1**).

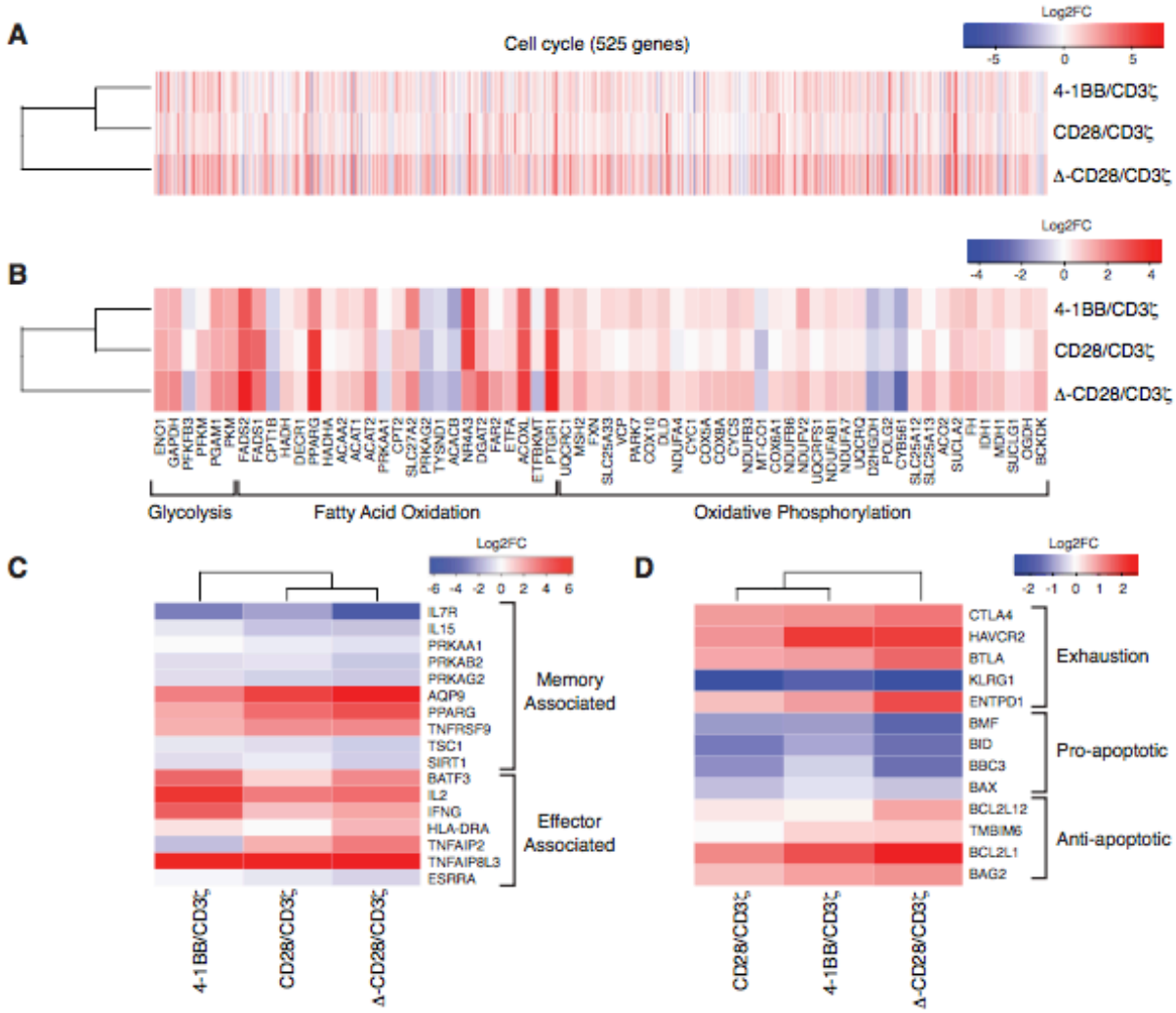

Figure 4-2. Transcriptome profiling of redirected T-cells. Heatmaps showing differentially regulated genes in **A** Cell cycle pathways (525 genes, enlisted in table S4-1) **B** Metabolism via glycolysis, fatty acid oxidation and oxidative phosphorylation **C** effector or memory phenotype in T-cells and **D** exhaustion and apoptosis. Color key corresponding to each heat map is presented on the upper right corner. Color codes represent Log fold change (Log_2FC) in gene expression of FAP-specific CAR^+CD8^+ cells over control CAR^+CD8^+ cells, after stimulation with FAP; CD28/CD3ζ (F19-CD28/CD3ζ over T1-CD28/CD3ζ), Δ-CD28/CD3z (F19-Δ-CD28/CD3ζ over T1-Δ-CD28/CD3ζ) and 4-1BB/CD3ζ (F19-4-1BB/CD3ζ over T1-4-1BB/CD3ζ). RNA sequencing was performed using 3 biological replicates.

In addition to increased cell-division, Δ-CD28/CD3ζ CAR-T cells showed relatively higher expression of genes that control cell metabolism such as glycolysis, fatty acid oxidation and oxidative phosphorylation (**figure 4-2 B**).

Consistent with this observation, the plasma membrane transporters which play a predominant role in cell metabolism [221] were most distinctly regulated in the Δ-CD28/CD3ζ specific co-stimulation (**figure S4-3 A**).

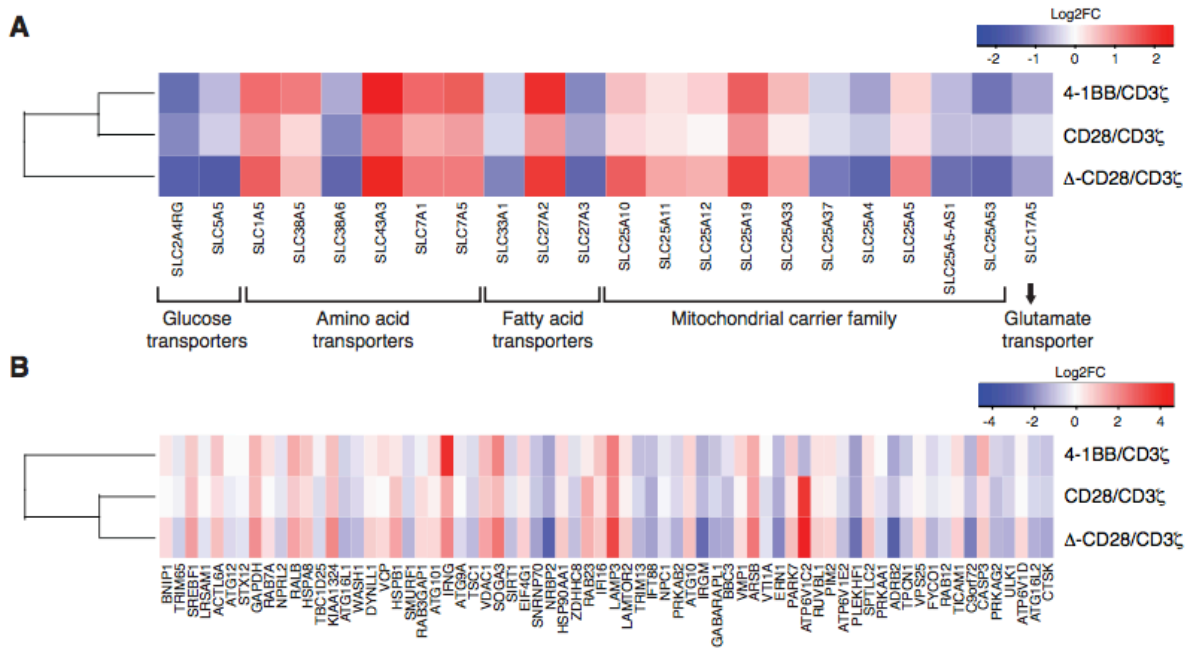

Figure S4-3. Heatmaps showing Log_2FC values of genes relevant to **A** Cell membrane transporters; Glucose transporters, Amino acid transporters, Fatty acid transporters, Mitochondrial carrier family, Glutamate transporter **B** Autophagy. Color key corresponding to each heat map is presented on the upper right corner. Color codes represent Log fold change (Log_2FC) in gene expression of FAP-specific CAR^+CD8^+ cells over control CAR^+CD8^+ cells, after stimulation with FAP: CD28/CD3ζ (F19-CD28/CD3ζ over T1-CD28/CD3ζ), Δ-CD28/CD3ζ (F19-Δ-CD28/CD3ζ over T1-Δ-CD28/CD3ζ) and 4-1BB/CD3ζ (F19-4-1BB/CD3ζ over T1-4-1BB/CD3ζ). RNA sequencing was performed using 3 biological replicates.

It is known that T-cells undergo dynamic changes in their metabolism during an immune response, and that metabolic changes can decide the differentiation and fate of T-cells [221]. Our findings indicate a highly proliferating, actively metabolizing and a more terminally differentiated cell like biology of redirected T-cells that received stimulation through the Δ-CD28/CD3ζ CAR. Further, we looked specifically into key signature markers that distinguish effector T-cells from memory T-cells. The expression of genes such as IL-7R, IL-15, AMPK (PRKAA1, PRKAB2 and PRKAG2), TSC1 (negative regulator of mTOR) and SIRT1, which provide a more memory like T-cell phenotype were increasingly reduced in Δ-CD28/CD3ζ when compared to 4-1BB/CD3ζ specific co-stimulation (**figure 4-2 C**). Activation and proliferation of effector T-cells is often accompanied by increased levels of exhaustion markers [219]. We found that although Δ-CD28/CD3ζ stimulation resulted in enhanced expression of exhaustion genes, e.g. CTLA4, BTLA, ENTPD1 (CD39) and HAVCR2 (Tim-3), it also demonstrated reduced expression of pre-apoptotic genes and increased expression of anti-apoptotic genes (**figure 4-2 D**). Besides, we also observed increased autophagy (enhanced upregulation of positive and down-regulation of negative regulators of autophagy) in redirected T-cells with Δ-CD28/CD3ζ co-stimulation (**figure S4-3 B**). Albeit,

the exact relation between autophagy and apoptosis is controversial, increasing research evidence indicates that autophagy can promote T-cell survival by negatively impacting cell death and plays a role in memory formation [222, 223]. Overall, we conclude that stimulation through the Δ-CD28/CD3ζ CAR imparts an exceedingly activated cell like profile to redirected T-cells, as demonstrated by a genetic signature consistent with enhanced proliferation, metabolism and exhaustion.

4.3.3 Lck lacking CD28 CAR expressed increased levels of exhaustion markers.

To validate our gene expression data, we looked into the expression of immune checkpoint markers such as TIM-3 and PD-1 upon antigen-specific stimulation of redirected T-cells by flow cytometry. In line with our gene expression data, we found a trend to highest expression of TIM-3 and PD-1 in the Δ-CD28/CD3ζ CAR redirected T-cells (**figure 4-3**).

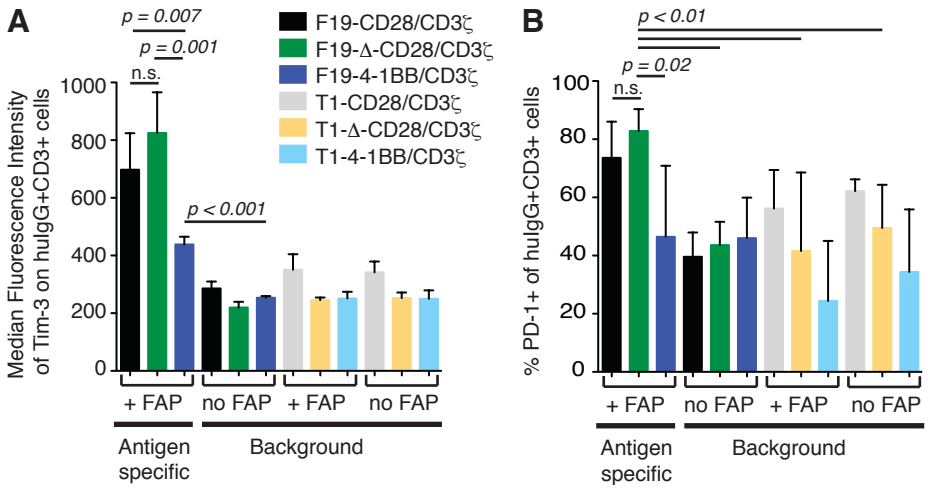

Figure 4-3. Expression of immune check point markers on redirected T-cells. FAP-specific CAR$^+$ (F19-CD28/CD3ζ, F19-Δ-CD28/CD3ζ, F19-4-1BB/CD3ζ) CD3$^+$ cells and control CAR$^+$ (T1-CD28/CD3ζ, T1-Δ-CD28/CD3ζ, T1-4-1BB/CD3ζ) CD3$^+$ cells were compared for **A** MFI of Tim3 on CAR$^+$ CD3$^+$ cells **B** frequency of PD-1$^+$ cells of CAR$^+$ CD3$^+$ cells in response to antigen-specific stimulation (FAP-specific CAR-T cells incubated with FAP) or background (FAP-specific CAR-T cells incubated with no FAP and control CAR-T cells incubated with or without FAP). Representative plots from one experiment with two buffy donors is shown (n=2). Data is presented as mean ± S.D. Statistics is done using unpaired t-test and p values are indicated.

Additionally, we also examined the phenotype of redirected T-cells with different co-stimulatory domains post antigen-specific stimulation. We observed that CAR transduced T-cells demonstrated in general, a more central memory and effector memory like phenotype compared to non-transduced T cells (**figure S4-4**). However, this effect was not antigen-specific. Additionally, no striking difference in T-cell phenotype was observed pertaining to a certain co-stimulation.

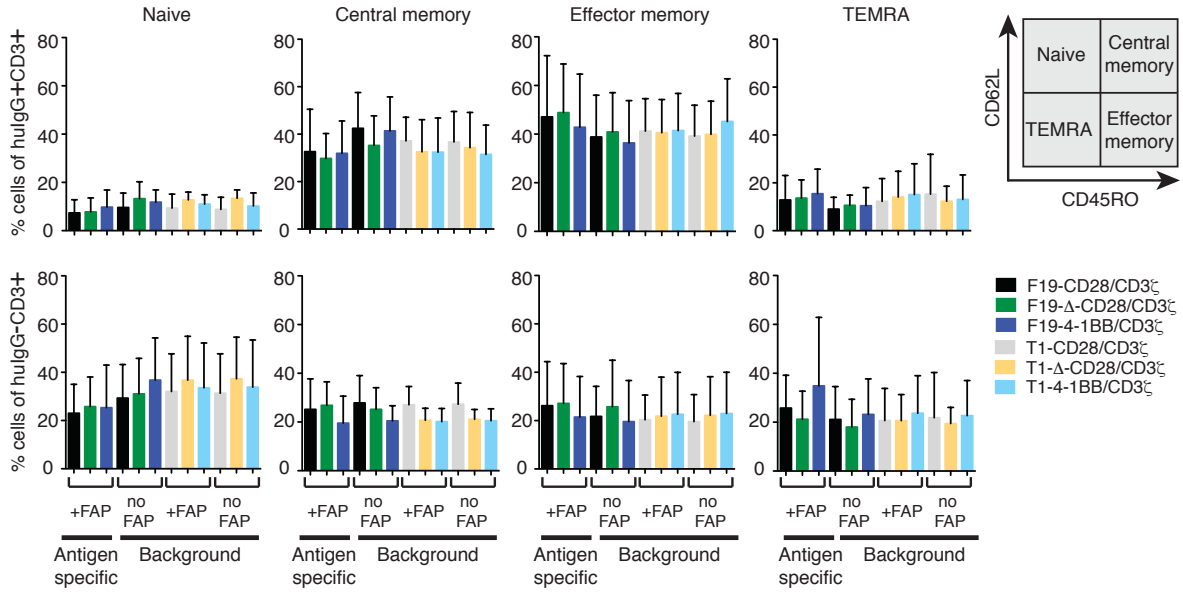

Figure S4-4. Memory marker profiling in CAR$^+$ and CAR$^-$ cells. CD3$^+$ cells obtained from buffy donors were transduced to express FAP-specific CARs (F19-CD28/CD3ζ, F19-Δ-CD28/CD3ζ, F19-4-1BB/CD3ζ) or control CARs (T1-CD28/CD3ζ, T1-Δ-CD28/CD3ζ, T1-4-1BB/CD3ζ). The resulting redirected T-cells (mixture of CAR transduced and un-transduced cells) were incubated with FAP or no FAP and stained for markers CD45RO and CD62L. Based on the cell surface expression of CD45RO and CD62L, the cell populations were sub-divided into; naive (CD45RO$^-$ CD62L$^+$), Central memory (CD45RO$^+$CD62L$^+$), Effector memory (CD45RO$^+$CD62L$^-$) and TEMRA (CD45RO$^-$CD62L$^-$). Top panel shows four sub-populations pre-gated on CAR$^+$ cells. Bottom panel shows the four subpopulations pre-gated on CAR- cells. Pooled data from six buffy donors is shown (n=3). Data is presented as mean ± S.D.

4.3.4 Aberrant Lck signaling through the CD28 CAR increases the proliferative-specificity of redirected T-cells

Next, we investigated the impact of different co-stimulations through the CAR on proliferation and anti-tumor efficacy of redirected T-cells *in vitro*. Over multiple experiments with several donors (n=8) we observed that CD28/CD3ζ CAR-T cells proliferated un-specifically. In contrast, the Δ-CD28/CD3ζ and 4-1BB/CD3ζ CAR-T cells proliferated equally well in a highly antigen-specific manner (**figure 4-4 A**). Additionally, we observed that the CD8$^+$ CAR-T cells demonstrated significantly higher non-specific proliferation compared to CD4$^+$ CAR-T cells (**figure S4-5**). Notably, all three co-stimulatory CAR constructs (CD28/CD3ζ, Δ-CD28/CD3ζ and 4-1BB/CD3ζ) demonstrated antigen-specific anti-tumor efficacy at different effector/target ratios (**figure 4-4 B**). Yet, the 4-1BB/CD3ζ CAR showed the least tumor cell lysis which was significantly different from the Δ-CD28/CD3ζ CAR. In addition to tumor cell lysis, all three CAR constructs exhibited antigen-specific IFN-γ and IL-2 release (**figure 4-4 C**). Likewise, the frequency of IL-2 and IFN-γ producing cells was elevated upon cognate antigen recognition (**figure 4-4 D**). Even though we observed significantly higher frequency of IL-2 producing cells in the 4-1BB/CD3ζ group (**figure 4-4 D**), the total amount of IL-2 secreted by these cells was very limited (**figure 4-4 C**). The reduced IL-2 release by the Δ-CD28/CD3ζ compared to CD28/CD3ζ CAR-T cells has already been reported before [216] and is a consequence of the missing lck signal (**figure 4-4 C**). Besides, Δ-CD28/CD3ζ CAR-T cells revealed

maximum antigen-specific IFN-γ release (**figure 4-4 C**). Taken together, our data demonstrate the superiority of Δ-CD28/CD3ζ CAR over others in terms of maximum antigen-specific proliferation, tumor cell lysis and cytokine release.

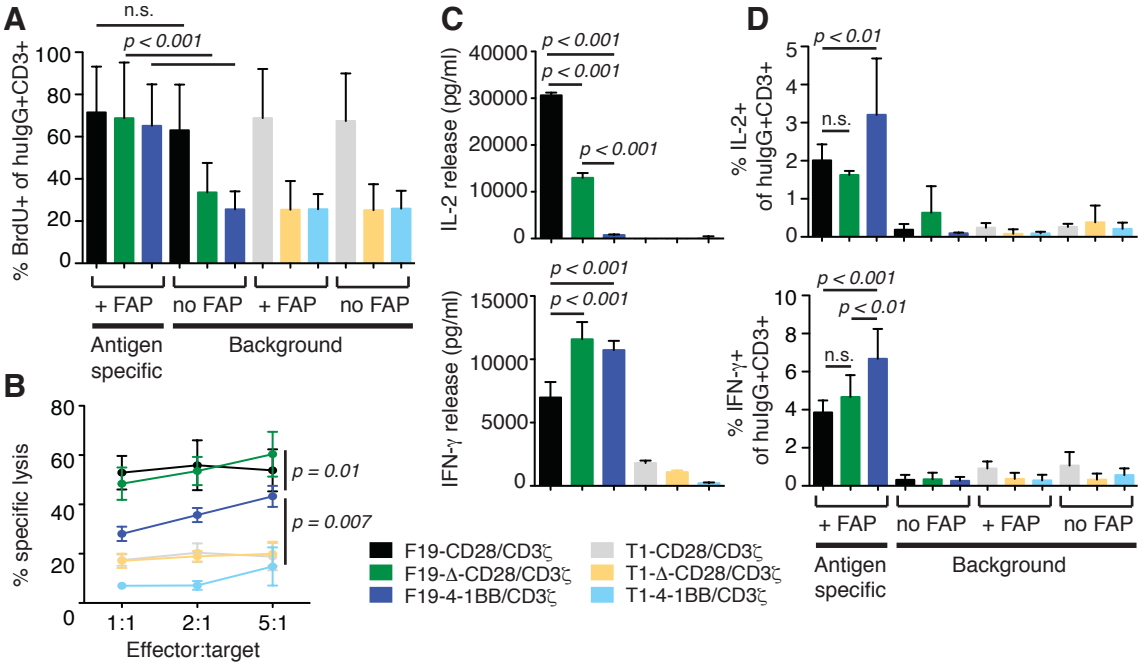

Figure 4-4. *In vitro* functional characterization of redirected T-cells with different co-stimulations. $CD3^+$ cells obtained from buffy donors were transduced to express FAP-specific CARs (F19-CD28/CD3ζ, F19-Δ-CD28/CD3ζ, F19-4-1BB/CD3ζ) or control CARs (T1-CD28/CD3ζ, T1-Δ-CD28/CD3ζ, T1-4-1BB/CD3ζ) **A** Proliferation was compared by culturing CAR transduced cells in BrdU supplemented medium and stimulating with (+FAP) or without antigen (no FAP). Frequency of proliferating cells was determined by first gating on $huIgG^+$ (CAR^+) cells followed by further selecting $BrdU^+$ cells. Pooled data from 8 buffy donors (n=4) is shown. Statistics is done using one way anova with tukey's post test for multiple comparison. **B** Redirected T-cells were co-cultured with HT1080FAP tumor cells at specified Effector/Target (E:T) ratios and tumor cell lysis was measured. Data from 2 representative donors is shown (n=4). P value is calculated using unpaired t-test **C** Cytokines IFN-γ and IL-2 quantified by ELISA in supernatant from co-culture of CAR-T cells with tumor cells. **D** Intra-cellular staining (ICS) to measure frequency of IFN-γ and IL-2 producing CAR-T cells in response to antigen-specific stimulation or no stimulation (background). These are representative plots from one experiment with 2 buffy donors (n=3). Statistics is done using one way anova with tukey's post test. Data is presented as mean ± S.D.

4.3.5 Lck lacking CD28 CAR-T cells show improved tumor control in combination with PD-1 blockade in tumor bearing humanized mice.

First and foremost to test the survival of redirected T-cells in humanized mice, we generated CAR transduced T-cells using splenocytes from donor humanized mice and injected them into recipient mice that were reconstituted from the autologous HSC donor (**figure 4-5 A**). After adoptive transfer of redirected T-cells and serial blood draws (**figure 4-5 B**), CAR-T cells could be detected in the peripheral blood with almost no

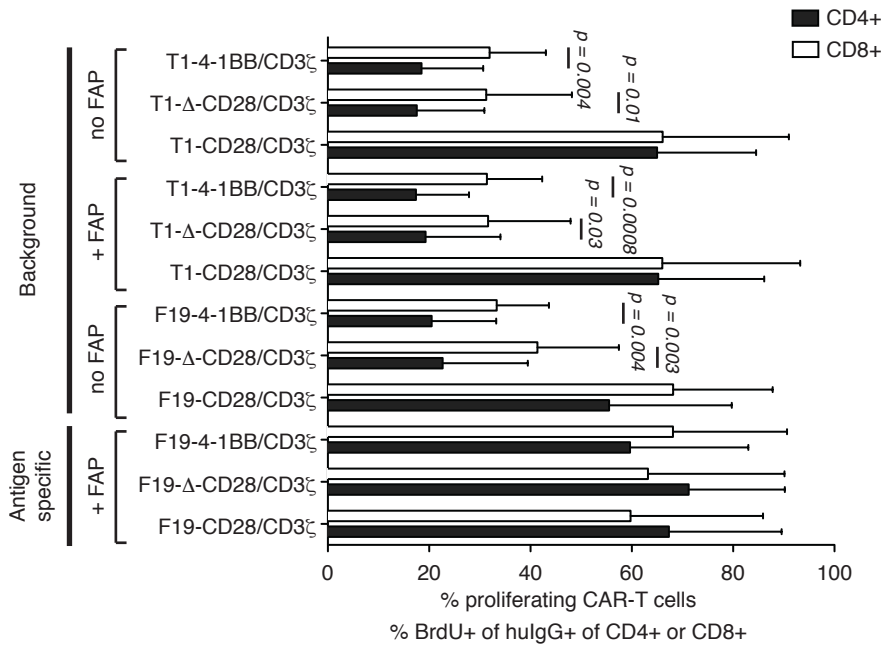

Figure S4-5. Comparing proliferation of CD4$^+$ and CD8$^+$ redirected T-cells. CD3$^+$ cells obtained from buffy donors were transduced to express FAP-specific CARs (F19-CD28/CD3ζ, F19-Δ-CD28/CD3ζ, F19-4-1BB/CD3ζ) or control CARs (T1-CD28/CD3ζ, T1-Δ-CD28/CD3ζ, T1-4-1BB/CD3ζ). The resulting redirected T-cells (mixture of CAR transduced and un-transduced CD4$^+$ and CD8$^+$ cells) were incubated with FAP or no FAP in BrdU supplemented medium. To identify proliferating CAR$^+$ cells of CD4$^+$ or CD8$^+$ lineage; we first gated on CD4$^+$ cells and CD8$^+$ cells individually, followed by gating on huIgG$^+$ cells and further selecting BrdU$^+$ cells. Figure shows frequency of proliferating CAR-T cells in response to antigen-specific stimulation (FAP-specific CAR-T cells incubated with FAP) or background proliferation (FAP specific CAR-T cells incubated without FAP or control CAR-T cells incubated with and without FAP) Pooled data from 8 buffy donors is shown (n=4). P values as mentioned are calculated using unpaired t-test. Data is presented as mean ± S.D.

significant difference between the groups. Up to at least 44 days, redirected T-cells persisted in the blood of humanized mice without any antigenic stimulus (**figure 4-5 C & D**). Additionally, we also examined the trafficking of these cells in organs of humanized mice. At day 44, we found these cells predominantly in the blood and in highest frequency of humanized NSG (huNSG) mice belonging to 4-1BB/CD3ζ group (75% mice) compared to CD28/CD3ζ (25% mice) or Δ-CD28/CD3ζ (40% mice) groups. In addition, we found CD28/CD3ζ redirected T-cells in the liver, spleen and BM of 50%, 25% and 50% of huNSG mice, respectively. Δ-CD28/CD3ζ redirected T-cells were observed in the BM of 40% huNSG mice only and 4-1BB/CD3ζ CAR-T cells in the liver of 25% of huNSG mice (**figure 4-5 E**).

After confirming the survival of redirected T-cells, we intended to investigate its impact on tumor development in huNSG mice. We injected human fibrosarcoma cells expressing FAP (HT1080FAP) in huNSG mice (**figure 4-6 A**). Prior to tumor inoculation, the expression of FAP and PD-L1 was confirmed by flow cytometry (**figure S4-6**). 96% of HT1080FAP tumor cells co-expressed FAP and PD-L1. The HT1080FAP tumor cell line is xenogeneic to the murine host and allogeneic to the reconstituted human immune compartment of the huNSG mice. To negate the possibility of the reconstituted human immune compartment impacting on the tumor

development (allogenicity of the tumor cell line towards the host immune cells), we examined the correlation of reconstitution frequency (% CD45$^+$ and % CD3$^+$ cells in blood) in huNSG mice with tumor development (after tumor inoculation and prior to injecting redirected T-cells).

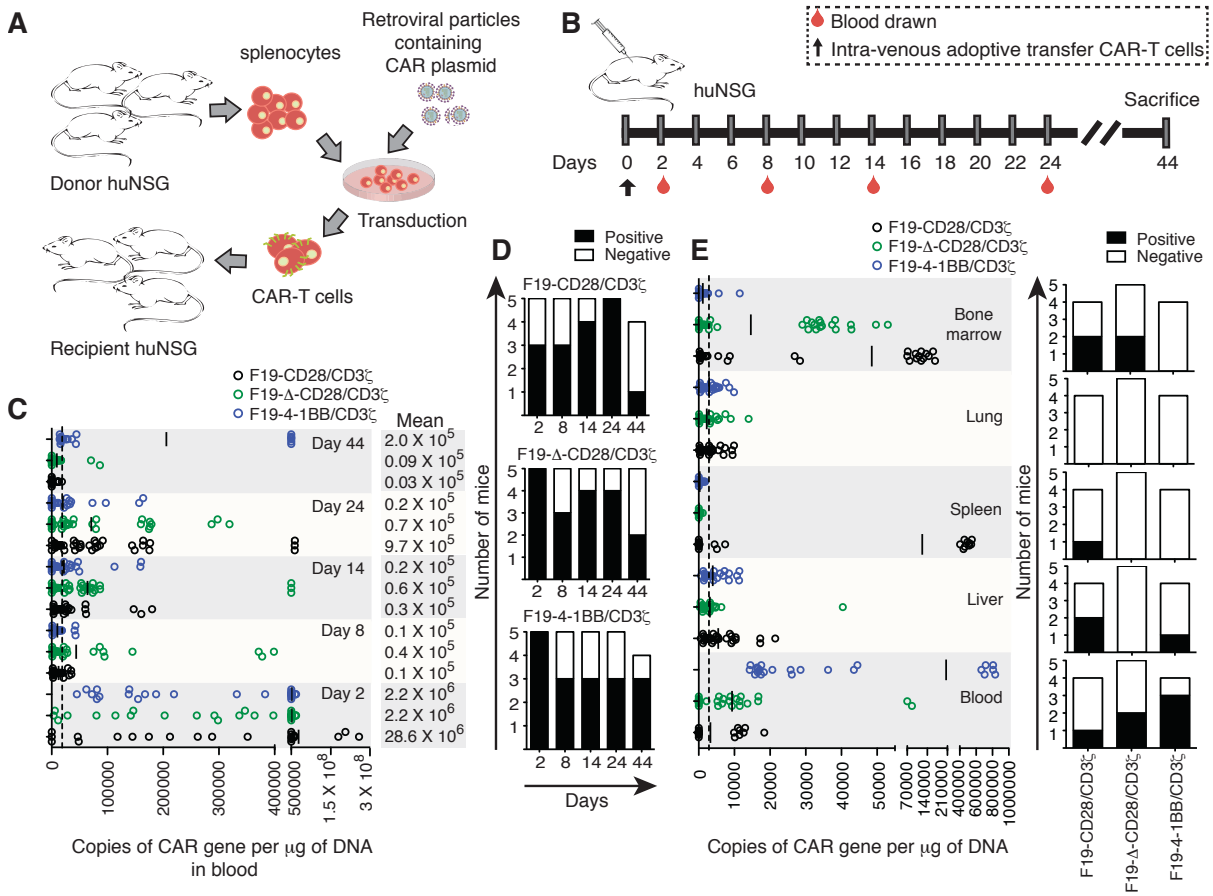

Figure 4-5. Survival of redirected T-cells in humanized mice. A Splenocytes were harvested from donor humanized NSG (huNSG) mice and transduced to express FAP-specific CARs with different co-stimulations (F19-CD28/CD3ζ, F19-Δ-CD28/CD3ζ and F19-4-1BB/CD3ζ). Redirected T-cells were then injected into recipient huNSG mice. **B** Time line of the adoptive transfer experiment is shown. Redirected T-cells were injected intra-venously at day 0. Blood was drawn at day 2, 8, 14, 24 and 44 after adoptive transfer. Mice were sacrificed at day 44 and organs were harvested. **C** Copies of CAR gene per μg of DNA in blood at day 2, 8, 14, 24 and 44 as quantified by qPCR. Mean CAR copies corresponding to each group and time point are indicated (-) and mentioned (right panel). Each circle represents one qPCR replicate (~6 replicates per mouse). Dashed line indicates detection threshold. **D** Number of mice (Y-axis) that showed positive CAR copies in the blood at specified time points (X-axis) in the F19-CD28/CD3ζ (top), F19-Δ-CD28/CD3ζ (middle) and F19-4-1BB/CD3ζ group (bottom). **E** Copies of CAR gene per μg of DNA in blood, liver, spleen, lungs and BM of harvested mice at day 44. Each circle illustrate one qPCR replicate (~6 replicates per mouse). Mean values are marked (-). Right panel shows number of mice (Y-axis) that showed positive CAR copies in corresponding organs in each group (X-axis). Representative data from one experiment with 5 mice per group is shown (n=3).

We found that tumor-take in huNSG mice was independent of the level of reconstitution (**figure S4-7 A**). The tumor bearing humanized mice were similarly distributed into the different experimental groups based on reconstitution in blood (% CD45$^+$) and tumor load (**figure S4-7 B**), prior to adoptive transfer of redirected T-cells.

As described previously, we used the peritoneal cavity to implant the tumor to have a physiological space, in which later redirected T-cells could be transferred in proximity to the tumor. Due to the strong expression of PD-L1 on the tumor cells (**figure S4-6**) and a high frequency of redirected T-cells expressing PD-1 (**figure 4-3 B**) the model allows for the testing of PD-1 blockade with T-cells expressing different CAR constructs.

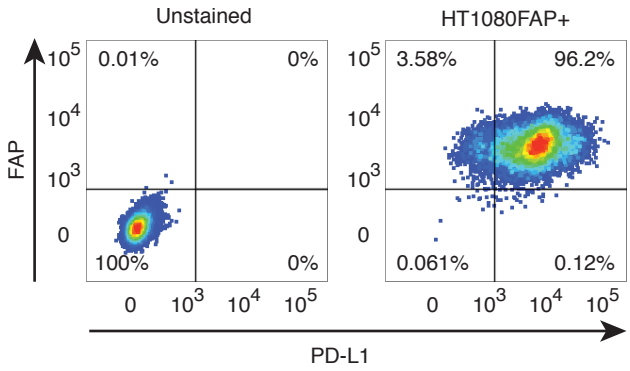

Figure S4-6. HT1080FAP cells stained for FAP and PD-L1 (right panel). Left panel indicates unstained cells.

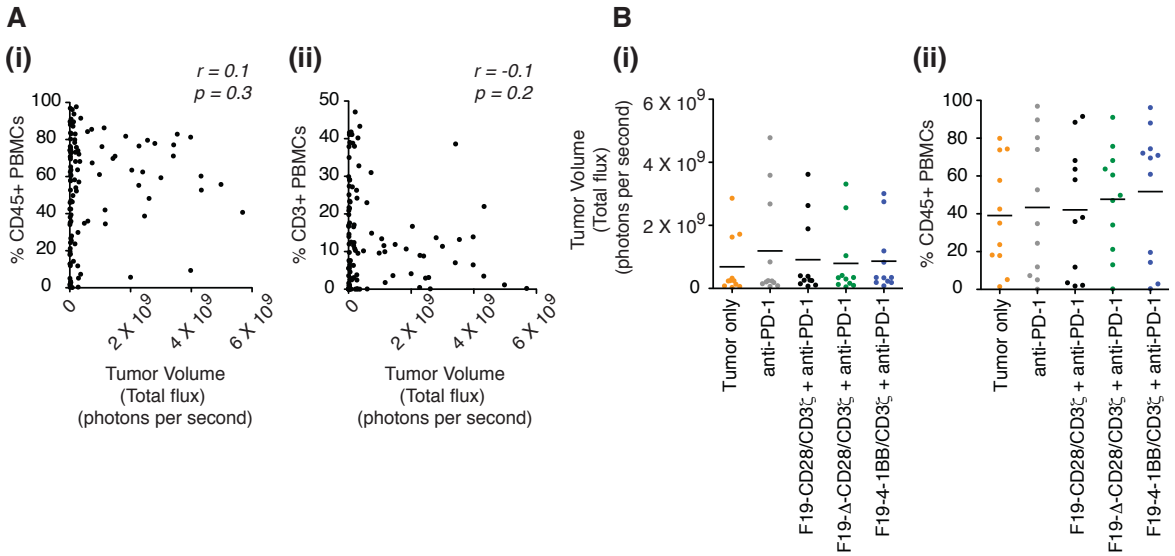

Figure S4-7. The allogenecity of reconstituted human immune compartment in humanized mice does not impact on tumor development. Humanized mice are reconstituted with donors that are allogeneic to FAP expressing tumor cell line (HT1080FAP). We thereby tested if the reconstituted immune cells of humanized mice would in general negatively impact on tumor development (pertaining to the allogenecity of the reconstituted immune compartment towards the injected tumor cells HT1080FAP) **A** Correlation of frequency of $CD45^+$ cells (left panel) and frequency of $CD3^+$ cells (right panel) in the blood of humanized mice with tumor volume (measured on IVIS; 1 day after tumor inoculation and prior to adoptive transfer of re-directed T-cells). Pearson correlation coefficient (*r*) and p value (*p*) is indicated (n = 117). **B** Mice were equally distributed in groups after tumor inoculation and before adoptive transfer of re-directed T-cells (day 2) based on tumor volume at day 1 (left panel) and human immune reconstitution in blood (as indicated by % $CD45^+$ cells in blood; right panel). Each dot represents one mouse (total mice per group = 11).

Before transfer, there was no *in vitro* effect of PD-1 blockade with regards to proliferation and antigen-specific cell killing by redirected T-cells (**figure S4-8**). After implantation of the tumor cells, functionally tested (*in vitro)* redirected T-cells (**figure 4-6 C & D**) were transferred in the peritoneal cavity and PD-1 blocking antibody was administered (**figure 4-6 B**). Surprisingly, only redirected T-cells expressing the F19-Δ-CD28/CD3ζ CAR induced significantly attenuated tumor growth (**figure 4-6 E**) and provided an improved survival of mice (**figure 4-6 F**).

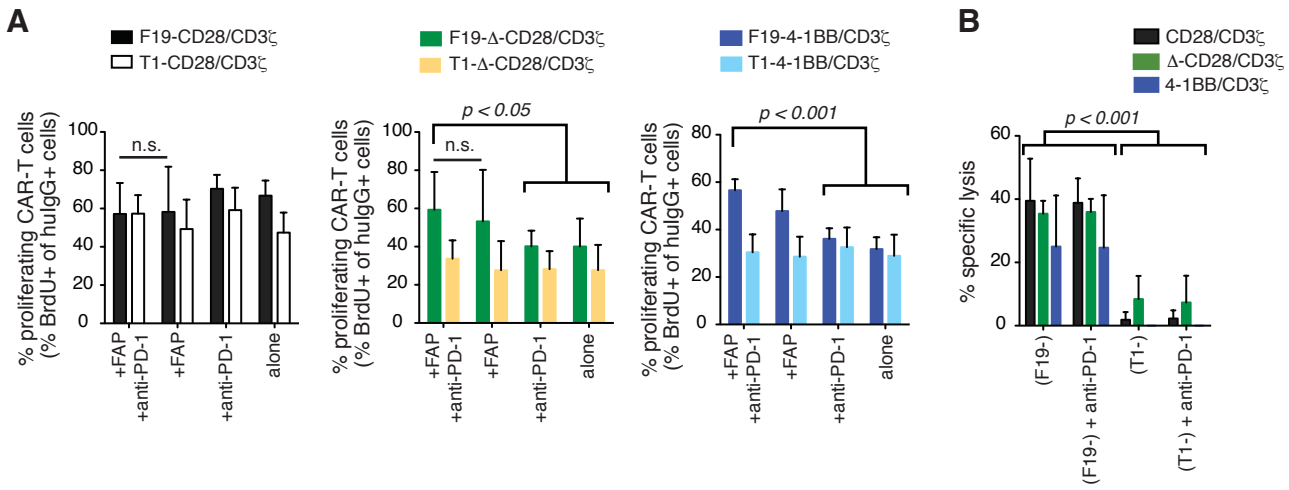

Figure S4-8. PD-1 blockade does not impact on proliferation and efficacy of re-directed T-cells *in-vitro*. A FAP-specific (F19) or control (T1) CAR-T cells with different co-stimulations (CD28/CD3ζ, Δ-CD28/CD3ζ or 4-1BB/CD3ζ) are seeded on recombinant human FAP coated plates (+FAP) or alone and with or without PD-1 blocking antibody (anti-PD-1). Proliferation of CAR-T cells is measured by BrdU proliferation assay and frequencies of proliferating CAR-T cells ($BrdU^+$ of $huIgG^+$) is plotted. **B** FAP-specific (F19) or control (T1) CAR-T cells with CD28, Δ-CD28 and 4-1BB co-stimulations (CD28/CD3ζ, Δ-CD28/CD3ζ and 4-1BB/CD3ζ, respectively) are co-incubated with FAP expressing tumor cells (HT1080FAP) with or without PD-1 blocking antibody (anti-PD-1). Lysis of HT1080FAP is measured and compared. Pooled data from four buffy donors in shown. P values are calculated using one way anova. Data is presented as mean ± S.D.

In this model, no redirected T-cells could be measured in the peripheral blood (**figure 4-7 A & figure S4-9**). Persistence of redirected T-cells could be identified in the Tumor Infiltrating Lymphocytes (TILs) and peritoneal lavage (**figure 4-7 A**). Interestingly, persistence was significantly enhanced in T-cells redirected by the 4-1BB/CD3ζ CAR contrasting anti-tumor efficacy. Nevertheless, only the number of redirected T-cell by the Δ-CD28/CD3ζ showed a significant inverse correlation with tumor development (**figure 4-7 B & figure S4-10**). Finally, there was no statistically significant difference in frequency of Tregs infiltrating tumors between the different CAR groups (**figure S4-11**) suggesting no prominent role of regulatory T-cells for the stronger therapeutic effect mediated by the Δ-CD28/CD3ζ CAR in combination with PD-1 checkpoint blockade.

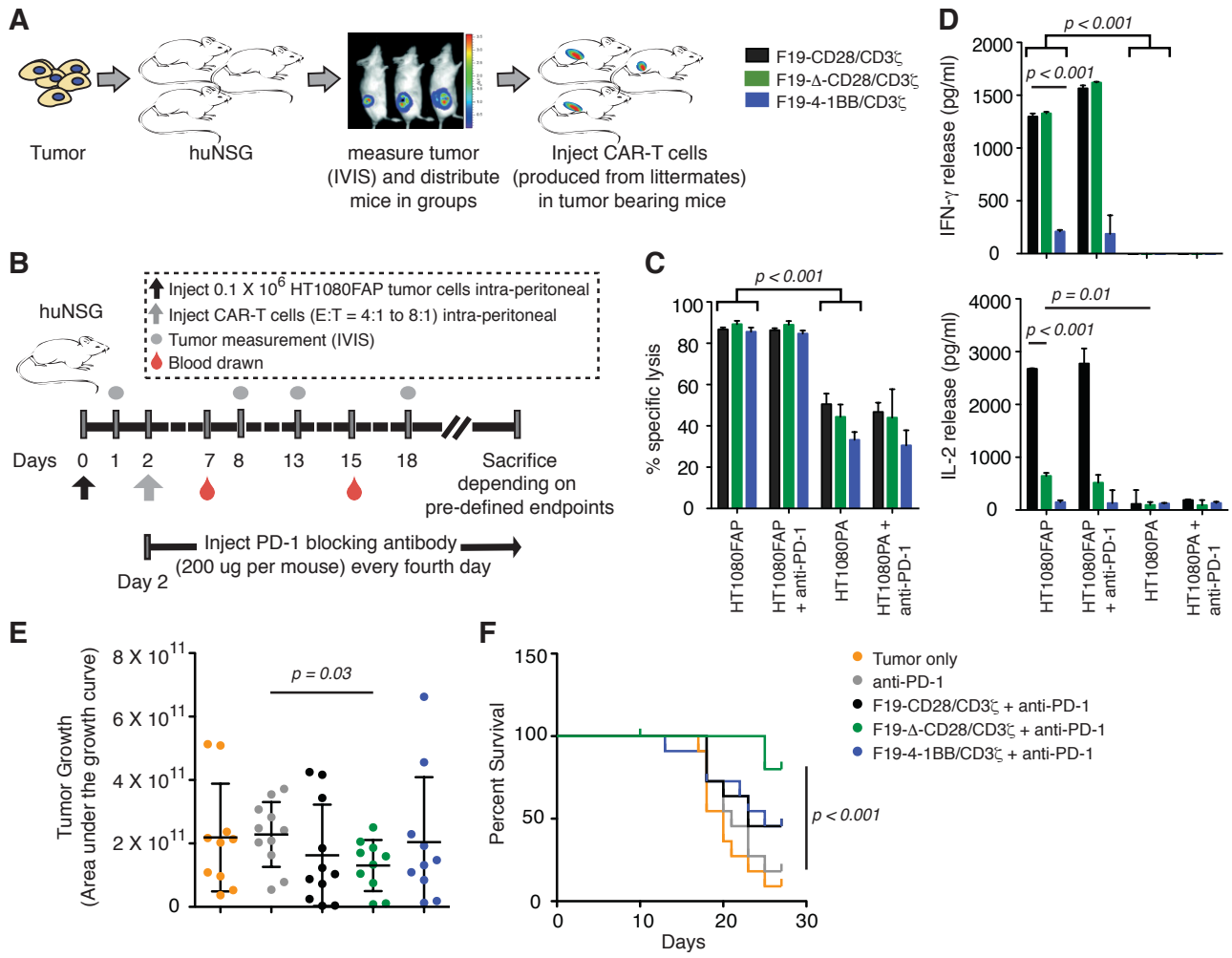

Figure 4-6. Adoptive transfer of redirected T-cells in tumor bearing humanized mice. A HT1080FAP cells were injected intra-peritoneally in huNSG mice. Tumor development was monitored and mice were distributed into groups (day 1) before injecting redirected T-cells, produced from donor matched littermates (day 2). **B** Timeline of adoptive transfer. Tumor cells were injected at day 0, followed by measuring tumor in IVIS at day 1. After grouping mice based on tumor development, redirected T-cells at E:T = 4:1 to 8:1 were injected at day 2. Blood was drawn on day 7, 15 and at the time of sacrifice. Tumor measurements were performed at day 1, 8, 13 and 18 post tumor injection. Mice were sacrificed based on pre-defined endpoints and the experiment was terminated at day 27. Starting from day 2, mice received PD-1 blocking antibody every fourth day. **C** FAP-specific redirected T-cells produced from donor matched littermates of huNSG, were co-cultivated with tumor cells expressing FAP (HT1080FAP) or no FAP (HT1080PA) with or without PD-1 blocking antibody (anti-PD-1). Tumor cell lysis was measured (n=2). **D** IFN-γ and IL-2 release in supernatants from co-culture of redirected T-cells with tumor cells was measured by ELISA (n=2). P-value calculated using unpaired t-test. **E** Tumor volume measured as photons per second (in IVIS) at day 1, 8, 13 and 18 was plotted and area under the tumor growth curve (AUC) was calculated for each mouse. Each dot represents the AUC of one mouse. Data is presented as mean ± S.D. P-value is calculated using mann whitney test. **F** Percentage of survival of mice is indicated by a kapplan meier curve. P value is calculated using log rank test. Cumulative data from 3 cohorts of mice in two independent experiments is shown (total mice per group = 11).

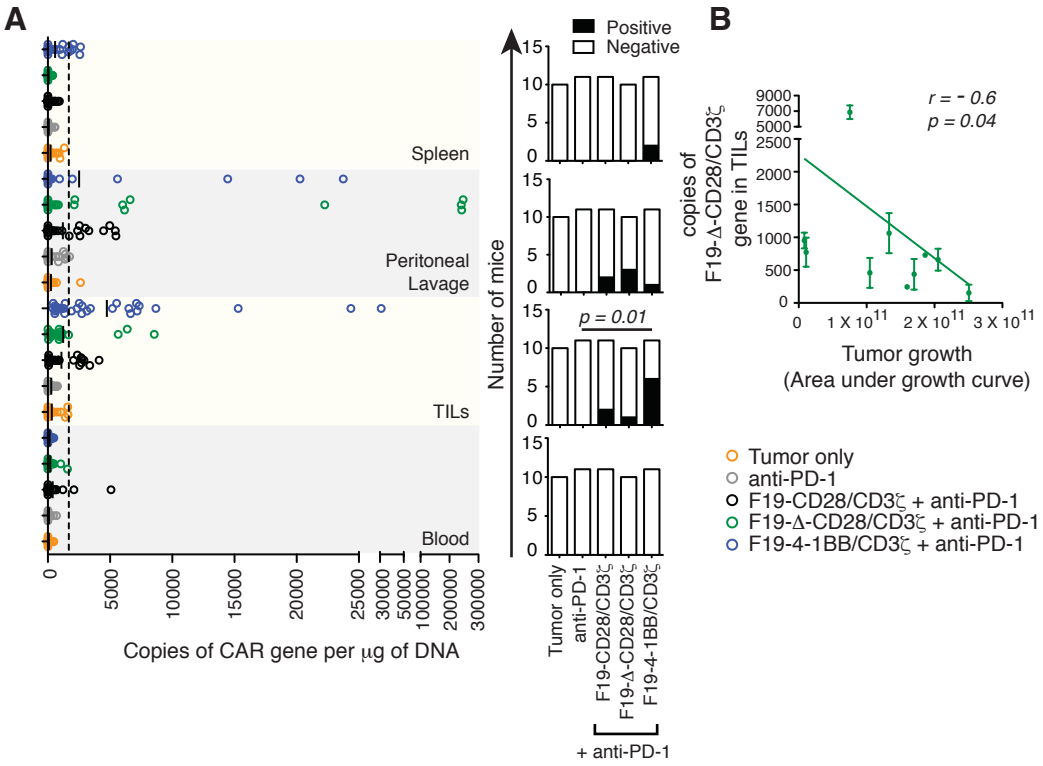

Figure 4-7. Persistence of redirected T-cells in Tumor Infiltrating lymphocytes (TILs) and Peritoneal Lavage (PL). A Copies of CAR gene per μg of DNA was quantified by qPCR in blood, TILs, PL and spleen of harvested mice (Left panel). Each circle indicates one qPCR replicate (total 3 replicates per mouse). Dashed line indicates detection threshold. Right panel indicates number of mice (Y-axis) from each group (X-axis) that showed positive CAR copies in the corresponding organ. P value is calculated using Fischer's exact test. **B** Correlation of copies of F19-Δ-CD28/CD3ζ gene in TILs with tumor growth (area under the curve). Data is presented as mean ± SEM. Spearman correlation coefficient (*r*) and p value (*p*) is mentioned. Each dot is one mouse (n = 11). Error bars depicts the variation between qPCR replicates.

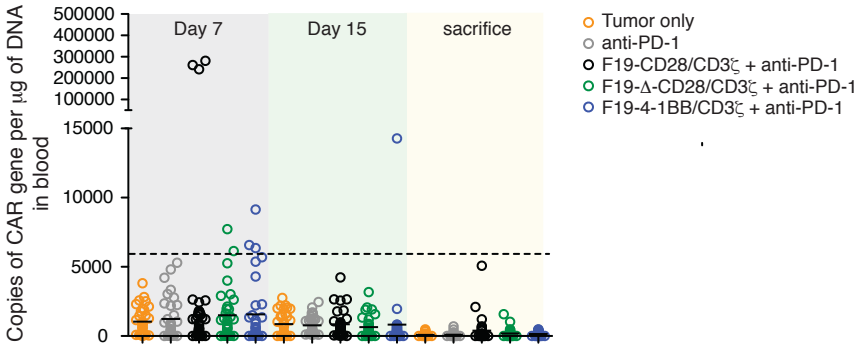

Figure S4-9. Re-directed T-cells did not show persistence in the blood of tumor bearing humanized mice. Copies of CAR gene per μg of DNA in blood is shown for each group. Each circle represents one qPCR replicate (total 3 replicates per mouse). Dashed line indicates background threshold level. Pooled data from three cohorts of mice with total 11 mice per group is shown.

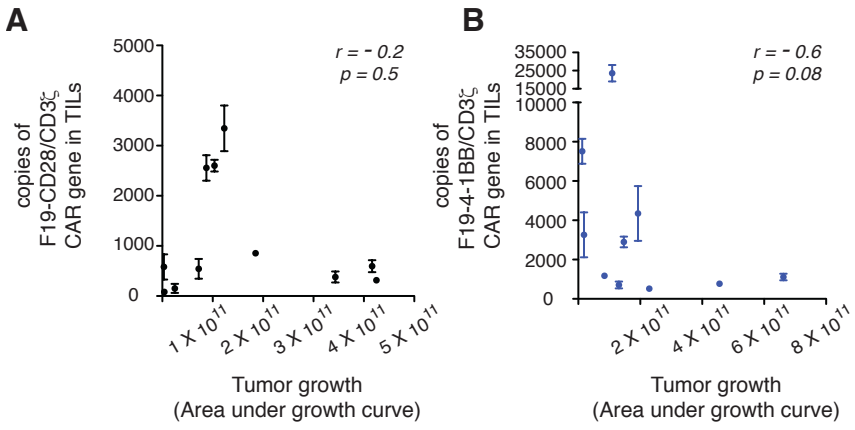

Figure S4-10. Correlation of **A** copies of F19-CD28/CD3ζ gene **B** copies of F19-4-1BB/CD3ζ gene in TILs with tumor growth (area under the curve). Data is presented as mean ± SEM. Spearman correlation coefficient (*r*) and p value (*p*) is mentioned. Each dot is one mouse (n = 11). Error bars depicts the variation between qPCR replicates.

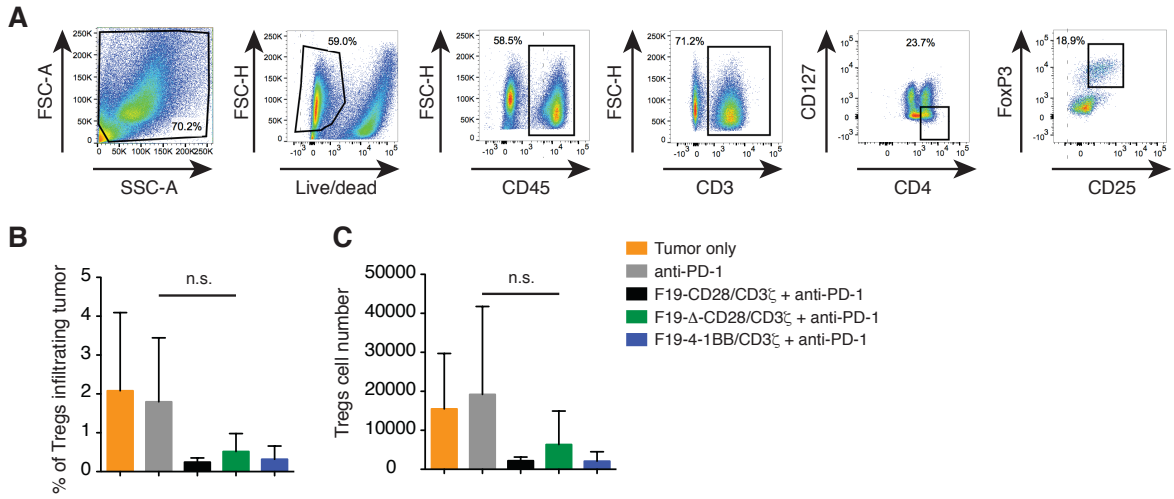

Figure S4-11. Staining for Tregs infiltrating tumor. Tumor Infiltrating Lymphocytes (TILs) from harvested mice were used to stain for Tregs. **A** To identify Tregs; we first gated on lymphocytes in the TILs, followed by selecting living cells and then $CD45^{+}$ cells, further gating $CD3^{+}$ cells and next $CD4^{+}CD127^{lo}$ and finally gating on $CD25^{hi}FoxP3^{+}$ (Tregs) cells **B** % of Tregs infiltrating tumors and **C** Tregs cell number is shown for each group. Pooled data from three cohorts of mice with total 11 mice per group is shown.

4.3.6 First-in-man adoptive transfer of lck lacking CD28 CAR showed persistence of redirected T cells up to 21 days.

Based on our initial data we designed a first-in-human clinical protocol [215] for the treatment of MPM patients with FAP-specific redirected T-cells to implement FAP-specific redirected T-cells as a platform for combination therapies as exemplarily tested in the previously described experiments. In this clinical trial, we aimed to use a new application method for the administration of redirected T-cells supported by our experience from mouse models. Redirected T-cells were injected in proximity to the malignant cells directly into the pleural infusion

(**figure 4-8 A**). To better characterize the injection site, pleural effusions of different patients with MPM were analyzed as first step. Some MPM pleural effusions showed prominent levels of TGF-β, IL-10 and VEGF suggesting an immune suppressive microenvironment (**figure S4-12**). However, these pleural effusions did not block in general the antigen-specific release of IFN-γ when compared to cell culture supernatant (**figure 4-8 B**). The first patient was treated 21 days after collection of autologous PBMCs and GMP redirection of his T-cells by the F19-Δ-CD28/CD3ζ against FAP (**figure 4-8 C**). At the day of transfer, the patient`s redirected T-cells were also tested *ex-vivo* (**figure 4-8 D**). These cells showed antigen-specific release of IFN-γ, IL-2, IL-10 and TNF-α.

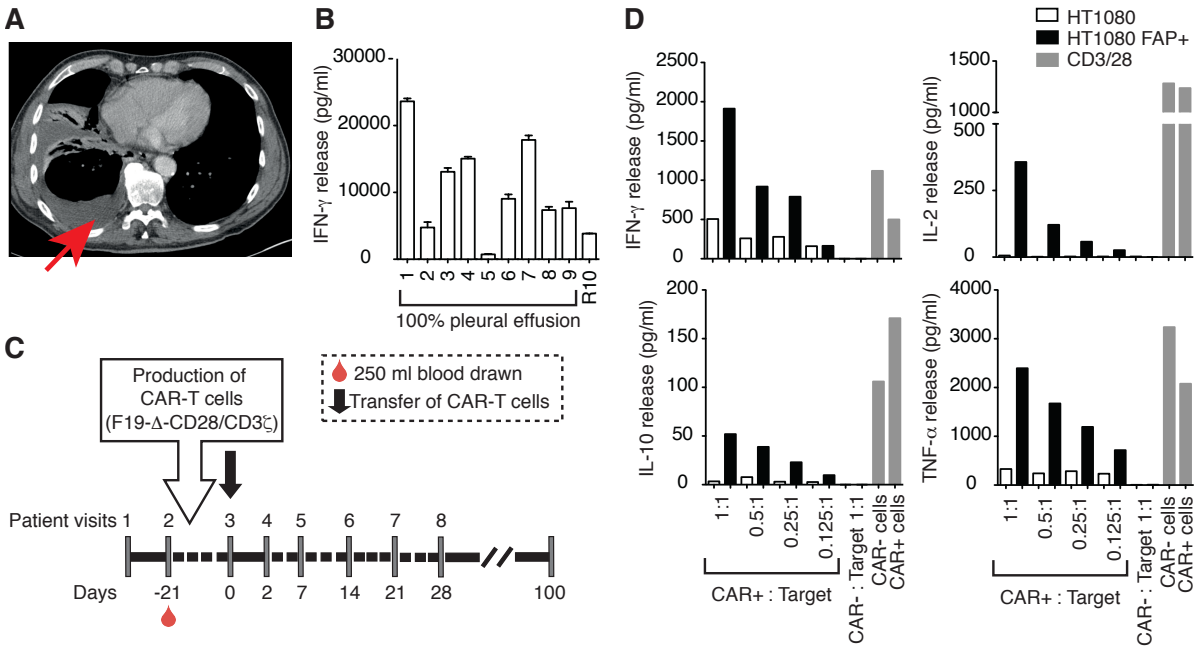

Figure 4-8. A shows CT scan of lung of first patient in the clinical trial (→ indicates the pleural effusion, in which the redirected T cells were injected **B** F19-Δ-CD28/CD3ζ redirected T cells were incubated with HT1080FAP target cell in pleural effusions from different donors (1-9) or culture media (R10) and IFN-γ release was measured by ELISA. **C** Time schedule of the clinical phase I trial **D** GMP produced, redirected FAP-specific T-cells were tested *in vitro* before transfer in different effector to target ratios and cytokines were measured. "CAR-" indicates un-transduced T-cells.

Next, the lymphocyte counts, cytokines and the CAR persistence was evaluated in the peripheral blood according to the study protocol (**figure 4-9**). Initially, lymphocyte counts and cytokines levels (IFN-γ, IL-2, IL-6, IL-10 and TNF-α) dropped, followed by an increase of IL-10 at later time points (**figure 4-9 A-C**). Most interestingly, we observed F19-Δ-CD28/CD3ζ CAR-T cell expansion which peaked in the peripheral blood at day 21 post infusion (**figure 4-9 D**).

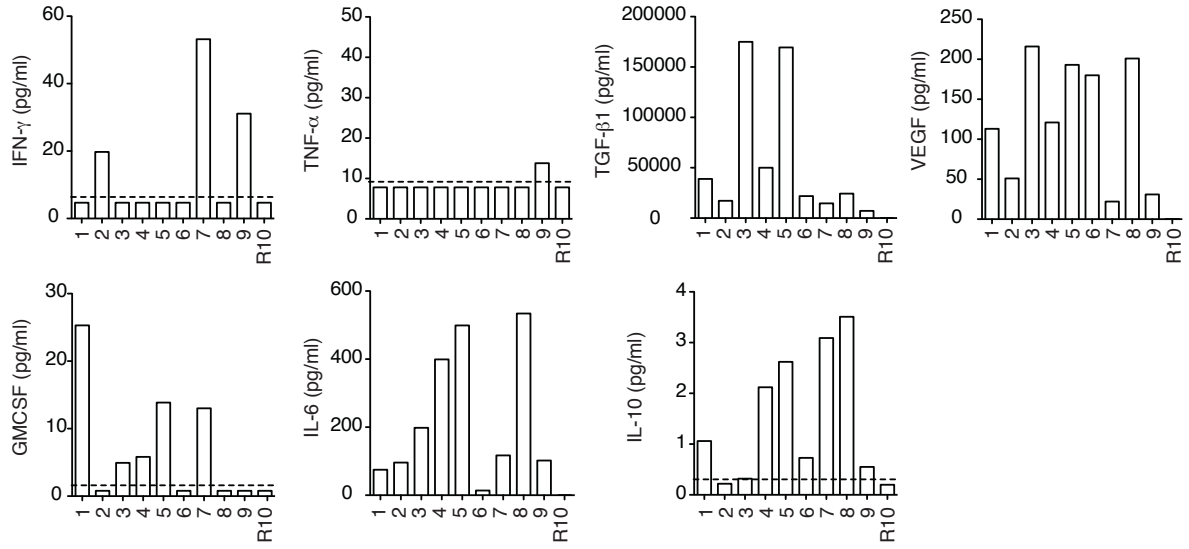

Figure S4-12. Baseline level of cytokines measured in pleural effusions from different donors (1-9) *ex-vivo* by ELISA (R10 culture medium alone as negative control).

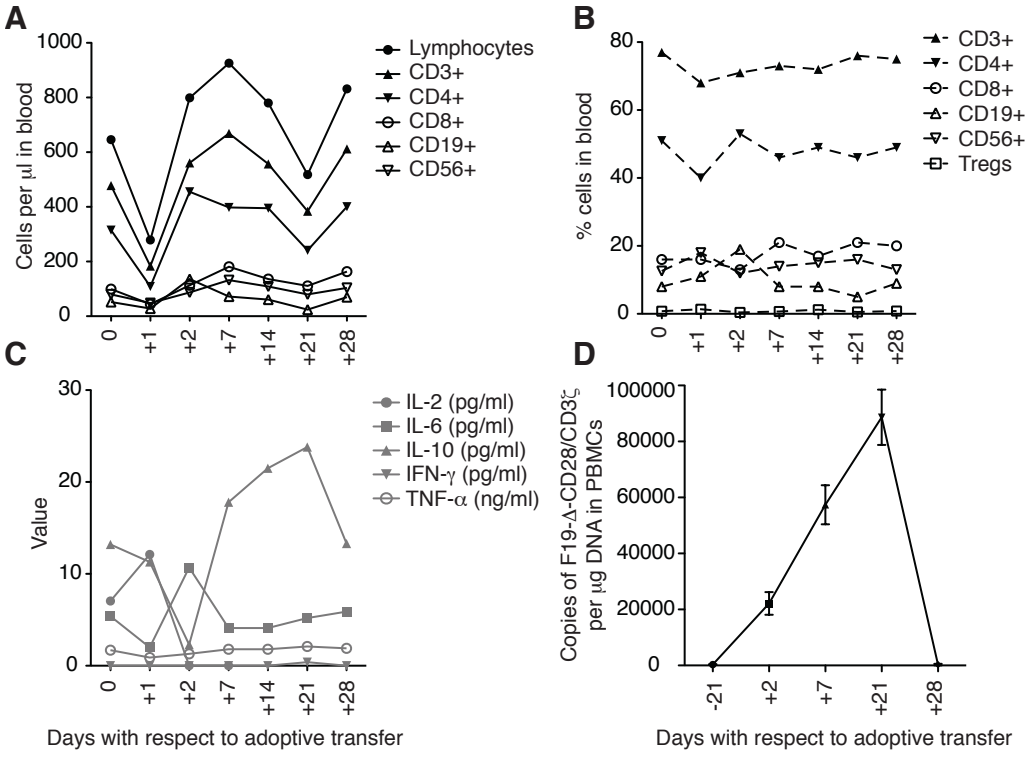

Figure 4-9. Cell counts, cytokine level and CAR copies measured between day 0 (day of transfer) and day +28 after transfer. A absolute counts of leukocyte subsets **B** percentages of leukocyte subsets **C** cytokine levels measured in the peripheral blood **D** copy numbers of the CAR (F19-Δ-CD28/CD3ζ) gene in the peripheral blood measured in relation to peripheral blood mononuclear cell (PBMC) DNA amount (per μg).

Table S4-1. List of differentially regulated cell-cycle genes

Category	HGNC symbol	Log2FC values			Category	HGNC symbol	Log2FC values		
		CD28/CD3ζ	Δ-CD28/CD3ζ	41BB/CD3ζ			CD28/CD3ζ	Δ-CD28/CD3ζ	41BB/CD3ζ
Actin related proteins	ACTR3	0.459	1.262	1.137	Cyclins	CCNA1	4.11	4.11	2.97
	AFAP1L2	3.349	4.678	3.349		CCNA2	1.31	3.37	1.85
	ANLN	1.102	2.612	0.665		CCNB1	1.33	2.98	1.16
	SMARCB1	0.107	0.640	0.186		CCNB2	1.14	3.54	1.97
	SMARCD3	-1.077	-2.228	-2.354		CCND1	2.06	1.79	-1.13
AMP activated protein kinases	PRKAA1	-0.449	-0.670	-0.035		CCND2	0.99	1.60	1.44
	PRKAB2	-0.617	-1.320	-0.748		CCND3	0.16	0.94	0.60
	PRKAG2	-1.052	-1.274	-0.708		CCNE1	1.01	2.22	1.35
Anaphase-promoting Complex-cyclosome	CDC20	1.567	3.674	1.596		CCNE2	0.51	1.89	1.31
	CDC20B	1.790	4.317	3.636		CCNF	0.63	1.83	0.83
	HSBP1L1	-0.623	-1.713	-0.843		CCNL2	-0.85	-1.56	-0.81
	HSP90AA1	0.320	0.963	0.613		CCNYL1	-0.60	-1.29	-0.80
	HSP90AB1	0.743	1.264	1.160	Cyclin dependent kinases	CDK1	1.34	3.49	1.89
	HSPA8	0.541	1.095	1.017		CDK10	-0.71	-0.99	-0.34
Apoptosis related	APITD1	0.526	1.264	1.033		CDK11B	-0.51	-0.61	-0.09
	BCL2L1	1.225	2.675	1.844		CDK2	0.89	1.76	1.18
	BID	-1.319	-1.445	-0.893		CDK20	-1.27	-2.10	-1.55
	DDIAS	1.208	2.677	1.827		CDK2AP1	0.79	1.62	0.65
	TRIAP1	0.064	0.643	0.369		CDK4	0.66	1.60	0.85
Aurora kinases	AUNIP	1.708	3.738	1.446		CDK6	1.63	2.14	1.75
	AURKA	1.462	2.980	1.701		CKS1B	0.93	2.35	1.36
	AURKB	0.874	3.062	1.381		CKS2	0.98	2.59	1.29
CDC25 phosphatases	CDC25A	1.307	2.847	1.013	Cyclin dependent kinase inhibitors	CDKN1A	1.08	1.86	1.65
	CDC25C	1.052	3.347	1.577		CDKN1B	-0.68	-1.51	-1.37
Cell division cycle associated	CDCA2	1.065	3.157	1.931		CDKN2C	0.32	1.33	0.18
	CDCA3	0.575	2.408	1.570		CDKN3	0.99	2.99	1.76
	CDCA4	0.567	1.338	1.088	DNA polymerases	POLA1	0.66	1.63	0.98
	CDCA5	1.028	3.508	1.947		POLA2	0.51	1.65	0.95
	CDCA7	0.990	2.046	0.907		POLE	0.28	1.05	0.69
	CDCA7L	1.306	2.441	2.044		POLE2	1.20	3.21	1.56
	CDCA8	0.877	3.111	1.568	Geminin	GMNN	0.79	1.81	0.54
Centromere and centrosomal protein	CENPA	0.942	2.793	2.027	Integrins	ITGA2	0.82	1.69	1.56
	CENPE	1.196	2.431	1.283		ITGA5	0.23	-1.43	-0.46
	CENPF	1.078	2.471	1.187		ITGB3BP	0.59	1.06	0.53
	CENPH	1.294	2.388	1.662		ITGB5	3.41	2.98	-1.64
	CENPI	1.216	2.630	0.768	Kinesins	KIF11	0.98	2.58	1.69
	CENPJ	0.855	1.450	1.199		KIF14	1.36	3.29	1.66
	CENPL	0.491	1.581	1.061		KIF15	1.27	3.69	2.39
	CENPM	0.754	2.876	1.658		KIF18A	0.85	2.20	1.50
	CENPN	0.938	2.744	1.561		KIF18B	0.80	3.49	1.70
	CENPO	0.428	1.761	1.303		KIF20A	1.02	3.18	1.37
	CENPP	0.609	2.514	1.345		KIF20B	0.88	1.46	1.15
	CENPQ	1.072	1.928	1.517		KIF23	0.93	2.88	1.44
	CENPT	-0.863	-1.445	-0.964		KIF2A	0.80	1.02	1.38
	CENPU	1.095	3.044	1.900		KIF2C	1.27	3.42	2.02
	CENPW	0.982	2.557	0.846		KIF4A	1.03	2.97	1.40
	CEP41	0.738	1.117	0.527		KIFC1	0.88	3.54	2.16
	CEP55	1.386	3.689	2.443	MAD2	MAD2L1	1.10	1.99	1.09
Cohesin and Condensin	CAPN3	-1.529	-2.618	-1.874	Minichromosome maintainance proteins	MCM10	1.68	3.65	1.50
	DSCC1	1.562	3.194	1.466		MCM2	1.28	2.98	1.68
	NCAPD2	0.500	1.353	0.907		MCM3	0.82	2.05	1.19
	NCAPD3	0.682	1.504	0.964		MCM4	0.95	2.47	1.35
	NCAPG	1.180	3.018	1.663		MCM5	0.78	1.91	1.47
	NCAPG2	1.063	2.483	1.513		MCM6	0.87	1.81	1.29
	NCAPH	0.806	2.234	1.527		MCM7	0.68	1.80	0.94
	SMC1A	0.625	1.406	0.862		MCM8	1.36	2.18	1.39
	SMC1B	2.123	2.448	1.720		MCMBP	0.52	1.20	0.99
	SMC2	1.039	2.048	1.488	Meiotic and Mitotic checkpoint proteins	BARD1	0.47	1.06	0.97
Cullin	CUL4A	-0.165	-0.461	0.110		BRIP1	0.99	2.09	1.24

Table S4-1. Continued

Category	HGNC symbol	Log2FC values		
		CD28/CD3ζ	Δ-CD28/CD3ζ	41BB/CD3ζ
Meiotic and Mitotic checkpoint proteins	BRCA1	1.39	2.96	1.74
	BRCA2	1.41	2.49	1.59
	BUB1	1.33	2.54	1.44
	BUB1B	1.00	2.33	1.40
	CDC6	1.42	3.39	1.59
	CHEK1	1.31	3.33	2.09
	CHEK2	0.02	0.70	0.05
	ERCC6L	1.37	3.13	1.14
	MYB	1.08	2.15	1.54
	MYBL2	1.13	3.45	1.24
	RAD51	1.31	3.81	2.40
	RAD51C	0.32	1.19	0.85
	RAD9B	0.35	1.65	1.49
	TICRR	1.34	3.26	1.88
	TOM1L2	-0.53	-1.07	-0.58
NIMA related kinases	NEK2	0.89	2.68	1.25
	NEK6	1.07	2.50	1.16
Nucleoporins	NUP155	0.65	0.96	0.41
	NUP205	0.70	1.03	0.43
	NUP210	0.05	0.62	0.48
	NUP37	1.07	1.73	1.03
	NUP62	0.44	1.12	0.66
Origin recognition complex	ORC1	1.26	3.26	2.00
	ORC6	0.66	2.12	1.36
Primase	PRIM1	0.88	1.83	1.45
	PRIM2	0.66	1.41	1.13
Proteasome related	PSMA2	0.64	1.33	1.02
	PSMA5	0.10	0.68	0.47
	PSMA6	0.44	0.99	0.98
	PSMA8	0.50	1.55	0.43
	PSMB2	0.16	0.83	0.46
	PSMB5	0.77	1.21	0.45
	PSMB7	0.20	0.88	0.50
	PSMB8	0.13	0.95	0.92
	PSMC3	0.23	1.12	0.63
	PSMD1	0.42	1.07	0.75
	PSMD14	0.57	1.16	0.93
	PSMD8	0.14	0.80	0.56
	PSME2	0.05	0.96	0.82
	PSME3	0.11	0.70	0.43
Transcription factors and associated genes	ATF5	-0.19	0.83	-0.01
	E2F1	0.80	2.62	1.33
	E2F2	0.62	3.07	1.64
	E2F3	-0.89	-1.41	-0.56
	E2F7	1.02	2.77	1.34
	E2F8	0.83	3.57	2.33
	E4F1	-0.70	-1.03	-0.51
	INSM1	4.04	3.45	0.17
	JUNB	1.21	1.56	0.52
	JUND	0.56	1.11	0.46
	MNT	-0.45	-0.67	-0.14
	RB1	0.18	0.58	0.69
	RBL1	0.33	0.67	0.83
	RBL2	-1.15	-1.70	-1.28
	TFDP1	0.36	1.00	0.74
TRIM family	TRIM13	-0.68	-1.26	-1.11
	TRIM25	0.70	1.22	0.94
	TRIM35	0.28	0.82	0.38
	TRIM38	-0.38	-0.81	-0.27
TRIM family	TRIM59	2.95	2.67	0.35
Tubulins	TUBA4A	0.66	1.32	1.15
	TUBB	0.93	2.89	1.48
	TUBB4B	0.49	1.81	0.89
	TUBE1	0.14	-0.74	0.09
	TUBG1	0.72	1.61	0.56
Other cell cycle associated genes	ACVR1B	1.52	1.09	-1.12
	ADAM17	-0.12	-0.63	-0.14
	ADARB1	-1.24	-1.86	-0.99
	ADGRL1	-0.59	-1.51	-1.52
	AGO4	-0.58	-1.28	-0.88
	AIF1	0.70	1.70	0.79
	AK1	-0.67	-1.33	-1.02
	AKAP8	-0.38	-0.66	-0.14
	ALYREF	0.27	1.15	0.69
	ANGEL2	-0.36	-1.09	-0.50
	APBB2	4.29	3.97	1.84
	APP	0.25	0.90	-0.53
	APPL2	-0.64	-1.46	-0.77
	ARNTL	-0.70	-1.35	-0.83
	ASPM	1.16	3.11	1.90
	ATAD5	1.27	2.33	1.63
	AXL	5.10	2.28	1.63
	BANF1	0.28	1.04	0.53
	BANP	-0.64	-0.96	-0.24
	BCKDK	0.92	1.28	0.53
	BIN1	-0.56	-1.07	-0.50
	BIRC5	0.89	3.10	1.29
	BLM	0.85	1.45	1.35
	BST2	0.70	1.52	0.93
	BTG4	4.03	3.20	1.92
	C10orf99	5.78	4.25	0.25
	CABLES1	1.23	1.89	0.00
	CABLES2	0.06	0.62	0.18
	CACNA1A	0.18	1.43	0.36
	CALR	-0.05	0.74	0.56
	CAMK1	1.47	2.42	2.08
	CASC5	1.02	3.07	2.04
	CAV1	3.63	3.85	3.34
	CCL3	2.13	3.91	4.02
	CCL4	1.61	1.82	2.61
	CCL5	-1.58	-1.86	-1.25
	CCP110	0.73	1.01	1.26
	CCR5	-1.78	-2.50	-0.81
	CD80	2.22	2.99	1.29
	CDC45	1.20	3.62	1.85
	CDK5RAP3	-1.05	-1.54	-0.99
	CDT1	1.11	3.45	1.54
	CETN3	0.87	1.52	1.02
	CGREF1	2.94	4.21	4.22
	CHAF1A	0.68	1.96	0.99
	CHAF1B	0.81	1.82	1.08
	CHMP7	-0.87	-1.44	-1.19
	CHTF18	0.21	1.01	0.66
	CIT	0.93	2.68	0.85
	CKAP5	0.52	1.18	0.63
	CLIC1	0.21	1.02	0.53
	CLSPN	1.05	3.56	1.70
	ESPL1	1.35	3.16	1.97

Table S4-1. Continued

Category	HGNC symbol	Log2FC values			Category	HGNC symbol	Log2FC values		
		CD28/CD3ζ	Δ-CD28/CD3ζ	41BB/CD3ζ			CD28/CD3ζ	Δ-CD28/CD3ζ	41BB/CD3ζ
Other cell cycle associated genes	CROCC	-0.89	-1.36	-0.73	Other cell cycle associated genes	HAUS3	-0.69	-0.91	-0.38
	CTC1	-1.32	-2.04	-1.43		HCFC1	0.16	0.82	0.59
	CTDSPL	1.39	2.62	-0.22		HECA	-0.54	-1.18	-0.68
	CXCR5	2.22	1.70	0.49		HELLS	0.91	1.86	1.25
	CYP1A1	2.02	2.79	1.28		HERC5	0.82	1.84	0.79
	CYP27B1	1.43	2.10	2.23		HJURP	0.94	3.25	2.23
	DBF4B	0.47	1.51	0.78		HMMR	1.63	3.92	2.34
	DCLRE1B	0.76	1.52	1.08		HYAL2	0.75	1.75	0.05
	DDIT3	-0.84	-1.46	-0.38		ICAM1	0.77	1.70	0.63
	DEPDC1	1.16	2.30	0.60		ID3	2.61	2.15	-0.03
	DEPDC1B	1.01	2.90	1.63		IFIT1	3.06	4.82	2.68
	DEPDC4	1.60	2.75	0.62		IFITM1	0.30	1.29	0.36
	DHCR24	1.29	2.70	1.27		IFITM2	0.31	1.21	0.35
	DHFR	0.64	1.63	0.47		IFNG	1.45	2.13	3.96
	DIXDC1	2.01	1.49	0.91		IGF1	3.76	5.29	3.21
	DLD	0.73	1.33	0.85		IL1A	4.59	5.46	4.03
	DLGAP5	1.15	3.29	1.65		IL1B	5.77	4.09	2.73
	DMC1	1.58	3.58	1.81		INCENP	0.45	1.62	0.98
	DNA2	1.12	2.02	1.54		INHBA	4.10	6.09	4.14
	DONSON	0.76	1.30	0.88		IQGAP3	1.43	3.40	1.30
	DSN1	0.54	1.04	0.63		IRF6	3.26	3.87	3.07
	DTL	1.67	3.71	1.91		KANK2	0.61	1.51	-1.24
	DTYMK	0.38	1.76	0.99		KIAA0101	1.10	3.69	2.29
	DYNLL1	0.10	0.88	0.29		KIZ	-0.84	-1.32	-1.40
	ECT2	0.99	2.31	0.98		KLHL21	-1.32	-1.72	-0.77
	EIF4G1	0.30	0.80	0.71		KLLN	1.71	1.63	0.90
	EME1	1.60	3.25	1.95		KNSTRN	0.83	1.57	1.04
	EML4	-0.44	-0.94	-0.37		KNTC1	1.15	2.04	1.47
	ENSA	0.02	0.62	0.37		KPNA2	0.72	2.04	0.99
	ERH	0.25	0.93	0.50		KPNA5	-0.89	-1.55	-1.12
	ERN1	-1.42	-2.08	-1.15		LAMP3	2.24	3.37	2.36
	ESCO2	1.44	3.74	2.42		LAMTOR2	0.22	0.96	0.49
	EXO1	1.40	3.23	1.50		LDLR	0.72	1.75	1.81
	EZH2	0.57	1.87	1.45		LGALS1	1.77	3.35	2.60
	FANCA	0.46	2.00	0.92		LGALS9	-0.24	1.72	0.01
	FANCD2	0.61	1.21	0.64		LIF	1.89	4.24	3.70
	FANCG	0.51	1.52	1.11		LIG1	0.60	1.28	1.09
	FANCI	0.90	2.37	1.25		LIN37	-0.63	-1.32	-0.78
	FBXO43	0.45	3.49	2.91		LIN52	0.31	0.86	0.93
	FBXO5	0.51	1.81	1.17		LIN9	0.77	1.15	0.21
	FBXW5	-0.78	-0.55	-0.26		LLGL2	-1.33	-2.79	-1.84
	FEN1	1.08	2.78	1.47		LPIN1	-0.72	-1.08	-0.50
	FER	1.29	1.17	0.55		LRRCC1	0.54	1.23	0.82
	FGFR1	0.78	1.94	0.09		LZTS2	-0.55	-1.22	-0.88
	FH	0.70	1.35	1.06		MAP3K8	1.11	1.38	0.53
	FOXM1	0.83	2.98	1.34		MAPK12	-0.86	-1.41	-0.99
	FOXO4	-0.63	-1.01	-0.37		MAPRE1	-0.07	0.45	0.25
	GAS6	-2.20	-3.62	-3.28		MASTL	0.89	1.52	1.21
	GDPD5	-0.52	-1.89	-1.53		MCTS1	0.26	0.77	0.43
	GEM	3.61	2.79	2.25		MDM4	-0.91	-1.42	-0.76
	GEN1	0.47	1.06	0.85		MELK	1.02	3.25	1.89
	GINS1	1.77	3.26	1.40		MIF	1.12	1.28	0.62
	GINS2	1.19	3.28	1.30		MIS18A	0.72	1.43	0.26
	GPR3	2.37	4.88	2.38		MKI67	1.22	3.63	2.37
	GPSM2	0.59	1.39	0.53		MLH1	0.47	1.07	1.12
	GSG2	0.83	2.69	1.45		MND1	1.38	3.57	1.58
	GTSE1	0.83	3.11	1.63		MNS1	1.79	2.96	-0.51
	H2AFX	0.30	1.87	1.54		MSH2	0.81	1.47	0.83
	HAUS1	0.46	1.08	0.87		MSH6	1.09	1.62	0.92

Table S4-1. Continued

Category	HGNC symbol	Log2FC values			Category	HGNC symbol	Log2FC values		
		CD28/CD3ζ	Δ-CD28/CD3ζ	41BB/CD3ζ			CD28/CD3ζ	Δ-CD28/CD3ζ	41BB/CD3ζ
Other cell cycle associated genes	MYH10	2.06	2.53	-0.04	Other cell cycle associated genes	PVR	1.87	2.41	0.71
	NABP2	0.23	0.94	0.54		RAB11FIP4	-0.87	-1.60	-0.90
	NACC2	-0.60	-1.20	-0.41		RAB3GAP1	0.55	0.63	-0.26
	NASP	0.56	1.42	0.58		RAB7A	-0.04	0.52	0.43
	NCAM1	1.62	1.83	-1.05		RACGAP1	0.68	2.01	1.36
	NDC1	0.98	1.30	0.60		RAD54B	1.47	2.22	1.27
	NDC80	0.59	1.75	1.49		RAD54L	1.50	3.81	1.78
	NDE1	0.41	0.93	0.67		RALB	0.89	1.60	1.48
	NEDD9	0.26	0.88	0.97		RAN	0.81	1.55	1.01
	NLGN3	-0.53	-1.37	-0.84		RANBP1	0.68	1.32	0.60
	NMT2	-1.14	-1.85	-1.29		RASSF4	1.83	2.86	0.17
	NPC1	-0.13	-0.64	-0.40		RBBP8	1.09	2.44	1.73
	NR4A1	2.01	1.09	0.59		RCC1	0.43	1.01	0.59
	NR4A3	3.52	1.97	3.36		RCC2	0.67	1.32	0.80
	NSMCE2	0.36	1.01	0.70		RDX	0.77	1.18	0.42
	NUBP1	0.15	0.65	0.84		RFWD3	0.63	1.20	0.75
	NUDT15	0.36	1.19	0.50		RGS14	-0.97	-1.26	-0.57
	NUF2	1.26	2.51	1.72		RHOA	0.03	0.53	0.45
	NUSAP1	0.58	2.25	1.50		RHOB	1.63	1.96	0.58
	OFD1	-0.60	-1.38	-0.65		RHOC	0.45	1.03	0.27
	OGDH	0.20	0.78	0.71		RIMS2	2.68	3.84	1.25
	OIP5	1.11	2.83	1.77		RNF212	-0.64	-1.76	-1.27
	PA2G4	0.43	0.98	0.83		RPA1	0.12	0.87	0.37
	PACSIN1	-3.00	-3.93	-1.23		RPA3	1.15	2.01	1.19
	PAK1	1.13	1.64	1.35		RPS6KA1	0.19	0.54	0.70
	PARD6B	-0.07	-1.14	-0.26		RRM1	0.96	2.36	1.32
	PARD6G	-1.02	-2.41	-1.21		RRM2	1.44	4.13	2.51
	PBK	1.30	3.11	1.84		RUVBL1	0.34	0.85	0.47
	PCBP4	-0.70	-1.36	-1.02		SAC3D1	0.02	1.05	0.42
	PCID2	-0.17	-0.71	-0.16		SAE1	0.34	1.17	0.63
	PCNA	0.99	2.56	1.78		SASS6	0.81	0.79	0.26
	PDCD4	-0.64	-1.19	-0.38		SCIMP	0.97	2.80	2.05
	PDXP	0.84	1.32	0.74		SDCCAG3	-0.74	-0.99	-0.46
	PEA15	0.43	0.87	-0.23		Sep 11	0.35	1.21	0.19
	PFDN1	0.06	0.68	0.51		SGO1	1.27	3.00	1.83
	PHLDA1	1.48	2.49	1.88		SGO2	1.28	2.22	1.45
	PIM2	0.22	0.77	0.48		SIRT1	-0.41	-1.08	-0.75
	PKD1	-0.35	-0.80	-0.23		SIRT7	-1.05	-1.37	-0.63
	PKMYT1	0.64	3.31	1.63		SKA1	0.73	3.13	2.14
	PKP4	0.65	0.96	0.22		SKA2	0.28	0.99	0.67
	PLA2G16	1.50	1.76	0.76		SKA3	1.14	3.72	2.00
	PLD2	-1.12	-1.69	-1.08		SKIL	-0.86	-2.07	-0.93
	PLK1	0.86	2.47	1.00		SLBP	0.26	0.89	0.79
	PLK4	0.96	2.19	1.59		SLC1A5	0.99	1.53	1.39
	PPIA	0.38	1.03	0.77		SLC25A33	0.18	0.88	0.64
	PPM1G	0.39	1.09	0.81		SLC52A1	-0.76	-2.43	-1.36
	PPP1CC	0.18	0.75	0.37		SLFN11	0.14	-0.89	-0.01
	PPP2R2B	-2.63	-2.60	-1.07		SLX1A	-0.20	-1.71	-0.45
	PPP2R5B	-0.17	-0.65	-0.06		SNAP25	5.32	7.22	5.96
	PRC1	0.34	1.34	0.37		SNX33	1.01	1.15	0.22
	PRMT1	0.29	1.10	0.83		SPAG5	0.88	2.33	1.28
	PRNP	-0.40	-1.01	-0.40		SPC24	0.72	2.77	1.27
	PRR11	1.30	3.49	2.38		SPC25	0.86	3.24	1.61
	PRR5	-0.77	-1.35	-0.94		SPDL1	0.60	1.39	0.73
	PSMC3IP	0.53	2.13	1.16		SPRY1	1.77	2.29	1.33
	PTPN11	0.83	1.29	0.71		SRC	1.27	1.48	-0.54
	PTPN3	2.95	4.57	2.07		STIL	1.00	2.64	1.57
	PTPRK	0.69	1.43	1.06		STMN1	0.85	2.95	1.90
	PTTG1	0.62	1.72	1.00		STRA8	4.17	3.82	0.78

Table S4-1. Continued

Category	HGNC symbol	Log2FC values			Category	HGNC symbol	Log2FC values		
		CD28/CD3ζ	Δ-CD28/CD3ζ	41BB/CD3ζ			CD28/CD3ζ	Δ-CD28/CD3ζ	41BB/CD3ζ
Other cell cycle associated genes	STX11	0.40	1.49	1.30	Other cell cycle associated genes	TSPYL2	-0.64	-1.27	-0.89
	STX2	-0.45	-0.82	-0.22		TTK	0.97	2.69	1.10
	STXBP1	1.53	1.16	0.62		TYMS	1.25	3.98	2.39
	SUN1	-0.36	-1.03	-0.48		UBE2C	0.67	3.25	1.32
	SUV39H1	0.70	1.75	1.04		UBE2L3	-0.05	0.59	0.37
	SUV39H2	1.43	2.35	1.50		UBE2S	0.39	1.69	0.84
	SYCE2	0.98	2.42	0.95		UHRF1	1.11	3.61	2.00
	SYTL1	-0.84	-1.86	-1.14		UHRF2	-0.15	-0.66	-0.27
	TAP1	0.10	1.09	0.83		USP39	-0.11	0.45	0.16
	TBRG1	-0.83	-1.38	-0.73		VRK1	0.72	1.37	1.02
	TC2N	-1.54	-2.67	-1.94		WDR62	0.28	2.01	1.15
	TERT	1.60	3.40	0.60		WDR76	1.04	2.19	1.73
	TEX11	3.85	3.22	3.78		WNT10B	-1.00	-3.09	-2.31
	TEX12	-0.58	-1.45	-0.77		XPC	-0.56	-0.88	-0.34
	TFRC	1.74	2.67	2.17		XRCC2	1.19	2.35	1.28
	THOC3	0.63	1.30	0.29		XRCC3	0.50	1.48	1.02
	TIMELESS	0.60	2.28	1.30		YEATS4	0.20	1.19	0.98
	TIPIN	1.08	1.90	0.93		YWHAE	0.99	1.69	0.52
	TMEM8B	-0.35	-0.77	-1.11		ZBTB49	-0.57	-1.37	-0.86
	TNFRSF4	1.91	3.09	1.25		ZFHX3	1.97	2.40	-0.75
	TOP2A	1.30	3.35	1.86		ZFP36L2	-0.03	-0.79	-1.08
	TP53	-0.14	0.69	0.64		ZNF655	-0.65	-1.17	-0.65
	TP63	2.20	5.06	2.16		ZPR1	-0.15	-0.37	0.18
	TP73	0.50	2.88	1.47		ZW10	0.50	1.09	0.55
	TPX2	0.84	2.56	1.42		ZWILCH	0.64	1.56	0.91
	TRIP13	1.14	3.33	1.09		ZWINT	0.96	3.32	1.63
	TSC1	-0.72	-1.19	-0.57					

4.4 Discussion

Malignant pleural mesothelioma (MPM) is a rare solid tumor, which originates from transformed cells of the mesothelium. About 70% of MPM patients have a record of asbestos exposure with a long latency up to decades between exposure and disease onset [224]. MPM is considered an incurable disease with a median survival of 2 years even when intensive multi-modality treatment is performed for localized disease [212, 225]. Even if asbestos is banned in the western world, there are events leading to large pollution with asbestos exposure like unforeseen natural calamities. In contrast, permanent release of asbestos is part of working processes in the developing world leading to asbestos exposure of workers and their families. Therefore, new therapeutic options are desperately needed for persons exposed to asbestos who thereafter develop MPM.

Beside therapies targeting molecular pathways of the malignant cells [226], immunotherapy is a novel therapeutic strategy to fight MPM [227]. Checkpoint blockade induced modest response rates and focused on the induction of a natural, active-specific immune response [213, 214]. As a more comprehensive approach, the combination of checkpoint inhibition and passive adoptive immune therapy could be proposed to overcome the shortcomings of a T-cell repertoire potentially not existing or not able to recognize malignant mesothelioma cells.

We previously investigated the potential therapeutic effect of FAP-specific, redirected T-cells as a new option for treatment of MPM [216]. All three histological subtypes of MPM demonstrated FAP expression by the tumor stroma and by most tumor cells [215]. Functional T-cells expressing anti-FAP CARs at high level could be generated by standard procedures and these redirected T-cells showed antigen-specific activity [216]. The most recent research in the field of redirected T-cells analyzes a multitude of different CAR constructs, of which CARs with CD28 or the 4-1BB co-stimulatory moiety are most frequently used. This led us to the question, which co-stimulation through the CAR would be most optimal combined with checkpoint blockade for MPM.

To more realistically access the *in vivo* function of redirected T-cells, we generated and utilized a humanized mouse model. HFL were clearly identified as optimal source for $CD34^+$ HSCs compared to apheresis products. The uniform development of T cells from HFL derived $CD34^+$ allowed us to utilize humanized mice as a source for the generation of redirected T-cells, which then could be used as autologous T-cells for transfer experiments. Thereby, we avoided development of GvHD after adoptive transfer and allogeneic rejection of the transferred, redirected T-cells.

However, there are some initial concerns about this model. First, the tumor cell line is allogeneic to the reconstituted immune compartment in humanized mice. Notably, even a small number of allogeneic tumor cells (0.1×10^6 HT1080FAP) resulted in a reliable tumor take allowing for the testing of redirected T-cells. This result is even more surprising since it is estimated that the humanized T-cell repertoire contains about 5% alloreactive T-cells, which had no effect on tumor take [228]. Therefore, the effects of redirected T-cells do not seem to be enhanced by allogeneic endogenous T-cells. Hence, the model system is potentially able to access the therapeutic impact of redirected T-cells.

Remarkably, we observed improved persistence of autologous redirected T-cells in humanized mice, considering previously observed survival of up to three weeks in NSG mice [229]. As expected, the 4-1BB/CD3ζ CAR performed best with regards to persistence until day 44 in the peripheral blood of humanized mice. Multiple reasons could be responsible for this observation. Humanized mice have low levels of human cytokines, which are essential to support transferred T-cells. *In vitro* redirected T-cells are dependent on continuous support from cytokines; IL-2, IL-7 and IL-15. Some animal models tried to overcome this limitation by expressing human cytokines, like IL-7 transgenic NSG mice and, therefore, are potential candidate models to further improve the herein presented model [230]. An alternative explanation for the rather short persistence could be that T-cells are not supported without antigen stimulation and/or HLA stimulation [231]. Nevertheless, even in the first patient - who could be seen as the ultimate host for his autologous redirected T cells – the CAR persisted not longer than 21 days in the peripheral blood. However, at multiple time-points, we detected increasing copy numbers of the CAR, suggesting expansion of the transferred redirected T-cells.

This rather short persistence in humanized mice and man may also be explained by the state of the T-cells. Due to the process by which redirected T-cells are produced, the main phenotypes of redirected T-cells are effector memory or effector phenotype [229]. When comparing T-cells expressing the Δ-CD28/CD3ζ, CD28/CD3ζ and 4-1BB/CD3ζ CAR, which had the same phenotype after production, differences could be observed regarding gene expression profiles induced by antigen stimulation. Previously, the comparison of the CARs using CD28 or 4-1BB highlighted the different gene expression profile indicating different metabolic programs [232]. The authors have shown that CAR-T cells with 4-1BB co-stimulation developed a central memory phenotype while CD28 co-stimulation yielded effector memory T-cells [232]. Noteworthy, in our experiments, the CD28/CD3ζ CAR showed unspecific proliferation. Similar observation was made before in a study by Long and colleagues. The authors reported antigen independent signaling in CD28 co-stimulatory CARs and claimed it to be due to physical interactions between CAR receptors, leading to self-association and aggregation on cell surface. The antigen independent tonic signaling through CD28/CD3ζ CAR in this study was attributed to the framework regions in the scFv fragments of the CD28 co-stimulatory CAR [233]. Our data indicates that lck deletion results in improved antigen specific proliferation.

The Δ-CD28/CD3ζ CAR appears to induce a new and distinct supra-physiological gene expression profile in activated $CD8^+$ T cells. It induced the expression of gene programs of effector and memory T-cells; glycolysis, exhaustion (effector programs) and fatty acid oxidation and anti-apoptosis (memory programs). This, in theory, advantageous combination did not result in prolonged persistence.

Despite all concerns, *in vivo* functionality of the redirected T-cells could be tested with some astonishing results. PD-L1 expression was detected in about 20-40% of the clinical cases [234]. First, this indicates the immune suppressive potential of MPM via immune checkpoints. Second, it gives a very strong rational to use checkpoint inhibitors blocking the PD-1/PD-L1 axis. In combination with PD-1 blockade only T-cells redirected by the Δ-CD28/CD3ζ CAR showed statistically significant tumor control. This effect was dependent on the transfer of FAP-specific, redirected T-cells underlining the presence of T-cells capable to recognize targets on

the tumor cells. In contrast, it was shown recently that redirected T-cells with CD28 co-stimulation showed increased *in vivo* functionality in a mesothelioma model using immune-compromised mice [158]. We speculate that the different results are, in part, attributable to interactions of the humanized immune system and the redirected T-cells. One potential argument could be clonal competition for cytokines, another, increased immune suppression by parts of humanized immune system in the tumor microenvironment (e.g. regulatory T cells). The novel model delineates the Δ-CD28/CD3ζ CAR as an attractive receptor to re-direct T-cell for the use in combination with blocking the PD-1/PD-L1 axis.

To overcome the PD-1 checkpoint different approaches can be employed. Recently, the CRISPR/CAS9 method was used to permanently interrupt PD-1 signalling in T-cells [163]. Considering safety, this approach is currently tested for low risk target structures like CD19 or CD20. For high risk target structures, the permanent PD-1 blockade comes with increased risk of uncontrollable on-target/off-tissue toxicity. We believe that for high risk targets the PD-1/PDL-1 blockade should be pursued with non-permanent approaches like blocking antibodies.

In contrast to hematological diseases, redirected T-cells against solid tumors have to migrate into the tumor issue. Published experimental data indicate that tumor blood vessels block the influx of T-cells, thereby prohibiting T-cell mediated anti-cancer responses [235]. Clinical trials already included this knowledge in the trial design. For example, interleukin-13 receptor alpha 2-specific, redirected T-cells were injected directly in the cavity of resected glioblastoma [150]. Our line of experimentation and the early clinical trial were focused on the local injection of redirected T-cells in body cavities harboring the tumor cells (intraperitoneal model system in mice and pleural effusion in the clinical trial). The experimental data indicate that redirected T-cells injected into a tumor bearing cavity encounter the tumor and cause tumor control.

Taken together, we describe here the first humanized mouse model for autologous redirected T-cells. This model showed that the local transplantation of FAP-specific redirected T-cells with a special CAR lacking lck signaling through CD28 co-stimulation, in combination with PD-1 blockade induced transient tumor control. Since FAP is expressed in 90% of all malignant epithelial tumors by activated fibroblasts, this therapeutic approach should be further investigated beyond MPM.

4.5 Author contributions

PG, JR, MP, PSc and SJ conducted experiments. AK analyzed RNA sequencing data. SS, MH, WJ, TW contributed in patient care. NK and MPr helped with *in vivo* tumor imaging. AS and ME collected clinical samples and performed pathological evaluations. AT performed GMP production of redirected T-cells and PSa did autologous transfer. RS contributed to shipping and storage of redirected T-cells. UP, RStu, WW and CR contributed to study design. CR designed CAR constructs. UP and CM designed experiments with humanized mice. PG and UP wrote manuscript.

4.6 Acknowledgements

We thank the first patient and his family for their strong will to support modern therapies in an open and positive manner. We would like to thank Dorothea Greuter, Claudia Bonvin and Claudia Matter for excellent technical assistance. We thank Hinrich Abken and Markus Chmielewski (University of Cologne, Germany) for the pBullet plasmid. We are indebted to Helga Bachmann for the data management. We further thank George Coukos, Silke Gillessen, Alexander Jetter, Georg Stüssi for volunteering for the safety board. We would like to thank Uta Henze from the SCRM for the quality control process. We express gratitude to Mark Robinson for his assistance and support in analysis of RNA sequencing data. The phase I study of testing of FAP-redirected T-cells in MPM was partly planned and designed at the 12th joint ECCO-AACR-EORTC-ESMO Workshop 'Methods in Clinical Cancer Research', Waldhaus Flims, Switzerland, 19 – 25 June 2010. We are grateful for the financial support by "Forschungskredit" University of Zurich, 54171101, Swiss Cancer League KFS-3115-02-2013 (UP), "Hoch spezialisierte Medizin" of the Canton Zurich (CR), Swiss Tumor Immunology Institute (CR & UP), and Zurich Cancer League (CM).

4.7 References

1. Sadelain, M., R. Brentjens, and I. Rivière, *The basic principles of chimeric antigen receptor design.* Cancer Discov, 2013. **3**(4): p. 388-98.
2. Sadelain, M., *CAR therapy: the CD19 paradigm.* J Clin Invest, 2015. **125**(9): p. 3392-400.
3. Kalos, M., et al., *T cells with chimeric antigen receptors have potent antitumor effects and can establish memory in patients with advanced leukemia.* Sci Transl Med, 2011. **3**(95): p. 95ra73.
4. Porter, D.L., et al., *Chimeric antigen receptor T cells persist and induce sustained remissions in relapsed refractory chronic lymphocytic leukemia.* Sci Transl Med, 2015. **7**(303): p. 303ra139.
5. Jackson, H.J., S. Rafiq, and R.J. Brentjens, *Driving CAR T-cells forward.* Nat Rev Clin Oncol, 2016. **13**(6): p. 370-83.
6. Weder, W., I. Opitz, and R. Stahel, *Multimodality strategies in malignant pleural mesothelioma.* Semin Thorac Cardiovasc Surg, 2009. **21**(2): p. 172-6.
7. Karrison, H.K., et al., *Phase II Trial of Pembrolizumab in patients with Malignant Mesothelioma (MM): Interim Analysis* Journal of Thoracic Oncology.
8. Quispel-Janssen, J., et al., *A Phase II Study of Nivolumab in Malignant Pleural Mesothelioma (NivoMes): with Translational Research (TR) Biopies*. 2017.
9. Petrausch, U., et al., *Re-directed T cells for the treatment of fibroblast activation protein (FAP)-positive malignant pleural mesothelioma (FAPME-1).* BMC Cancer, 2012. **12**: p. 615.
10. Schuberth, P.C., et al., *Treatment of malignant pleural mesothelioma by fibroblast activation protein-specific re-directed T cells.* J Transl Med, 2013. **11**: p. 187.
11. Kofler, D.M., et al., *CD28 costimulation Impairs the efficacy of a redirected t-cell antitumor attack in the presence of regulatory t cells which can be overcome by preventing Lck activation.* Mol Ther, 2011. **19**(4): p. 760-7.
12. Li, Y. and R.J. Kurlander, *Comparison of anti-CD3 and anti-CD28-coated beads with soluble anti-CD3 for expanding human T cells: differing impact on CD8 T cell phenotype and responsiveness to restimulation.* J Transl Med, 2010. **8**: p. 104.
13. Wei, F., et al., *Strength of PD-1 signaling differentially affects T-cell effector functions.* Proc Natl Acad Sci U S A, 2013. **110**(27): p. E2480-9.
14. Brenchley, J.M., et al., *Expression of CD57 defines replicative senescence and antigen-induced apoptotic death of CD8+ T cells.* Blood, 2003. **101**(7): p. 2711-20.
15. O'Sullivan, D. and E.L. Pearce, *Targeting T cell metabolism for therapy.* Trends Immunol, 2015. **36**(2): p. 71-80.
16. Xu, X., et al., *Autophagy is essential for effector CD8(+) T cell survival and memory formation.* Nat Immunol, 2014. **15**(12): p. 1152-61.
17. Kovacs, J.R., et al., *Autophagy promotes T-cell survival through degradation of proteins of the cell death machinery.* Cell Death Differ, 2012. **19**(1): p. 144-52.
18. Teta, M.J., et al., *US mesothelioma patterns 1973-2002: indicators of change and insights into background rates.* Eur J Cancer Prev, 2008. **17**(6): p. 525-34.
19. Opitz, I., et al., *Incidence and management of complications after neoadjuvant chemotherapy followed by extrapleural pneumonectomy for malignant pleural mesothelioma.* Eur J Cardiothorac Surg, 2006. **29**(4): p. 579-84.
20. Jakobsen, J.N. and J.B. Sorensen, *Review on clinical trials of targeted treatments in malignant mesothelioma.* Cancer Chemother Pharmacol, 2011. **68**(1): p. 1-15.
21. Izzi, V., et al., *Immunity and malignant mesothelioma: from mesothelial cell damage to tumor development and immune response-based therapies.* Cancer Lett, 2012. **322**(1): p. 18-34.
22. Suchin, E.J., et al., *Quantifying the frequency of alloreactive T cells in vivo: new answers to an old question.* J Immunol, 2001. **166**(2): p. 973-81.

23. Schuberth, P.C., et al., *Effector memory and central memory NY-ESO-1-specific re-directed T cells for treatment of multiple myeloma.* Gene Ther, 2012.
24. van Lent, A.U., et al., *IL-7 enhances thymic human T cell development in "human immune system" Rag2-/-IL-2Rgammac-/- mice without affecting peripheral T cell homeostasis.* J Immunol, 2009. **183**(12): p. 7645-55.
25. Billerbeck, E., et al., *Characterization of human antiviral adaptive immune responses during hepatotropic virus infection in HLA-transgenic human immune system mice.* J Immunol, 2013. **191**(4): p. 1753-64.
26. Kawalekar, O.U., et al., *Distinct Signaling of Coreceptors Regulates Specific Metabolism Pathways and Impacts Memory Development in CAR T Cells.* Immunity, 2016. **44**(2): p. 380-90.
27. Long, A.H., et al., *4-1BB costimulation ameliorates T cell exhaustion induced by tonic signaling of chimeric antigen receptors.* Nat Med, 2015. **21**(6): p. 581-90.
28. Cedrés, S., et al., *Analysis of expression of programmed cell death 1 ligand 1 (PD-L1) in malignant pleural mesothelioma (MPM).* PLoS One, 2015. **10**(3): p. e0121071.
29. Cherkassky, L., et al., *Human CAR T cells with cell-intrinsic PD-1 checkpoint blockade resist tumor-mediated inhibition.* J Clin Invest, 2016. **126**(8): p. 3130-44.
30. Rupp, L.J., et al., *CRISPR/Cas9-mediated PD-1 disruption enhances anti-tumor efficacy of human chimeric antigen receptor T cells.* Sci Rep, 2017. **7**(1): p. 737.
31. Motz, G.T., et al., *Tumor endothelium FasL establishes a selective immune barrier promoting tolerance in tumors.* Nat Med, 2014. **20**(6): p. 607-15.
32. Brown, C.E., et al., *Regression of Glioblastoma after Chimeric Antigen Receptor T-Cell Therapy.* N Engl J Med, 2016. **375**(26): p. 2561-9.

Chapter-5

Conclusions and outlook

5.1 Conclusions and Outlook

Adoptive T-cell transfer and checkpoint blockade have both shown dramatic success in clinics against several types of cancers. However, both of these approaches are still at a formative stage with remarkable potential. Increasing research efforts aim to further optimize and expand these strategies to other cancer types. There is a substantial motivation to use a combination of checkpoint inhibition and adoptive cell therapy (ACT). Adoptive T-cells need a permissive environment to provide maximum antitumor effects. Checkpoint blocking antibodies eliminate T-cell inhibition, however, their effectiveness count upon the existence of a functional T-cell repertoire, specifically targeting tumor cells. Providing both tumor-targeting T cells and removing the T-cell inhibitory stimulus through checkpoint blockade may generate outcomes preferable to those produced by either approach alone. Optimization of such a combinatorial regime and pre-clinical evaluation is essential, since every tumor type is unique and can respond differently. Overall, the combined approach need to be tailored based on the tumor type, genetics and disease status of patients with a long-term aim to increase the effectiveness and reduce toxicities in patients.

In this study, we aimed to examine the synergistic effect of checkpoint blockade and ACT. We generated T-cells genetically engineered to target tumors expressing Fibroblast Activation Protein (FAP) through the introduction of Chimeric antigen receptor (CAR) and tested FAP-specific CAR-T cells in combination with PD-1 blockade. One of the main asset to CAR technology is the modular nature of CAR architecture, encompassing extracellular antigen-binding domain fused to intracellular T-cell co-stimulatory and signalling domains, which allows for continuous refinement and optimization of T-cell function by replacement of the CAR endo-domains. We were interested to study the impact of different co-stimulatory endo-domains on the overall anti-tumor efficacy and possible clinical outcome of FAP-specific redirected T-cells. In clinics, the most successful CARs targeting CD19 antigen in B-cell malignancies have employed 4-1BB or CD28 co-stimulatory domains. These co-stimulatory CARs have shown variable efficacy and persistence in a largely diverse patient population.

Parallel to the regularly used CD28 and 4-1BB co-stimulatory domains, we investigated a unique co-stimulatory domain, which is a modification of CD28 domain, generated by site directed mutagenesis. Our *in vitro* data showed enhanced anti-tumor functionality of redirected T-cells carrying the modified CD28 endo-domain (Δ-CD28) CAR, in terms of antigen-specific proliferation, maximum anti-tumor efficacy, cytokine release and metabolism. The Δ-CD28 co-stimulation has not been extensively pre-clinically studied before and has previously never been tested in clinical trials.

For *in vivo* pre-clinical evaluation of different co-stimulatory CARs, we employed a humanized mouse model. The purpose was to use a model system that could outline an interplay of human immune interactions supporting or masking the effect of redirected T-cells in combination with PD-1 blockade. We believed that humanized mice would provide a robust model system to study our therapeutic approach and would result in a more reliable extrapolation of our findings from bench to clinics.

Firstly, we could show that irrespective of the type of co-stimulation, redirected T-cells survive in humanized mice at least until day 44 after injection. Next, humanized mice could engraft an allogenic FAP+ tumor, showing that the reconstituted human immune compartments lack functional capacity to provide any protective effect against the transplanted tumor on its own. In fact, administering the PD-1 blocking antibody alone also did not potentiate tumor regression through allogeneic mismatch. Nevertheless, the functionality of FAP-specific redirected T-cells was tested in this model and notably, only redirected T-cells with Δ-CD28 CAR showed protection against tumor in combination with PD-1 blockade. This correlates well with our *in vitro* data where the Δ-CD28 CAR showed maximum cytotoxicity and antigen-specific IFN-γ release. In tumor bearing humanized mice, we injected CAR-T cells at an effector/target ratio of 4:1. Presumably, at a further higher effector/target ratios, we might observe protective effects in other groups; CD28 and 4-1BB. Considering that cytokine release syndrome (CRS) is a major side-effect of CAR-T cell approach, it is important to balance efficacy and toxicity and is preferable to administer a minimal dose that can elicit relevant anti-tumor responses.

In our approach, we chose fibroblast activation protein (FAP) as the target antigen. FAP Is a cell surface protease that is not expressed in normal tissues and mostly expressed in activated fibroblasts responding to pathologic situations that involve inflammation such as, arthritis, wounding, fibrosis and cancer [236]. The restricted and stable genetic expression of FAP makes it an attractive target for anti-cancer immunotherapies. However, a previous study has reported lethal bone toxicity and cachexia in mice due to immune-targeting of FAP [237]. These findings were attributed to low levels of FAP expression on bone marrow stem cells. Thus, future pre-clinical and clinical evaluation while targeting FAP, needs to be dealt with maximum caution.

Immunotherapies so far have shown limited success in solid cancers, mainly because of the biological complexity of the microenvironment in solid tumors. Given the key role of tumor stroma in mediating invasion, progression and metastasis of cancer and the extensive cross-talk between tumor cells and stroma [238], targeting both tumor and its micro-environment could provide an advantage. FAP is an ideal candidate in this situation since it is expressed on tumor cells as well as stromal fibroblasts of more than 90% of human epithelial cancers [239]. Thus, FAP can serve as an ideal antigen for synergistic targeting of tumor cells and microenvironment potentially leading to enhanced effects. Retrospectively, other approaches using anti-FAP antibodies and anti-FAP vaccines have successfully shown inhibition of tumor growth and prolonged survival in mouse models [240, 241]. The advantage of the CAR approach is that effector T-cell responses can be generated against cell surface antigens, which do not require presentation on MHC molecules, like FAP. The long-term aim is to generate tumor-targeting T cells which at a minimal dose, engraft, proliferate, persist and retain memory that can be further re-challenged to resume cytotoxic functions.

We extended our preclinical findings and started a first phase-I clinical study evaluating toxicity and feasibility of FAP targeting redirected T-cells with Δ-CD28 costimulatory CARs in patients with malignant pleural mesothelioma (MPM) disease. MPM is a rare and malignant cancer caused by exposure to asbestos. The primary mesothelioma tumors are formed in the pleura, a thin membrane of cells between the linings of the lungs and

chest wall. MPM is an occupational disease and is common in people working at construction sites, shipyards or production units, who are exposed to asbestos. It can take between 10 to 50 years for cancer to develop after exposure [242]. Nearly 2500 people every year are diagnosed with MPM. Due to occupational nature, MPM is more common in men than women (5:1 ratio) and more prevalent in old aged people due to longer latency periods [242]. MPM is almost always a fatal disease. The current prognosis using standard treatment options (surgery, chemotherapy and radiotherapy) is only 6-12 months, since a vast majority of patients are diagnosed in an advanced stage. Australia has one of the highest incidences of MPM on a population basis in the world since it was one of the largest consumers of asbestos in the post world war II period [243].

Although it has been 50 years since the first MPM incidence was discovered [242], until now, there are no established personalized or targeted approaches to treat the disease. Conventional treatment options, like surgery, radiation or chemotherapy, have not yielded significant improvements in prognosis. In fact, for many patients, surgery is not an option due to diffused neoplastic growth and a locally advanced disease [244]. Similarly, there is no evidence of survival benefit to MPM patients from radiotherapy [245]. Chemotherapy, on the other hand has shown improved response rates and survival [242]. The trimodality treatment approach that includes chemotherapy, surgery and radiotherapy has shown to provide a median survival of 29 months in MPM patients [246, 247].

Other novel biomarkers in MPM are beginning to be known and can be exploited to develop targeted therapies. At histological level, apart from FAP, MPM cells showed the expression of the antigens calretinin, thrombomodulin, mesothelin and cytokeratin-5 [248]. Genetic alterations in MPM include mutations in three key tumor suppressor genes, cyclin-dependent kinase inhibitor 2A/alternative reading frame (CDKN2A/ARF), neurofibromatosis type 2 (NF2) and BRCA1-associated protein-1 (BAP1) [249]. Apart from this, upregulation of epidermal growth factor receptor (EGFR), vascular endothelial growth factor (VEGF) was observed in MPM [242]. EGFR inhibitors tested *in vitro* have shown inhibition of MPM cell growth [250]. Several angiogenesis inhibitors have been tested in clinical trials including avastin, vatalanib, thalidomide and sorafenib and showed modest activities in MPM patients [251].

Aside from FAP, mesothelin, another cell surface antigen expressed in MPM, has been exploited as a target for CAR-T cell therapy. One of the major concern while designing targeted therapies against mesothelin is, its low-level expression on normal mesothelial cells [252]. A phase-I study using second generation mesothelin-specific 4-1BB CARs employed mRNA electroporation method to induce transient expression of CAR [141, 253]. This was aimed to reduce on-target/off-tumor toxicities. 4 patients with mesothelioma or pancreatic tumors were treated with mesothelin CARs [141, 253]. Autologous T-cells electroporated with mRNA for CAR were well tolerated and did not show off-target toxicities. Moderate clinical responses were observed in this study and CAR-T cells were detected in the tumors. Additionally, there was a transient elevation in cytokine levels, including IL-12, IL-6, G-CSF, MCP-1, IL1Rα, and RANTES in the serum of mesothelioma patients. No severe cytokine release syndrome (CRS) was reported. Later, a serious adverse event was reported as one patients

developed severe anaphylaxis and cardiac arrest after the third infusion of mesothelin CAR-T cells [141]. This reaction was accompanied by elevated levels of IgE antibody directed against the murine scFv of the mesothelin CAR [141].

In our first trial subject, we injected $1X10^6$ anti-FAP CAR with Δ-CD28 co-stimulation and showed that this dose was well tolerated and did not lead to any toxicities. Further, CAR-T cells expanded in the blood of the patient and could be detected until day 21. In our studies, we used retrovirus mediated gene transfer method to generate CAR-T cells. This approach requires heavy pre-activation of T-cells to induce proliferation, which might result in loss of functionality or early exhaustion. In future, lentivirus mediated gene delivery methods, that can infect non- proliferating cells, should be explored.

Choosing an appropriate co-stimulation domain is essential for the optimal activity and persistence of CAR T-cells. However, the ideal co-stimulation may depend on several factors, namely, antigen density, CAR stoichiometry, binding affinity of the CAR and the immunological microenvironment around tumors [252]. For our future studies, we have generated anti-FAP CARs with different binding affinities, but same epitope specificity, and harbouring either of these co-stimulations, namely CD28, Δ-CD28 and 4-1BB. It would be interesting to test the impact of co-stimulation on the threshold of CAR-mediated T-cell activation. Furthermore, it will be interesting to explore combinations of particular co-stimulation and affinity that could be used in case of tumors with low antigen density. Consequently, CAR-T cells can be efficiently used to target tumors that heavily downregulate expression of cell surface antigens. Overall, these varying affinities would help to optimize CAR sensitivity to an individual tumor type before clinical application.

On the whole, in this study, we have described a direct bench to beside translation of FAP-specific redirected T-cells by showing the translational application of our findings in the first MPM patient. This is just the starting point for investigations using immune modulatory anti-cancer drugs and adoptive T-cell therapy. Looking at the most recent data presented at the annual meeting of the American society of clinical oncology (ASCO2017), immune modulation in future, will reach out far beyond checkpoint inhibition involving other approaches such as, manipulation of immune cell metabolism, chemokines and cytokines as well as employing agonistic antibodies to co-stimulatory receptors on immune cells. The aim for the future is to transfer T-cells that could give the right cellular effector cell population to act in a modulated immune environment, able to fight cancer.

Chapter-6

Materials and Methods

6.1 Materials

6.1.1 Reagents and kits

Reagent	Manufacturer
0.25% Trypsin-EDTA	Invitrogen/Life Technologies
Alexa Fluor 647 Antibody Labeling Kit	Invitrogen
APC BrdU Flow Kit	BD Biosciences
BD OptEIA Set Human IFNγ	BD Biosciences
BD OptEIA Set Human IL-2	BD Biosciences
Brefeldin A	Sigma
CD3 microbead kit	Miltenyi Biotech
CD34 microbead kit	Miltenyi Biotech
CD8 microbead kit	Miltenyi Biotech
Dimethyl sulphoxide (DMSO)	Sigma
DMEM (Dulbecco modified eagle's medium) with 4.5 g/L D-glucose, L-glutamine and pyruvate	GIBCO
DNeasy blood and tissue kit	Qiagen
Dynabeads human T-cell activator CD3/28	Life Technologies
eBioscience Intracellular Fixation and Permeabilization Buffer Set	eBioscience
Fetal Bovine Serum	Biochrom
Fugene HD transfection reagent	Promega
Genticin selective antibiotic, G418	Sigma Aldrich
Hank's Balanced Salt Solution (HBSS) (containing $CaCl_2$ and $MgCl_2$)	GIBCO/LifeTechnologies
Human CD3 and CD28 co-stimulatory antibodies	eBioscience
Hygromycin B	Invitrogen
KAPA HIFI ploymerase	KAPA Biosystems
L-Glutamine	GIBCO
LIVE⁄DEAD Fixable Dead Cell Stain Kit	Invitrogen
Magnetic-activated cell sorting (MACS) buffer prepared using 1% FBS, 2mM ethylenediaminetetraacetic acid (EDTA) in PBS	
Non-essential amino acids solution (NEAA)	GIBCO
Penicillin-streptomycin	GIBCO/Invitrogen
Phosphate buffered saline (PBS), purchased otherwise prepared as; 8g/L NaCl, 0.2g/L KCl, 1.15g/L Na_2HPO_4 and 0.2 g/L KH_2PO_4 at a pH 7.3	GIBCO/Life Technologies
PKH26 general cell membrane labelling kit	Sigma
PMA, Ionomycin	Sigma
PureYield plasmid maxiprep kit	Promega

PureYield plasmid miniprep kit	Promega
Recombinant human Fibroblast activation protein (FAP)	R and D Systems
Recombinant human interleukin-15 (IL-15)	Miltenyi Biotech
Recombinant human interleukin-2 (IL-2)	Peprotech
Recombinant human interleukin-7 (IL-7)	Miltenyi Biotech
RPMI 1640 with 2mM L-glutamine	GIBCO
Taqman Universal PCR mastermix	Applied Biosystems
Trypan Blue stain 0.4%	GIBCO/LifeTechnologies
XenoLight D-Luciferin - K+ Salt Bioluminescent Substrate	Perkin Elmer
Zymo Quick-RNA microprep kit	Lucerna-Chem

6.1.2 Anti-human antibodies for flow cytometry

Marker	Fluorochrome	Company	Catalogue no	Clone
BrdU	APC	eBioscience	17-5071-42	Bu20A
CCR7	PECF594	BD Biosciences	562381	150503
CD127	PE/Dazzle 594	Biolegend	351336	A019D5
CD14	FITC	BD Biosciences	557153	MSE2
CD19	PE/Cy5	Biolegend	302210	HIB19
CD25	APC	eBioscience	17-0259-42	BC96
CD3	PE/Cy7	Biolegend	300420	UCHT1
CD34	APC	Invitrogen	CD34-581-05	581
CD38	PE	Biolegend	303506	HIT2
CD4	Bv510	Biolegend	317444	OKT4
CD4	PB	Biolegend	300521	RPA-T4
CD45	PB	Biolegend	304029	HI30
CD45	APC	BD Biosciences	555485	HI30
CD45RA	Bv605	Biolegend	304134	HI100
CD45RO	Bv785	Biolegend	304234	UCHL1
CD57	PB	Biolegend	322316	HCD57
CD62L	Bv510	BD Biosciences	563203	SK11
CD69	FITC	BD Biosciences	555530	FN50
CD8	PerCP	Biolegend	344708	SK1
CD8	PE	BD Biosciences	561950	RPA-T8
CD8	FITC	eBioscience	11-0088-42	RPA-T8
FoxP3	PE	eBioscience	12-4776-42	PCH101
HLA-DR	FITC	Biolegend	307804	L243
HLA-DR	FITC	BD Biosciences	556643	G46-6
IFN-γ	PE/Cy7	eBioscience	25-7319-82	4S.B3
IgG	PE	Southern Biotech	2043-09	2043-09
IL-2	APC	eBioscience	17-7029-41	MQ1-17H12
NkP46	APC	BD Biosciences	558051	9E2
PD-1	PE/Dazzle 594	Biolegend	329940	EH12.2H7
Tim-3	Alexa Fluor 488	R and D systems	FAB2365G	344823

6.1.3 Plasmids for retroviral transduction

Helper plasmids for retroviral transduction (kindly provided by Prof. Hinrich Abken, Köln, Germany)	
pCOLT-GaIV (#392)	Retroviral helper vector coding for GALV env protein. Described by Weijtens et. al.
pHIT60 (#393)	Retroviral helper vector coding for MLV gag and pol proteins. Described by Weijtens et. al.
Plasmids with CAR transgene. Binding domain of CAR (scFv) was cloned into pBullet vector. pBullet vector described by Hombach et. al. [254] **containing the CAR backbone without the binding domain (scFv) was provided by Prof. Hinrich Abken, Köln, Germany.**	
T1-CD28/CD3ζ	pBullet vector with expression cassette coding for a fusion protein consisting of a Lκ-leader sequence, the T1 scFv recognizing the HLA-A*02:01/NY-ESO-$1_{157-165}$ complex [229], a modified human CH_2CH_3 IgG domain that prevents binding to FcγR (described by Hombach et. al. [255]) and a CD28/CD3ζ domain.
T1-Δ-CD28/CD3ζ	pBullet vector with expression cassette coding for a fusion protein consisting of a Lκ-leader sequence, the T1 scFv recognizing the HLA-A*02:01/NY-ESO-$1_{157-165}$ complex, a modified human CH_2CH_3 IgG domain, a mutated CD28 domain which prevents binding of Lck upon T-cell activation (described by Kofler et. al. [217]) and a CD3ζ domain.
T1-4-1BB/CD3ζ	pBullet vector with expression cassette coding for a fusion protein consisting of a Lκ-leader sequence, the T1 scFv recognizing the HLA-A*02:01/NY-ESO-$1_{157-165}$ complex, a modified human CH_2CH_3 IgG domain and a 4-1BB/CD3ζ domain.
F19-CD28/CD3ζ	pBullet vector with expression cassette coding for a fusion protein consisting of a Lκ-leader sequence, the F19 antibody [256] derived scFv binding to human FAP, a modified human CH_2CH_3 IgG domain and a CD28/CD3ζ domain.
F19-Δ-CD28/CD3ζ	pBullet vector with expression cassette coding for a fusion protein consisting of a Lκ-leader sequence, the F19 scFv recognizing human FAP, a modified human CH_2CH_3 IgG domain, a mutated CD28 domain which prevents binding of Lck upon T-cell activation (described by Kofler et. al. [217]) and a CD3ζ domain.
F19-4-1BB/CD3ζ	pBullet vector with expression cassette coding for a fusion protein consisting of a Lκ-leader sequence, the F19 scFv binding to human FAP, a modified human CH_2CH_3 IgG domain and a 4-1BB/CD3ζ domain.

6.1.4 Primers for quantitative Real-Time PCR (qRT-PCR)

Primer name	**Sequence 5'-3'**
scF19_fwd	GAA GAT GAG CTG CAA GAC CA
scF19_rev	GCC CTT GAA CTT CTG GTT GT
F19_oligo (probe)	-(6FAM)-GTACACCATCCACTGGGTCC-(TAMRA)-

6.2 Methods

6.2.1 Cell culture

293T cells were purchased from ATCC (Manassas, VA, USA) and maintained in standard D10 medium; DMEM supplemented with 10% Fetal Bovine Serum (FBS), 50 U/ml Penicillin and 50 μg/ml streptomycin. HT1080FAP and HT1080PA cell lines were generated by stably transfecting HT1080 cells with human FAP or mock plasmid, respectively in addition to the luciferase plasmid, as described previously [216]. HT1080FAP and HT1080PA cell lines were maintained in standard R10 medium (RPMI + 10% FBS + 50U/ml Penicillin and 50 μg/ml streptomycin) supplemented with 150 μg/ml Hygromycin B. Additionally, 200 μg/ml G418 was added to the medium for culturing HT1080FAP cells. T-cell medium (TCM) included RPMI with 2mM L-glutamine, 10% FBS, 50 U/ml penicillin, 50 μg/ml streptomycin and 1X NEAA (Non-essential amino acids solution).

6.2.2 Generation of CAR constructs and retroviral transduction of T-cells

The single chain variable fragment (scFv) of the FAP-specific CAR (F19) [216] and the NY-ESO-1 specific CAR (T1); which serves as a control CAR (recognizing the HLA-A*02:01/NY-ESO-$1_{157\text{-}165}$ peptide complex) [229] flanked by NCOI and BamHI restriction sites, was cloned into pBullet vector [257] containing a human Δ-CH2/CH3 domain, either of the co-stimulatory domains (CD28, Δ-CD28 or 4-1BB) and CD3ζ domain. The human CH2/CH3 domain has been modified to reduce FcγR binding and thereby minimizes the risk of off-target T-cell activation by CAR binding to $Fc\gamma R^+$ cells [255]. Additionally, the Δ-CD28 is a modification of the CD28 co-stimulatory domain (generated by site directed mutagenesis) which is devoid of lck kinase binding site, to avoid IL-2 release and subsequent persistence of T-reg cells [217]. The resulting CAR constructs were termed as, FAP-specific; F19-CD28/CD3ζ, F19-Δ-CD28/CD3ζ or F19-4-1BB/CD3ζ and NY-ESO-1-specific; T1-CD28/CD3ζ, T1-Δ-CD28/CD3ζ or T1-4-1BB/CD3ζ.

For retroviral transduction, CD3+ or CD8+ T-cells were purified from healthy buffy donors using CD3 or CD8 microbeads, respectively and employing MACS technology (Miltenyi). Positive selection typically resulted in a ≥ 95% pure T-cell population. The cells were further activated with CD3/CD28 human T-cell activator dynabeads at a bead to cell ratio of 1:5 in T-cell medium (TCM) supplemented with cytokines; IL-2 (200 IU/ml), IL-7 (10 ng/ml) and IL-15 (10 ng/ml) at 37°C, 5% CO_2. After 48 hr, the beads were removed and activated T-cells were resuspended in TCM supplemented with cytokines. Next, transduction was carried out by co-culturing/overlaying the resulting T-cell suspension on 293T cells that were transiently producing high titers of retrovirus particles carrying the genomic information of the CAR (293T cells pre-transfected overnight with helper plasmids and insert plasmid containing the CAR transgene using fugene transfection reagent at a fugene/DNA ratio 4:1 (μl/μg)). The transduction was carried out for 48 hr. Later, cells were expanded for 2 days in TCM supplemented with cytokines at 37°C, 5% CO_2 . Transduction efficacy was determined by staining for CAR

receptor using anti-human IgG antibody and subsequently analysing the cells by flow cytometry, before putting the cells in experiment.

6.2.3 Flow cytometry

Analysis of FAP expression was performed using the humanized F19 antibody [216] directly labeled with Alexa Fluor 647 (Alexa Fluor® 647 Antibody Labeling Kit; Invitrogen) according to the manufacturer's protocol.
For staining surface markers, cells were washed in flow cytometry (FACS) buffer (PBS + 2% FBS + 0.1% sodium azide and 1mM EDTA) and stained with fluorochrome labelled antibodies for 20 min at 4°C. LIVE⁄DEAD Fixable Dead Cell Stain Kit (Invitrogen) was used for staining dead cells. After washing with FACS buffer, cells were fixed in 3% paraformaldehyde solution (PFA) for 10 minutes, followed by a subsequent wash and acquisition on a flow cytometer.
For intracellular stainings, cells were stimulated with antigen or PMA (10ng/ml) and ionomycin (500ng/ml) in medium supplemented with Brefeldin-A (BFA; ratio BFA:medium = 1:2000). Cell surface staining was performed as described above. This was followed by fixation and permeabilization using 250μl of cytofix/cytoperm solution (eBiosciences) for 20 minutes at 4°C. After washing with 1X perm/wash buffer (eBiosciences), cells were incubated with antibodies for intracellular markers for 30 minutes at 4°C. After another round of washing, cells were acquired on flow cytometer. All samples were measured on a FACSCanto II or LSR Fortessa cytometer (BD Biosciences). Data was analyzed using FlowJo software (Treestar). Dead cells were excluded from the analysis.

6.2.4 Cytotoxicity assays

To evaluate the cytotoxic capacity of redirected T-cells against the antigen (FAP)-specific target (HT1080FAP) or non specific (HT1080PA) tumor cells, cytotoxicity assays were performed as previously described [258]. Briefly, tumor cells were labelled with a dye that intercalates into the plasma membrane; PKH26 (Sigma Aldrich). Labelled tumor cells were then co-incubated with CAR-T cells at indicated effector/target ratios. After 8 hrs cells were harvested; TO-PRO-3 iodide, a membrane impermeable DNA stain was added at 0.5 μM final concentration and cells were analyzed by flow cytometry. The target cells can be identified by PKH26 red fluorescence and lysed targets can be distinguished from unlysed by their ability to retain the TO-PRO-3 DNA stain. Background cell death (spontaneous lysis) was obtained by incubating only target cells in medium. The percentage of specific lysis was calculated as: "Spontaneous lysis" = 100% - % dead target cells in medium alone; "Targeted lysis" = 100% - % of dead target cells in T-cell and target cell co-culture condition; % specific lysis = 100 - ((Targeted lysis/Spontaneous lysis) X 100).

6.2.5 Proliferation assays

Proliferation of T-cells was determined *in vitro* using bromodeoxyuridine (BrdU) APC flow kit. Briefly, 24 well cell culture plates were coated with 2ug/ml recombinant human FAP at 4°C overnight. 0.2 X 10^6 CAR-T cells were seeded per well on FAP coated plates (total cell density not exceeding 2 X 10^6 per ml) and incubated at 37°C and 5% CO_2. After 72 hours, BrdU was added to the medium at final concentration of 10 μM followed by further incubation for 72 hours. The cells were harvested and intra-nuclear staining for BrdU was performed as per manufacturer's instructions followed by analysis on a flow cytometer.

6.2.6 Measurements for cytokine release

Cytokine production was assessed by sandwich ELISA assays. Supernatants of co-cultivated effector and target cells were collected after 12 hours of incubation. IFN-γ and IL-2 levels were detected using BD OptEIA set human IFN-γ and BD OptEIA set human IL-2 kits, respectively, according to the manufacturer's instruction (BD Biosciences).

From the patient, cytokines IL-2, IL-6, IL-10, IFN-γ and TNF-α were measured using a multiplexed particle-based flow cytometric cytokine assay [259]. Cytokine Luminex kits were purchased from R&D Systems (Oxon, UK) and used as per manufacturer's instructions. The analysis was conducted on a flow cytometer (Guava EasyCyte Plus, Millipore, Zug, Switzerland).

6.2.7 Library preparation for RNA sequencing

$CD8^+$ T-cells isolated from each of three individual buffy donors (N=3) using CD8 microbeads (Miltenyi Biotech) were transduced to express FAP-specific; F19-CD28/CD3ζ, F19-Δ-CD28/CD3ζ or F19-4-1BB/CD3ζ or NY-ESO-1-specific; T1-CD28/CD3ζ, T1-Δ-CD28/CD3ζ or T1-4-1BB/CD3ζ CARs. After transduction, the cells were stimulated with recombinant human FAP for 6 days and CAR^+ T-cells were flow sorted on an Aria III cell sorter (BD Biosciences). Average 1 X 10^6 sorted CAR^+CD8^+ cells with purity > 95% were used for RNA extraction using Zymo Quick RNA MicroPrep kit (Lucerna-Chem, Luzern, Switzerland) as per manufacturer's instructions. The quantity and quality of isolated RNA was determined with Qubit (1.0) Fluorometer (Life Technologies) and a Bioanalyzer 2100 (Agilent, Waldbronn, Germany). Samples with RNA Integrity Number (RIN) ≥ 7 were used for library preparation. Average RIN = 9.6 (n=16). The TruSeq Stranded mRNA Sample Prep Kit (Illumina, CA, USA) was used in library preparation. Briefly, total RNA samples (100ng) were poly-A selected and then reverse-transcribed into double stranded cDNA with Actinomycin added during first-strand synthesis. The cDNA samples were fragmented, end-repaired and adenylated before ligation of TruSeq adapters. Fragments containing TruSeq adapters on both ends were selectively enriched with PCR. The quality and quantity of the enriched libraries was validated using Qubit Fluorometer and Bioanalyzer 2100. The resulting product which is a smear with an average fragment size of approximately 360bp was normalized to 10nM in Tris-Cl 10mM, pH8.5 with 0.1% Tween-20.

Cluster generation was done using the TruSeq SR Cluster Kit v4-cBot-HS (Illumina) using 8pM of pooled normalized libraries on the cBOT. Sequencing was performed on the Illumina HiSeq 2500 single end 125 bp using the TruSeq SBS kit v4-HS (Illumina) at the Functional Genomics Center Zurich (FGCZ).

6.2.8 RNA sequencing data analysis

Illumina raw reads were separated by barcodes. Quality checks for raw sequencing reads was performed using FastQC program [260]. Reads with low quality ends (phred quality score <20) were subsequently filtered and mapped to the human reference genome (hg38, build GRCh38, downloaded from the UCSC genome browser [http://genome.ucsc.edu]) using TopHat. Gene expression levels were quantified using RSEM software package [261]. Differential expression analysis was performed using Bioconductor edgeR software package. Normalization and filtering of genes was carried out using edgeR. Only those genes expressed above 0.5 counts-per- million (CPM) in at least two of three biological replicates were retained for further analysis. TMM method (Trimmed mean of M-values) was used to normalize the compositional biases between libraries [262]. Limma package [263] was used to analyse differential gene expression. Read counts were transformed (log_2CPM) using voom function in the Limma package. Mean variance relationship was taken into account while transforming the data. Following voom transformation, lmfit function of Limma was used to fit linear model for each gene and assess differential expression. Differential gene expression was calculated in terms of Log fold change (Log_2FC) of antigen-specific stimulation (through FAP-specific CARs) over background (Control CARs). Genes with false discovery rate (FDR) value < 0.05 were considered differentially expressed and were subjected to Gene enrichment analysis using CAMERA also referred to as Competitive gene set test [264]. Inter-gene correlations were assessed within each gene set. Using CAMERA, we reported enriched pathways corresponding to the differentially expressed genes. Pathways with FDR < 0.05 were selected. We further focused our analysis on pathways that were unique to Δ-CD28 co-stimulation through the CAR (Log_2FC of F19-Δ-CD28/CD3ζ over T1-Δ-CD28/CD3ζ. Next, we selected a subset of relevant immune-linked pathways and identified commonly associated genes and their pattern of regulation.

6.2.9 Isolation of hematopoietic stem cells (HSCs)

Human fetal liver (HFL) at a gestational age between 17 to 22 weeks was obtained from Advanced Bioscience Resources (Alameda, CA, USA). Isolation of $CD34^+$ cells from HFL was performed as per the established protocol described previously [265]. Leukapheresis products were left overs from patients which initially were allocated autologous $CD34^+$ transplantation but did not need further treatment (obtained from Department of Oncology, University Hospital Zurich, Switzerland). The leukapheresis bag was thawed at 37°C in water bath and diluted 1:20 in PBS supplemented with 20% FBS and 0.4% EDTA (0.5M) (Life Technologies). PBMCs were isolated by density gradient centrifugation on Ficoll (GE Healthcare, UK) and resuspended in standard R10 medium at cell

density of 4 X 10^6 cells per ml. This was followed by double gradient centrifugation to further remove the contaminating monocytes from PBMCs. For double gradient centrifugation "solution-A" (per 50 ml - mixed 23.13 ml Percoll solution (GE Healthcare) with 1.87 ml 10-fold PBS) and "solution-B" (46% of solution-A in R10) were prepared. PBMC suspension was overlayered on solution-B at a volume of 1:1. This was followed by centrifugation at 500G for 30 min at room temperature. The white ring of monocytes formed at the interphase was discarded and the pellet of lymphocytes was collected. $CD34^+$ cells were isolated from the lymphocytes by positive selection using CD34 microbeads (Miltenyi Biotech) as per manufacturer's instructions. Purity of CD34 fraction was assessed by FACS and the cells were cryopreserved (RPMI + 7.5% DMSO + 20% FBS) for further use.

6.2.10 Generation of humanized mice

NSG mice were obtained from the Jackson Laboratory, and bred and raised under specific pathogen-free conditions at the Biologisches Zentrallabor (BZL), University Hospital Zurich, Switzerland. Newborn NSG mice (1 to 5 days old) were irradiated with 1 Gy and injected intrahepatically 5–7 hours later with 2×10^5 $CD34^+$ human hematopoietic progenitor cells obtained from HFL or with 2×10^6 $CD34^+$ obtained from leukapheresis product. The reconstitution of human immune system components in the peripheral blood of humanized NSG mice (huNSG) was analyzed 12 weeks after engraftment as described previously [204]. Before experiment, age matched mice (12-20 weeks old) were equally distributed in groups based on human immune reconstitution in blood.

6.2.11 Adoptive transfer of redirected T-cells in humanized mice

To test the survival of redirected T-cells, 0.2 X 10^6 CAR^+CD3^+ cells (F19-CD28/CD3ζ or F19-Δ-CD28/CD3ζ or F19-4-1BB/CD3ζ produced from harvested splenocytes of donor huNSG mice, were intra-venously injected into recipient huNSG mice (reconstituted with same $CD34^+$ HSCs as donor huNSG mice). Persistence of redirected T-cells in the blood was measured by qPCR at indicated time points in the timeline (fig. 5b). Mice were harvested at day 44 followed by screening for presence redirected T-cells in blood and other abdominal organs (liver, lung, spleen, bone marrow) by qPCR. To test the anti-tumor efficacy of redirected T-cells in humanized mice, luciferase expressing HT1080FAP tumor cells (0.1 X 10^6 cells per mouse) were injected intra-peritoneally (i.p.). Tumor development at day 1 was measured by *in vivo* bioluminescence imaging and based on the tumor burden, mice were equally distributed in groups. This was followed by adoptive transfer of redirected T-cells i.p. at effector/target (E:T) ratio of 4:1 to 8:1. In addition to this, mice were injected intra-peritoneally with PD-1 blocking antibody (200µg per mouse), every fourth day. Tumor measurements were performed several times during the experiment (timeline indicated in fig. 6b). For *in vivo* tumor imaging, mice were anesthetized with 2% isoflurane and i.p. injected with 150 mg/kg D-Luciferin (PerkinElmer, MA, USA) and signals were visualized using IVIS 200 Caliper (Caliper Life Sciences, MA, USA). Monitoring of mice was started immediately after D-Luciferin

injection and lasted up to 30 min to obtain the peak photon emission of each animal. For imaging purposes, a pseudocolor map representing light intensity was superimposed over a whole-body image. Throughout the experiment, all the bioluminescence signals were measured using the same settings; exposure time = 1 sec, binning = small and F-stop = 2. The bioluminescence emission was measured as Total Flux (photons/second) and quantified for each animal using software Living Image 3.2 (Caliper Life Sciences). A constant region of interest was designated around the torso of each animal to avoid any incoherence. Mice were regularly monitored by body weight measurements and were euthanized if their body weight increased or decreased by more than 15% or if mice displayed persistent signs of discomfort or deviations from normal behaviour.

6.2.12 Isolation of cells from humanized mouse tissues

Spleens were mechanically disrupted using the plunger of a syringe and filtered through 70μm cell strainer followed by separation of mononuclear cells using density gradient centrifugation employing ficoll. Livers and tumors were minced in HBSS (Thermo Fischer Scientific) containing 2% FBS, 0.4mg/ml collagenase-D and 20ug/ml DNAse (Roche, Basel, Switzerland). Lungs were minced in R10 containing 25mM Hepes (Thermo Fischer Scientific), 50ug/ml DNAse and 0.4mg/ml collagenase-A (Roche). This was followed by digestion of organs at 37°C for 30 min and then filtering the suspension through 70μm nylon cell strainers. Mononuclear cells from liver, lungs and tumor infiltrating lymphocytes (TILs) were further separated using a percoll gradient. Lysis of erythrocytes in the whole blood was done using Ack lysing buffer (Thermo Fischer Scientific). Bone marrow (BM) cells were harvested by inserting a needle into the opening of the bone and flushing out cells using 0.5-3 ml PBS. To obtain peritoneal lavage, 5ml of PBS was injected intra-peritoneally (IP) followed by gentle massaging and collection of fluid using a second syringe. The resulting single cell suspensions obtained were then used for subsequent analysis and for isolation of DNA.

6.2.13 Quantitative Real Time PCR to detect redirected T-cells

Cellular DNA was extracted using DNeasy blood and tissue kit (Qiagen, Hilden, Germany). Total DNA concentration was measured using nanodrop (Thermo Scientific). 300ng of total cellular DNA was added per well into 384 well lightcycler plates (Sarstedt, Nümbrecht, Germany). CAR DNA was quantified by real-time PCR using primers; scF19_fwd, scF19_rev and probe F19_oligo and Taqman Universal PCR Master Mix. The samples were measured in a CFX-384 Touch Real-Time PCR Detection System (Bio-Rad, CA, USA). All samples were tested at least in triplicates.

6.2.14 Clinical trial design

The primary objective was to test safety of a fixed single dose of $1x10^6$ adoptively transferred FAP-specific redirected T-cells in the pleural effusion in patients with MPM. Therefore, all grade III and IV adverse events

(AE), and severe adverse events (SAE) were measured. Main inclusion criteria were a histologically confirmed MPM, and the patient had not to be candidate for pleuropneumectomy. Main exclusion criteria were any autoimmune conditions, allogeneic transplants and any clinical relevant arteriopathies including stroke and coronary heart syndrome. For the safety assessment grade III and IV AEs and SAEs were collected until day +35. The primary safety variables are abnormalities, which are judged to be treatment-related and dose limiting (DLT) by an independent safety monitoring board after the patient passed day +35. GMP grade redirected T-cells were produced by retroviral transfer by EUFETS, Idar-Oberstein, Germany. The study schedule is given in **figure 4-8 C**. The research project was carried out in accordance to the research plan and with principles enunciated in the current version of the Declaration of Helsinki (DoH), the Essentials of Good Epidemiological Practice issued by Public Health Schweiz (EGEP), the Swiss Law and Swiss regulatory authority's requirements as applicable. The clinical trial for the complete recruitment is still ongoing. No primary endpoints are reported in this study.

6.2.15 Statistical analysis

Data was analyzed with Graph Pad Prism version 5.00 for Mac (GraphPad Software, San Diego, CA). Student's unpaired t-tests were performed between two groups of interest. For comparison between multiple groups, we used one way annova test using tukey's post test for multiple comparisons. Survival analysis was performed employing Kaplan Meier survival curves and statistical significance was calculated using log-rank test.

6.2.16 Study Approval

All animal experiments were performed in accordance with the Swiss federal and cantonal laws on animal protection KEK-ZH-Nr. 2011-0498, KEVT 10/2013 and 41/2016). The clinical trial was reviewed and approved by the cantonal ethics committee of Zürich, Switzerland (ethical committee KEK-ZH-Nr. 2012-0106, registered under NCT01722149). Written informed consent was received from the participant prior to inclusion in the study.

Chapter-7

References

7.1 References

1. Kenderian, S.S., D.L. Porter, and S. Gill, *Chimeric Antigen Receptor T Cells and Hematopoietic Cell Transplantation: How Not to Put the CART Before the Horse.* Biol Blood Marrow Transplant, 2017. **23**(2): p. 235-246.
2. Pandya, P.H., et al., *The Immune System in Cancer Pathogenesis: Potential Therapeutic Approaches.* J Immunol Res, 2016. **2016**: p. 4273943.
3. Collaborators, G.R.F., *Global, regional, and national comparative risk assessment of 79 behavioural, environmental and occupational, and metabolic risks or clusters of risks, 1990-2015: a systematic analysis for the Global Burden of Disease Study 2015.* Lancet, 2016. **388**(10053): p. 1659-1724.
4. Siegel, R.L., K.D. Miller, and A. Jemal, *Cancer Statistics, 2017.* CA Cancer J Clin, 2017. **67**(1): p. 7-30.
5. Pinho, S.S. and C.A. Reis, *Glycosylation in cancer: mechanisms and clinical implications.* Nat Rev Cancer, 2015. **15**(9): p. 540-55.
6. Sharma, S., T.K. Kelly, and P.A. Jones, *Epigenetics in cancer.* Carcinogenesis, 2010. **31**(1): p. 27-36.
7. Allison, K.H. and G.W. Sledge, *Heterogeneity and cancer.* Oncology (Williston Park), 2014. **28**(9): p. 772-8.
8. Jamal-Hanjani, M., et al., *Tracking the Evolution of Non-Small-Cell Lung Cancer.* N Engl J Med, 2017. **376**(22): p. 2109-2121.
9. Fedele, C., R.W. Tothill, and G.A. McArthur, *Navigating the challenge of tumor heterogeneity in cancer therapy.* Cancer Discov, 2014. **4**(2): p. 146-8.
10. Hanahan, D. and R.A. Weinberg, *The hallmarks of cancer.* Cell, 2000. **100**(1): p. 57-70.
11. Dunn, G.P., L.J. Old, and R.D. Schreiber, *The immunobiology of cancer immunosurveillance and immunoediting.* Immunity, 2004. **21**(2): p. 137-48.
12. Hanahan, D. and R.A. Weinberg, *Hallmarks of cancer: the next generation.* Cell, 2011. **144**(5): p. 646-74.
13. Yang, Y., *Cancer immunotherapy: harnessing the immune system to battle cancer.* J Clin Invest, 2015. **125**(9): p. 3335-7.
14. Chow, M.T., A. Möller, and M.J. Smyth, *Inflammation and immune surveillance in cancer.* Semin Cancer Biol, 2012. **22**(1): p. 23-32.
15. Kim, R., M. Emi, and K. Tanabe, *Cancer immunoediting from immune surveillance to immune escape.* Immunology, 2007. **121**(1): p. 1-14.
16. Swann, J.B. and M.J. Smyth, *Immune surveillance of tumors.* J Clin Invest, 2007. **117**(5): p. 1137-46.
17. Dunn, G.P., et al., *A critical function for type I interferons in cancer immunoediting.* Nat Immunol, 2005. **6**(7): p. 722-9.
18. Dighe, A.S., et al., *Enhanced in vivo growth and resistance to rejection of tumor cells expressing dominant negative IFN gamma receptors.* Immunity, 1994. **1**(6): p. 447-56.
19. Kaplan, D.H., et al., *Demonstration of an interferon gamma-dependent tumor surveillance system in immunocompetent mice.* Proc Natl Acad Sci U S A, 1998. **95**(13): p. 7556-61.
20. van den Broek, M.E., et al., *Decreased tumor surveillance in perforin-deficient mice.* J Exp Med, 1996. **184**(5): p. 1781-90.
21. Bolitho, P., et al., *Perforin-mediated suppression of B-cell lymphoma.* Proc Natl Acad Sci U S A, 2009. **106**(8): p. 2723-8.
22. Smyth, M.J., et al., *Perforin-mediated cytotoxicity is critical for surveillance of spontaneous lymphoma.* J Exp Med, 2000. **192**(5): p. 755-60.

23. Shankaran, V., et al., *IFNgamma and lymphocytes prevent primary tumour development and shape tumour immunogenicity.* Nature, 2001. **410**(6832): p. 1107-11.
24. Smyth, M.J., et al., *Differential tumor surveillance by natural killer (NK) and NKT cells.* J Exp Med, 2000. **191**(4): p. 661-8.
25. Street, S.E., E. Cretney, and M.J. Smyth, *Perforin and interferon-gamma activities independently control tumor initiation, growth, and metastasis.* Blood, 2001. **97**(1): p. 192-7.
26. Girardi, M., et al., *Regulation of cutaneous malignancy by gammadelta T cells.* Science, 2001. **294**(5542): p. 605-9.
27. Svane, I.M., et al., *Chemically induced sarcomas from nude mice are more immunogenic than similar sarcomas from congenic normal mice.* Eur J Immunol, 1996. **26**(8): p. 1844-50.
28. Engel, A.M., et al., *MCA sarcomas induced in scid mice are more immunogenic than MCA sarcomas induced in congenic, immunocompetent mice.* Scand J Immunol, 1997. **45**(5): p. 463-70.
29. Smyth, M.J., G.P. Dunn, and R.D. Schreiber, *Cancer immunosurveillance and immunoediting: the roles of immunity in suppressing tumor development and shaping tumor immunogenicity.* Adv Immunol, 2006. **90**: p. 1-50.
30. Dranoff, G., *Cytokines in cancer pathogenesis and cancer therapy.* Nat Rev Cancer, 2004. **4**(1): p. 11-22.
31. Howell, W.M., V. Carter, and B. Clark, *The HLA system: immunobiology, HLA typing, antibody screening and crossmatching techniques.* J Clin Pathol, 2010. **63**(5): p. 387-90.
32. Choo, S.Y., *The HLA system: genetics, immunology, clinical testing, and clinical implications.* Yonsei Med J, 2007. **48**(1): p. 11-23.
33. Neefjes, J., et al., *Towards a systems understanding of MHC class I and MHC class II antigen presentation.* Nat Rev Immunol, 2011. **11**(12): p. 823-36.
34. Hansen, V.L. and R.D. Miller, *The Evolution and Structure of Atypical T Cell Receptors.* Results Probl Cell Differ, 2015. **57**: p. 265-78.
35. Malissen, B., et al., *Integrative biology of T cell activation.* Nat Immunol, 2014. **15**(9): p. 790-7.
36. Germain, R.N., *T-cell development and the CD4-CD8 lineage decision.* Nat Rev Immunol, 2002. **2**(5): p. 309-22.
37. Gascoigne, N.R., *Do T cells need endogenous peptides for activation?* Nat Rev Immunol, 2008. **8**(11): p. 895-900.
38. Hogquist, K.A. and S.C. Jameson, *The self-obsession of T cells: how TCR signaling thresholds affect fate 'decisions' and effector function.* Nat Immunol, 2014. **15**(9): p. 815-23.
39. Angus, K.L. and G.M. Griffiths, *Cell polarisation and the immunological synapse.* Curr Opin Cell Biol, 2013. **25**(1): p. 85-91.
40. Freiberg, B.A., et al., *Staging and resetting T cell activation in SMACs.* Nat Immunol, 2002. **3**(10): p. 911-7.
41. Wülfing, C., et al., *Costimulation and endogenous MHC ligands contribute to T cell recognition.* Nat Immunol, 2002. **3**(1): p. 42-7.
42. Bromley, S.K., et al., *The immunological synapse and CD28-CD80 interactions.* Nat Immunol, 2001. **2**(12): p. 1159-66.
43. Gutcher, I. and B. Becher, *APC-derived cytokines and T cell polarization in autoimmune inflammation.* J Clin Invest, 2007. **117**(5): p. 1119-27.
44. Schmidt, A., N. Oberle, and P.H. Krammer, *Molecular mechanisms of treg-mediated T cell suppression.* Front Immunol, 2012. **3**: p. 51.
45. Maxwell, J.R., et al., *Danger and OX40 receptor signaling synergize to enhance memory T cell survival by inhibiting peripheral deletion.* J Immunol, 2000. **164**(1): p. 107-12.
46. Sanchez, P.J., et al., *Combined TLR/CD40 stimulation mediates potent cellular immunity by regulating dendritic cell expression of CD70 in vivo.* J Immunol, 2007. **178**(3): p. 1564-72.

47. Mullen, A.C., et al., *Role of T-bet in commitment of TH1 cells before IL-12-dependent selection.* Science, 2001. **292**(5523): p. 1907-10.
48. Pennock, N.D., et al., *T cell responses: naive to memory and everything in between.* Adv Physiol Educ, 2013. **37**(4): p. 273-83.
49. Fields, P.E., S.T. Kim, and R.A. Flavell, *Cutting edge: changes in histone acetylation at the IL-4 and IFN-gamma loci accompany Th1/Th2 differentiation.* J Immunol, 2002. **169**(2): p. 647-50.
50. Taylor-Robinson, A.W. and R.S. Phillips, *Functional characterization of protective CD4+ T-cell clones reactive to the murine malaria parasite Plasmodium chabaudi.* Immunology, 1992. **77**(1): p. 99-105.
51. Goswami, R. and M.H. Kaplan, *A brief history of IL-9.* J Immunol, 2011. **186**(6): p. 3283-8.
52. Stockinger, B., M. Veldhoen, and B. Martin, *Th17 T cells: linking innate and adaptive immunity.* Semin Immunol, 2007. **19**(6): p. 353-61.
53. Breitfeld, D., et al., *Follicular B helper T cells express CXC chemokine receptor 5, localize to B cell follicles, and support immunoglobulin production.* J Exp Med, 2000. **192**(11): p. 1545-52.
54. Fontenot, J.D., M.A. Gavin, and A.Y. Rudensky, *Foxp3 programs the development and function of CD4+CD25+ regulatory T cells.* Nat Immunol, 2003. **4**(4): p. 330-6.
55. Broere, F., et al., *T cell subsets and T cell-mediated immunity*. 2011, Principles of Immunopharmacology.
56. Spear, P., et al., *NKG2D ligands as therapeutic targets.* Cancer Immun, 2013. **13**: p. 8.
57. Zamai, L., et al., *Natural killer (NK) cell-mediated cytotoxicity: differential use of TRAIL and Fas ligand by immature and mature primary human NK cells.* J Exp Med, 1998. **188**(12): p. 2375-80.
58. Wink, D.A., et al., *Nitric oxide and redox mechanisms in the immune response.* J Leukoc Biol, 2011. **89**(6): p. 873-91.
59. Chan, T., et al., *Enhanced T-cell immunity induced by dendritic cells with phagocytosis of heat shock protein 70 gene-transfected tumor cells in early phase of apoptosis.* Cancer Gene Ther, 2007. **14**(4): p. 409-20.
60. Schiavoni, G., F. Mattei, and L. Gabriele, *Type I Interferons as Stimulators of DC-Mediated Cross-Priming: Impact on Anti-Tumor Response.* Front Immunol, 2013. **4**: p. 483.
61. Boon, T. and P. van der Bruggen, *Human tumor antigens recognized by T lymphocytes.* J Exp Med, 1996. **183**(3): p. 725-9.
62. Mosmann, T.R., *Cytokines, differentiation and functions of subsets of CD4 and CD8 T cells.* Behring Inst Mitt, 1995(96): p. 1-6.
63. Bubeník, J., *MHC class I down-regulation: tumour escape from immune surveillance? (review).* Int J Oncol, 2004. **25**(2): p. 487-91.
64. Adam, J.K., B. Odhav, and K.D. Bhoola, *Immune responses in cancer.* Pharmacol Ther, 2003. **99**(1): p. 113-32.
65. Turnis, M.E., L.P. Andrews, and D.A. Vignali, *Inhibitory receptors as targets for cancer immunotherapy.* Eur J Immunol, 2015. **45**(7): p. 1892-905.
66. Moh, M.C. and S. Shen, *The roles of cell adhesion molecules in tumor suppression and cell migration: a new paradox.* Cell Adh Migr, 2009. **3**(4): p. 334-6.
67. Rabinovich, G.A., D. Gabrilovich, and E.M. Sotomayor, *Immunosuppressive strategies that are mediated by tumor cells.* Annu Rev Immunol, 2007. **25**: p. 267-96.
68. Koh, Y.T., M.L. García-Hernández, and W.M. Kast, *Tumor Immune Escape Mechanisms* Cancer Drug Discovery and Development: Cancer Drug Resistance.
69. Wherry, E.J. and M. Kurachi, *Molecular and cellular insights into T cell exhaustion.* Nat Rev Immunol, 2015. **15**(8): p. 486-99.
70. Angelosanto, J.M., et al., *Progressive loss of memory T cell potential and commitment to exhaustion during chronic viral infection.* J Virol, 2012. **86**(15): p. 8161-70.

71. Brooks, D.G., D.B. McGavern, and M.B. Oldstone, *Reprogramming of antiviral T cells prevents inactivation and restores T cell activity during persistent viral infection.* J Clin Invest, 2006. **116**(6): p. 1675-85.
72. Frebel, H., et al., *Programmed death 1 protects from fatal circulatory failure during systemic virus infection of mice.* J Exp Med, 2012. **209**(13): p. 2485-99.
73. Nishimura, H., et al., *Development of lupus-like autoimmune diseases by disruption of the PD-1 gene encoding an ITIM motif-carrying immunoreceptor.* Immunity, 1999. **11**(2): p. 141-51.
74. McKinney, E.F., et al., *T-cell exhaustion, co-stimulation and clinical outcome in autoimmunity and infection.* Nature, 2015. **523**(7562): p. 612-6.
75. Dong, H., et al., *Tumor-associated B7-H1 promotes T-cell apoptosis: a potential mechanism of immune evasion.* Nat Med, 2002. **8**(8): p. 793-800.
76. Fourcade, J., et al., *PD-1 is a regulator of NY-ESO-1-specific CD8+ T cell expansion in melanoma patients.* J Immunol, 2009. **182**(9): p. 5240-9.
77. Gassner, F.J., et al., *Chemotherapy-induced augmentation of T cells expressing inhibitory receptors is reversed by treatment with lenalidomide in chronic lymphocytic leukemia.* Haematologica, 2014. **99**(5): p. 67-9.
78. Lee, P.P., et al., *Characterization of circulating T cells specific for tumor-associated antigens in melanoma patients.* Nat Med, 1999. **5**(6): p. 677-85.
79. Baitsch, L., et al., *Exhaustion of tumor-specific CD8⁺ T cells in metastases from melanoma patients.* J Clin Invest, 2011. **121**(6): p. 2350-60.
80. Catakovic, K., et al., *T cell exhaustion: from pathophysiological basics to tumor immunotherapy.* Cell Commun Signal, 2017. **15**(1): p. 1.
81. Barber, D.L., et al., *Restoring function in exhausted CD8 T cells during chronic viral infection.* Nature, 2006. **439**(7077): p. 682-7.
82. Yokosuka, T., et al., *Programmed cell death 1 forms negative costimulatory microclusters that directly inhibit T cell receptor signaling by recruiting phosphatase SHP2.* J Exp Med, 2012. **209**(6): p. 1201-17.
83. Parry, R.V., et al., *CTLA-4 and PD-1 receptors inhibit T-cell activation by distinct mechanisms.* Mol Cell Biol, 2005. **25**(21): p. 9543-53.
84. Patsoukis, N., et al., *Selective effects of PD-1 on Akt and Ras pathways regulate molecular components of the cell cycle and inhibit T cell proliferation.* Sci Signal, 2012. **5**(230): p. ra46.
85. Park, H.J., et al., *PD-1 upregulated on regulatory T cells during chronic virus infection enhances the suppression of CD8+ T cell immune response via the interaction with PD-L1 expressed on CD8+ T cells.* J Immunol, 2015. **194**(12): p. 5801-11.
86. Paley, M.A., et al., *Progenitor and terminal subsets of CD8+ T cells cooperate to contain chronic viral infection.* Science, 2012. **338**(6111): p. 1220-5.
87. Blackburn, S.D., et al., *Selective expansion of a subset of exhausted CD8 T cells by alphaPD-L1 blockade.* Proc Natl Acad Sci U S A, 2008. **105**(39): p. 15016-21.
88. Intlekofer, A.M. and C.B. Thompson, *At the bench: preclinical rationale for CTLA-4 and PD-1 blockade as cancer immunotherapy.* J Leukoc Biol, 2013. **94**(1): p. 25-39.
89. He, J., et al., *Development of PD-1/PD-L1 Pathway in Tumor Immune Microenvironment and Treatment for Non-Small Cell Lung Cancer.* Sci Rep, 2015. **5**: p. 13110.
90. Byun, D.J., et al., *Cancer immunotherapy - immune checkpoint blockade and associated endocrinopathies.* Nat Rev Endocrinol, 2017. **13**(4): p. 195-207.
91. Iwai, Y., et al., *Cancer immunotherapies targeting the PD-1 signaling pathway.* J Biomed Sci, 2017. **24**(1): p. 26.
92. Robert, C., et al., *Nivolumab in previously untreated melanoma without BRAF mutation.* N Engl J Med, 2015. **372**(4): p. 320-30.

93. Gettinger, S.N., et al., *Overall Survival and Long-Term Safety of Nivolumab (Anti-Programmed Death 1 Antibody, BMS-936558, ONO-4538) in Patients With Previously Treated Advanced Non-Small-Cell Lung Cancer.* J Clin Oncol, 2015. **33**(18): p. 2004-12.
94. Brahmer, J., et al., *Nivolumab versus Docetaxel in Advanced Squamous-Cell Non-Small-Cell Lung Cancer.* N Engl J Med, 2015. **373**(2): p. 123-35.
95. Borghaei, H., et al., *Nivolumab versus Docetaxel in Advanced Nonsquamous Non-Small-Cell Lung Cancer.* N Engl J Med, 2015. **373**(17): p. 1627-39.
96. Herbst, R.S., et al., *Pembrolizumab versus docetaxel for previously treated, PD-L1-positive, advanced non-small-cell lung cancer (KEYNOTE-010): a randomised controlled trial.* Lancet, 2016. **387**(10027): p. 1540-50.
97. Westin, J.R., et al., *Safety and activity of PD1 blockade by pidilizumab in combination with rituximab in patients with relapsed follicular lymphoma: a single group, open-label, phase 2 trial.* Lancet Oncol, 2014. **15**(1): p. 69-77.
98. Armand, P., et al., *Disabling immune tolerance by programmed death-1 blockade with pidilizumab after autologous hematopoietic stem-cell transplantation for diffuse large B-cell lymphoma: results of an international phase II trial.* J Clin Oncol, 2013. **31**(33): p. 4199-206.
99. Postow, M.A., et al., *Nivolumab and ipilimumab versus ipilimumab in untreated melanoma.* N Engl J Med, 2015. **372**(21): p. 2006-17.
100. Weber, J.S., et al., *Nivolumab versus chemotherapy in patients with advanced melanoma who progressed after anti-CTLA-4 treatment (CheckMate 037): a randomised, controlled, open-label, phase 3 trial.* Lancet Oncol, 2015. **16**(4): p. 375-84.
101. Ribas, A., et al., *Association of Pembrolizumab With Tumor Response and Survival Among Patients With Advanced Melanoma.* JAMA, 2016. **315**(15): p. 1600-9.
102. Rosenberg, S.A. and N.P. Restifo, *Adoptive cell transfer as personalized immunotherapy for human cancer.* Science, 2015. **348**(6230): p. 62-8.
103. DELORME, E.J. and P. ALEXANDER, *TREATMENT OF PRIMARY FIBROSARCOMA IN THE RAT WITH IMMUNE LYMPHOCYTES.* Lancet, 1964. **2**(7351): p. 117-20.
104. Fefer, A., *Immunotherapy and chemotherapy of Moloney sarcoma virus-induced tumors in mice.* Cancer Res, 1969. **29**(12): p. 2177-83.
105. Morgan, D.A., F.W. Ruscetti, and R. Gallo, *Selective in vitro growth of T lymphocytes from normal human bone marrows.* Science, 1976. **193**(4257): p. 1007-8.
106. Rosenberg, S.A., et al., *Regression of established pulmonary metastases and subcutaneous tumor mediated by the systemic administration of high-dose recombinant interleukin 2.* J Exp Med, 1985. **161**(5): p. 1169-88.
107. Eberlein, T.J., M. Rosenstein, and S.A. Rosenberg, *Regression of a disseminated syngeneic solid tumor by systemic transfer of lymphoid cells expanded in interleukin 2.* J Exp Med, 1982. **156**(2): p. 385-97.
108. Rosenberg, S.A., et al., *Use of tumor-infiltrating lymphocytes and interleukin-2 in the immunotherapy of patients with metastatic melanoma. A preliminary report.* N Engl J Med, 1988. **319**(25): p. 1676-80.
109. Rosenberg, S.A., et al., *Treatment of patients with metastatic melanoma with autologous tumor-infiltrating lymphocytes and interleukin 2.* J Natl Cancer Inst, 1994. **86**(15): p. 1159-66.
110. Dudley, M.E., et al., *Cancer regression and autoimmunity in patients after clonal repopulation with antitumor lymphocytes.* Science, 2002. **298**(5594): p. 850-4.
111. Gattinoni, L., et al., *Removal of homeostatic cytokine sinks by lymphodepletion enhances the efficacy of adoptively transferred tumor-specific CD8+ T cells.* J Exp Med, 2005. **202**(7): p. 907-12.

112. Rosenberg, S.A., et al., *Durable complete responses in heavily pretreated patients with metastatic melanoma using T-cell transfer immunotherapy.* Clin Cancer Res, 2011. **17**(13): p. 4550-7.
113. Goff, S.L., et al., *Randomized, Prospective Evaluation Comparing Intensity of Lymphodepletion Before Adoptive Transfer of Tumor-Infiltrating Lymphocytes for Patients With Metastatic Melanoma.* J Clin Oncol, 2016. **34**(20): p. 2389-97.
114. Tran, E., et al., *T-Cell Transfer Therapy Targeting Mutant KRAS in Cancer.* N Engl J Med, 2016. **375**(23): p. 2255-2262.
115. Besser, M.J., et al., *Minimally cultured or selected autologous tumor-infiltrating lymphocytes after a lympho-depleting chemotherapy regimen in metastatic melanoma patients.* J Immunother, 2009. **32**(4): p. 415-23.
116. Stanislawski, T., et al., *Circumventing tolerance to a human MDM2-derived tumor antigen by TCR gene transfer.* Nat Immunol, 2001. **2**(10): p. 962-70.
117. Gao, L., et al., *Selective elimination of leukemic CD34(+) progenitor cells by cytotoxic T lymphocytes specific for WT1.* Blood, 2000. **95**(7): p. 2198-203.
118. de Witte, M.A., et al., *Targeting self-antigens through allogeneic TCR gene transfer.* Blood, 2006. **108**(3): p. 870-7.
119. Morgan, R.A., et al., *Cancer regression in patients after transfer of genetically engineered lymphocytes.* Science, 2006. **314**(5796): p. 126-9.
120. Maher, J., *Immunotherapy of malignant disease using chimeric antigen receptor engrafted T cells.* ISRN Oncol, 2012. **2012**: p. 278093.
121. Dai, H., et al., *Chimeric Antigen Receptors Modified T-Cells for Cancer Therapy.* J Natl Cancer Inst, 2016. **108**(7).
122. Fesnak, A.D., C.H. June, and B.L. Levine, *Engineered T cells: the promise and challenges of cancer immunotherapy.* Nat Rev Cancer, 2016. **16**(9): p. 566-81.
123. Yu, S., et al., *Chimeric antigen receptor T cells: a novel therapy for solid tumors.* J Hematol Oncol, 2017. **10**(1): p. 78.
124. Gross, G., T. Waks, and Z. Eshhar, *Expression of immunoglobulin-T-cell receptor chimeric molecules as functional receptors with antibody-type specificity.* Proc Natl Acad Sci U S A, 1989. **86**(24): p. 10024-8.
125. Kalaitsidou, M., et al., *CAR T-cell therapy: toxicity and the relevance of preclinical models.* Immunotherapy, 2015. **7**(5): p. 487-97.
126. Sha, H.H., et al., *Chimaeric antigen receptor T-cell therapy for tumour immunotherapy.* Biosci Rep, 2017. **37**(1).
127. Chmielewski, M. and H. Abken, *TRUCKs: the fourth generation of CARs.* Expert Opin Biol Ther, 2015. **15**(8): p. 1145-54.
128. Carter, R.H. and D.T. Fearon, *CD19: lowering the threshold for antigen receptor stimulation of B lymphocytes.* Science, 1992. **256**(5053): p. 105-7.
129. Engel, P., et al., *Abnormal B lymphocyte development, activation, and differentiation in mice that lack or overexpress the CD19 signal transduction molecule.* Immunity, 1995. **3**(1): p. 39-50.
130. Rickert, R.C., K. Rajewsky, and J. Roes, *Impairment of T-cell-dependent B-cell responses and B-1 cell development in CD19-deficient mice.* Nature, 1995. **376**(6538): p. 352-5.
131. Shank, B.R., et al., *Chimeric Antigen Receptor T Cells in Hematologic Malignancies.* Pharmacotherapy, 2017. **37**(3): p. 334-345.
132. Brentjens, R.J., et al., *Eradication of systemic B-cell tumors by genetically targeted human T lymphocytes co-stimulated by CD80 and interleukin-15.* Nat Med, 2003. **9**(3): p. 279-86.
133. Maus, M.V., et al., *Antibody-modified T cells: CARs take the front seat for hematologic malignancies.* Blood, 2014. **123**(17): p. 2625-35.

134. Kochenderfer, J.N., et al., *Eradication of B-lineage cells and regression of lymphoma in a patient treated with autologous T cells genetically engineered to recognize CD19.* Blood, 2010. **116**(20): p. 4099-102.
135. Kochenderfer, J.N., et al., *Adoptive transfer of syngeneic T cells transduced with a chimeric antigen receptor that recognizes murine CD19 can eradicate lymphoma and normal B cells.* Blood, 2010. **116**(19): p. 3875-86.
136. Pegram, H.J., et al., *Tumor-targeted T cells modified to secrete IL-12 eradicate systemic tumors without need for prior conditioning.* Blood, 2012. **119**(18): p. 4133-41.
137. Davila, M.L., et al., *CD19 CAR-targeted T cells induce long-term remission and B Cell Aplasia in an immunocompetent mouse model of B cell acute lymphoblastic leukemia.* PLoS One, 2013. **8**(4): p. e61338.
138. Paszkiewicz, P.J., et al., *Targeted antibody-mediated depletion of murine CD19 CAR T cells permanently reverses B cell aplasia.* J Clin Invest, 2016. **126**(11): p. 4262-4272.
139. Rivière, I. and M. Sadelain, *Chimeric Antigen Receptors: A Cell and Gene Therapy Perspective.* Mol Ther, 2017. **25**(5): p. 1117-1124.
140. Lamers, C.H., et al., *Immune responses to transgene and retroviral vector in patients treated with ex vivo-engineered T cells.* Blood, 2011. **117**(1): p. 72-82.
141. Maus, M.V., et al., *T cells expressing chimeric antigen receptors can cause anaphylaxis in humans.* Cancer Immunol Res, 2013. **1**(1): p. 26-31.
142. Makita, S., K. Yoshimura, and K. Tobinai, *Clinical development of anti-CD19 chimeric antigen receptor T-cell therapy for B-cell non-Hodgkin lymphoma.* Cancer Sci, 2017.
143. Atanackovic, D., et al., *Chimeric Antigen Receptor (CAR) therapy for multiple myeloma.* Br J Haematol, 2016. **172**(5): p. 685-98.
144. Kalos, M., et al., *T cells with chimeric antigen receptors have potent antitumor effects and can establish memory in patients with advanced leukemia.* Sci Transl Med, 2011. **3**(95): p. 95ra73.
145. Brentjens, R.J., et al., *CD19-targeted T cells rapidly induce molecular remissions in adults with chemotherapy-refractory acute lymphoblastic leukemia.* Sci Transl Med, 2013. **5**(177): p. 177ra38.
146. Brudno, J.N., et al., *Allogeneic T Cells That Express an Anti-CD19 Chimeric Antigen Receptor Induce Remissions of B-Cell Malignancies That Progress After Allogeneic Hematopoietic Stem-Cell Transplantation Without Causing Graft-Versus-Host Disease.* J Clin Oncol, 2016. **34**(10): p. 1112-21.
147. Xu, X.J. and Y.M. Tang, *Cytokine release syndrome in cancer immunotherapy with chimeric antigen receptor engineered T cells.* Cancer Lett, 2014. **343**(2): p. 172-8.
148. Geyer, M.B. and R.J. Brentjens, *Review: Current clinical applications of chimeric antigen receptor (CAR) modified T cells.* Cytotherapy, 2016. **18**(11): p. 1393-1409.
149. Morgan, R.A., et al., *Case report of a serious adverse event following the administration of T cells transduced with a chimeric antigen receptor recognizing ERBB2.* Mol Ther, 2010. **18**(4): p. 843-51.
150. Brown, C.E., et al., *Regression of Glioblastoma after Chimeric Antigen Receptor T-Cell Therapy.* N Engl J Med, 2016. **375**(26): p. 2561-9.
151. Katz, S.C., et al., *Phase I Hepatic Immunotherapy for Metastases Study of Intra-Arterial Chimeric Antigen Receptor-Modified T-cell Therapy for CEA+ Liver Metastases.* Clin Cancer Res, 2015. **21**(14): p. 3149-59.
152. Louis, C.U., et al., *Antitumor activity and long-term fate of chimeric antigen receptor-positive T cells in patients with neuroblastoma.* Blood, 2011. **118**(23): p. 6050-6.
153. Ahmed, N., et al., *Human Epidermal Growth Factor Receptor 2 (HER2) -Specific Chimeric Antigen Receptor-Modified T Cells for the Immunotherapy of HER2-Positive Sarcoma.* J Clin Oncol, 2015. **33**(15): p. 1688-96.

154. Newick, K., et al., *CAR T Cell Therapy for Solid Tumors.* Annu Rev Med, 2017. **68**: p. 139-152.
155. John, L.B., et al., *Anti-PD-1 antibody therapy potently enhances the eradication of established tumors by gene-modified T cells.* Clin Cancer Res, 2013. **19**(20): p. 5636-46.
156. Moon, E.K., et al., *Multifactorial T-cell hypofunction that is reversible can limit the efficacy of chimeric antigen receptor-transduced human T cells in solid tumors.* Clin Cancer Res, 2014. **20**(16): p. 4262-73.
157. Sheppard, D., *Dominant negative mutants: tools for the study of protein function in vitro and in vivo.* Am J Respir Cell Mol Biol, 1994. **11**(1): p. 1-6.
158. Cherkassky, L., et al., *Human CAR T cells with cell-intrinsic PD-1 checkpoint blockade resist tumor-mediated inhibition.* J Clin Invest, 2016. **126**(8): p. 3130-44.
159. Shin, J.H., et al., *Positive conversion of negative signaling of CTLA4 potentiates antitumor efficacy of adoptive T-cell therapy in murine tumor models.* Blood, 2012. **119**(24): p. 5678-87.
160. Liu, X., et al., *A Chimeric Switch-Receptor Targeting PD1 Augments the Efficacy of Second-Generation CAR T Cells in Advanced Solid Tumors.* Cancer Res, 2016. **76**(6): p. 1578-90.
161. Prosser, M.E., et al., *Tumor PD-L1 co-stimulates primary human CD8(+) cytotoxic T cells modified to express a PD1:CD28 chimeric receptor.* Mol Immunol, 2012. **51**(3-4): p. 263-72.
162. Suarez, E.R., et al., *Chimeric antigen receptor T cells secreting anti-PD-L1 antibodies more effectively regress renal cell carcinoma in a humanized mouse model.* Oncotarget, 2016. **7**(23): p. 34341-55.
163. Rupp, L.J., et al., *CRISPR/Cas9-mediated PD-1 disruption enhances anti-tumor efficacy of human chimeric antigen receptor T cells.* Sci Rep, 2017. **7**(1): p. 737.
164. Holzapfel, B.M., et al., *Concise review: humanized models of tumor immunology in the 21st century: convergence of cancer research and tissue engineering.* Stem Cells, 2015. **33**(6): p. 1696-704.
165. Goldman, J.P., et al., *Enhanced human cell engraftment in mice deficient in RAG2 and the common cytokine receptor gamma chain.* Br J Haematol, 1998. **103**(2): p. 335-42.
166. Perrin, S., *Preclinical research: Make mouse studies work.* Nature, 2014. **507**(7493): p. 423-5.
167. Holzapfel, B.M., et al., *Humanised xenograft models of bone metastasis revisited: novel insights into species-specific mechanisms of cancer cell osteotropism.* Cancer Metastasis Rev, 2013. **32**(1-2): p. 129-45.
168. Thibaudeau, L., et al., *Mimicking breast cancer-induced bone metastasis in vivo: current transplantation models and advanced humanized strategies.* Cancer Metastasis Rev, 2014. **33**(2-3): p. 721-35.
169. Burkhardt, A.M. and A. Zlotnik, *Translating translational research: mouse models of human disease.* Cell Mol Immunol, 2013. **10**(5): p. 373-4.
170. Brehm, M.A., et al., *Generation of improved humanized mouse models for human infectious diseases.* J Immunol Methods, 2014. **410**: p. 3-17.
171. Shultz, L.D., et al., *Humanized mice for immune system investigation: progress, promise and challenges.* Nat Rev Immunol, 2012. **12**(11): p. 786-98.
172. King, M.A., et al., *Human peripheral blood leucocyte non-obese diabetic-severe combined immunodeficiency interleukin-2 receptor gamma chain gene mouse model of xenogeneic graft-versus-host-like disease and the role of host major histocompatibility complex.* Clin Exp Immunol, 2009. **157**(1): p. 104-18.
173. Tanner, A., et al., *Humanized mice as a model to study human hematopoietic stem cell transplantation.* Stem Cells Dev, 2014. **23**(1): p. 76-82.
174. Rämer, P.C., et al., *Mice with human immune system components as in vivo models for infections with human pathogens.* Immunol Cell Biol, 2011. **89**(3): p. 408-16.
175. Werner-Klein, M., et al., *Immune humanization of immunodeficient mice using diagnostic bone marrow aspirates from carcinoma patients.* PLoS One, 2014. **9**(5): p. e97860.

176. Lang, J., et al., *Generation of hematopoietic humanized mice in the newborn BALB/c-Rag2null Il2rγnull mouse model: a multivariable optimization approach.* Clin Immunol, 2011. **140**(1): p. 102-16.
177. Legrand, N., K. Weijer, and H. Spits, *Experimental models to study development and function of the human immune system in vivo.* J Immunol, 2006. **176**(4): p. 2053-8.
178. Kikuchi, K. and M. Kondo, *Developmental switch of mouse hematopoietic stem cells from fetal to adult type occurs in bone marrow after birth.* Proc Natl Acad Sci U S A, 2006. **103**(47): p. 17852-7.
179. Brehm, M.A., et al., *Overcoming current limitations in humanized mouse research.* J Infect Dis, 2013. **208 Suppl 2**: p. S125-30.
180. Lan, P., et al., *Reconstitution of a functional human immune system in immunodeficient mice through combined human fetal thymus/liver and CD34+ cell transplantation.* Blood, 2006. **108**(2): p. 487-92.
181. Melkus, M.W., et al., *Humanized mice mount specific adaptive and innate immune responses to EBV and TSST-1.* Nat Med, 2006. **12**(11): p. 1316-22.
182. Rongvaux, A., et al., *Human hemato-lymphoid system mice: current use and future potential for medicine.* Annu Rev Immunol, 2013. **31**: p. 635-74.
183. Biswas, S., et al., *Humoral immune responses in humanized BLT mice immunized with West Nile virus and HIV-1 envelope proteins are largely mediated via human CD5+ B cells.* Immunology, 2011. **134**(4): p. 419-33.
184. van der Stegen, S.J., M. Hamieh, and M. Sadelain, *The pharmacology of second-generation chimeric antigen receptors.* Nat Rev Drug Discov, 2015. **14**(7): p. 499-509.
185. Porter, D.L., et al., *Chimeric antigen receptor T cells persist and induce sustained remissions in relapsed refractory chronic lymphocytic leukemia.* Sci Transl Med, 2015. **7**(303): p. 303ra139.
186. Mak, I.W., N. Evaniew, and M. Ghert, *Lost in translation: animal models and clinical trials in cancer treatment.* Am J Transl Res, 2014. **6**(2): p. 114-8.
187. Day, C.P., G. Merlino, and T. Van Dyke, *Preclinical mouse cancer models: a maze of opportunities and challenges.* Cell, 2015. **163**(1): p. 39-53.
188. Shultz, L.D., F. Ishikawa, and D.L. Greiner, *Humanized mice in translational biomedical research.* Nat Rev Immunol, 2007. **7**(2): p. 118-30.
189. Morton, J.J., et al., *Humanized Mouse Xenograft Models: Narrowing the Tumor-Microenvironment Gap.* Cancer Res, 2016. **76**(21): p. 6153-6158.
190. de Visser, K.E., A. Eichten, and L.M. Coussens, *Paradoxical roles of the immune system during cancer development.* Nat Rev Cancer, 2006. **6**(1): p. 24-37.
191. McCune, J.M., et al., *The SCID-hu mouse: murine model for the analysis of human hematolymphoid differentiation and function.* Science, 1988. **241**(4873): p. 1632-9.
192. Namikawa, R., et al., *Long-term human hematopoiesis in the SCID-hu mouse.* J Exp Med, 1990. **172**(4): p. 1055-63.
193. Kyoizumi, S., et al., *Implantation and maintenance of functional human bone marrow in SCID-hu mice.* Blood, 1992. **79**(7): p. 1704-11.
194. Carballido, J.M., et al., *Generation of primary antigen-specific human T- and B-cell responses in immunocompetent SCID-hu mice.* Nat Med, 2000. **6**(1): p. 103-6.
195. Mosier, D.E., et al., *Transfer of a functional human immune system to mice with severe combined immunodeficiency.* Nature, 1988. **335**(6187): p. 256-9.
196. Hesselton, R.M., et al., *High levels of human peripheral blood mononuclear cell engraftment and enhanced susceptibility to human immunodeficiency virus type 1 infection in NOD/LtSz-scid/scid mice.* J Infect Dis, 1995. **172**(4): p. 974-82.

197. Tereb, D.A., et al., *Human T cells infiltrate and injure pig coronary artery grafts with activated but not quiescent endothelium in immunodeficient mouse hosts.* Transplantation, 2001. **71**(11): p. 1622-30.
198. Ito, M., et al., *NOD/SCID/gamma(c)(null) mouse: an excellent recipient mouse model for engraftment of human cells.* Blood, 2002. **100**(9): p. 3175-82.
199. Ishikawa, F., et al., *Development of functional human blood and immune systems in NOD/SCID/IL2 receptor {gamma} chain(null) mice.* Blood, 2005. **106**(5): p. 1565-73.
200. Traggiai, E., et al., *Development of a human adaptive immune system in cord blood cell-transplanted mice.* Science, 2004. **304**(5667): p. 104-7.
201. Lepus, C.M., et al., *Comparison of human fetal liver, umbilical cord blood, and adult blood hematopoietic stem cell engraftment in NOD-scid/gammac-/-, Balb/c-Rag1-/-gammac-/-, and C.B-17-scid/bg immunodeficient mice.* Hum Immunol, 2009. **70**(10): p. 790-802.
202. Miller, J.S., et al., *Single adult human CD34(+)/Lin-/CD38(-) progenitors give rise to natural killer cells, B-lineage cells, dendritic cells, and myeloid cells.* Blood, 1999. **93**(1): p. 96-106.
203. Huang, S. and L.W. Terstappen, *Lymphoid and myeloid differentiation of single human CD34+, HLA-DR+, CD38- hematopoietic stem cells.* Blood, 1994. **83**(6): p. 1515-26.
204. Shultz, L.D., et al., *Human lymphoid and myeloid cell development in NOD/LtSz-scid IL2R gamma null mice engrafted with mobilized human hemopoietic stem cells.* J Immunol, 2005. **174**(10): p. 6477-89.
205. Takenaka, K., et al., *Polymorphism in Sirpa modulates engraftment of human hematopoietic stem cells.* Nat Immunol, 2007. **8**(12): p. 1313-23.
206. Yahata, T., et al., *Functional human T lymphocyte development from cord blood CD34+ cells in nonobese diabetic/Shi-scid, IL-2 receptor gamma null mice.* J Immunol, 2002. **169**(1): p. 204-9.
207. Gimeno, R., et al., *Monitoring the effect of gene silencing by RNA interference in human CD34+ cells injected into newborn RAG2-/- gammac-/- mice: functional inactivation of p53 in developing T cells.* Blood, 2004. **104**(13): p. 3886-93.
208. Tonomura, N., et al., *Antigen-specific human T-cell responses and T cell-dependent production of human antibodies in a humanized mouse model.* Blood, 2008. **111**(8): p. 4293-6.
209. Sadelain, M., R. Brentjens, and I. Rivière, *The basic principles of chimeric antigen receptor design.* Cancer Discov, 2013. **3**(4): p. 388-98.
210. Sadelain, M., *CAR therapy: the CD19 paradigm.* J Clin Invest, 2015. **125**(9): p. 3392-400.
211. Jackson, H.J., S. Rafiq, and R.J. Brentjens, *Driving CAR T-cells forward.* Nat Rev Clin Oncol, 2016. **13**(6): p. 370-83.
212. Weder, W., I. Opitz, and R. Stahel, *Multimodality strategies in malignant pleural mesothelioma.* Semin Thorac Cardiovasc Surg, 2009. **21**(2): p. 172-6.
213. Karrison, H.K., et al., *Phase II Trial of Pembrolizumab in patients with Malignant Mesothelioma (MM): Interim Analysis* Journal of Thoracic Oncology.
214. Quispel-Janssen, J., et al., *A Phase II Study of Nivolumab in Malignant Pleural Mesothelioma (NivoMes): with Translational Research (TR) Biopies*. 2017.
215. Petrausch, U., et al., *Re-directed T cells for the treatment of fibroblast activation protein (FAP)-positive malignant pleural mesothelioma (FAPME-1).* BMC Cancer, 2012. **12**: p. 615.
216. Schuberth, P.C., et al., *Treatment of malignant pleural mesothelioma by fibroblast activation protein-specific re-directed T cells.* J Transl Med, 2013. **11**: p. 187.
217. Kofler, D.M., et al., *CD28 costimulation Impairs the efficacy of a redirected t-cell antitumor attack in the presence of regulatory t cells which can be overcome by preventing Lck activation.* Mol Ther, 2011. **19**(4): p. 760-7.
218. Li, Y. and R.J. Kurlander, *Comparison of anti-CD3 and anti-CD28-coated beads with soluble anti-CD3 for expanding human T cells: differing impact on CD8 T cell phenotype and responsiveness to restimulation.* J Transl Med, 2010. **8**: p. 104.

219. Wei, F., et al., *Strength of PD-1 signaling differentially affects T-cell effector functions.* Proc Natl Acad Sci U S A, 2013. **110**(27): p. E2480-9.
220. Brenchley, J.M., et al., *Expression of CD57 defines replicative senescence and antigen-induced apoptotic death of CD8+ T cells.* Blood, 2003. **101**(7): p. 2711-20.
221. O'Sullivan, D. and E.L. Pearce, *Targeting T cell metabolism for therapy.* Trends Immunol, 2015. **36**(2): p. 71-80.
222. Xu, X., et al., *Autophagy is essential for effector CD8(+) T cell survival and memory formation.* Nat Immunol, 2014. **15**(12): p. 1152-61.
223. Kovacs, J.R., et al., *Autophagy promotes T-cell survival through degradation of proteins of the cell death machinery.* Cell Death Differ, 2012. **19**(1): p. 144-52.
224. Teta, M.J., et al., *US mesothelioma patterns 1973-2002: indicators of change and insights into background rates.* Eur J Cancer Prev, 2008. **17**(6): p. 525-34.
225. Opitz, I., et al., *Incidence and management of complications after neoadjuvant chemotherapy followed by extrapleural pneumonectomy for malignant pleural mesothelioma.* Eur J Cardiothorac Surg, 2006. **29**(4): p. 579-84.
226. Jakobsen, J.N. and J.B. Sorensen, *Review on clinical trials of targeted treatments in malignant mesothelioma.* Cancer Chemother Pharmacol, 2011. **68**(1): p. 1-15.
227. Izzi, V., et al., *Immunity and malignant mesothelioma: from mesothelial cell damage to tumor development and immune response-based therapies.* Cancer Lett, 2012. **322**(1): p. 18-34.
228. Suchin, E.J., et al., *Quantifying the frequency of alloreactive T cells in vivo: new answers to an old question.* J Immunol, 2001. **166**(2): p. 973-81.
229. Schuberth, P.C., et al., *Effector memory and central memory NY-ESO-1-specific re-directed T cells for treatment of multiple myeloma.* Gene Ther, 2012.
230. van Lent, A.U., et al., *IL-7 enhances thymic human T cell development in "human immune system" Rag2-/-IL-2Rgammac-/- mice without affecting peripheral T cell homeostasis.* J Immunol, 2009. **183**(12): p. 7645-55.
231. Billerbeck, E., et al., *Characterization of human antiviral adaptive immune responses during hepatotropic virus infection in HLA-transgenic human immune system mice.* J Immunol, 2013. **191**(4): p. 1753-64.
232. Kawalekar, O.U., et al., *Distinct Signaling of Coreceptors Regulates Specific Metabolism Pathways and Impacts Memory Development in CAR T Cells.* Immunity, 2016. **44**(2): p. 380-90.
233. Long, A.H., et al., *4-1BB costimulation ameliorates T cell exhaustion induced by tonic signaling of chimeric antigen receptors.* Nat Med, 2015. **21**(6): p. 581-90.
234. Cedrés, S., et al., *Analysis of expression of programmed cell death 1 ligand 1 (PD-L1) in malignant pleural mesothelioma (MPM).* PLoS One, 2015. **10**(3): p. e0121071.
235. Motz, G.T., et al., *Tumor endothelium FasL establishes a selective immune barrier promoting tolerance in tumors.* Nat Med, 2014. **20**(6): p. 607-15.
236. Zi, F., et al., *Fibroblast activation protein α in tumor microenvironment: recent progression and implications (review).* Mol Med Rep, 2015. **11**(5): p. 3203-11.
237. Tran, E., et al., *Immune targeting of fibroblast activation protein triggers recognition of multipotent bone marrow stromal cells and cachexia.* J Exp Med, 2013. **210**(6): p. 1125-35.
238. Berraondo, P., V. Umansky, and I. Melero, *Changing the tumor microenvironment: new strategies for immunotherapy.* Cancer Res, 2012. **72**(20): p. 5159-64.
239. Jiang, G.M., et al., *The application of the fibroblast activation protein α-targeted immunotherapy strategy.* Oncotarget, 2016. **7**(22): p. 33472-82.
240. Kraman, M., et al., *Suppression of antitumor immunity by stromal cells expressing fibroblast activation protein-alpha.* Science, 2010. **330**(6005): p. 827-30.

241. Jiang, G.M., et al., *Curcumin combined with FAPαc vaccine elicits effective antitumor response by targeting indolamine-2,3-dioxygenase and inhibiting EMT induced by TNF-α in melanoma.* Oncotarget, 2015. **6**(28): p. 25932-42.
242. Porpodis, K., et al., *Malignant pleural mesothelioma: current and future perspectives.* J Thorac Dis, 2013. **5 Suppl 4**: p. S397-406.
243. van Zandwijk, N., et al., *Guidelines for the diagnosis and treatment of malignant pleural mesothelioma.* J Thorac Dis, 2013. **5**(6): p. E254-307.
244. Treasure, T. and A. Sedrakyan, *Pleural mesothelioma: little evidence, still time to do trials.* Lancet, 2004. **364**(9440): p. 1183-5.
245. Alberts, A.S., et al., *Malignant pleural mesothelioma: a disease unaffected by current therapeutic maneuvers.* J Clin Oncol, 1988. **6**(3): p. 527-35.
246. Krug, L.M., et al., *Multicenter phase II trial of neoadjuvant pemetrexed plus cisplatin followed by extrapleural pneumonectomy and radiation for malignant pleural mesothelioma.* J Clin Oncol, 2009. **27**(18): p. 3007-13.
247. Bölükbas, S., et al., *Survival after trimodality therapy for malignant pleural mesothelioma: Radical Pleurectomy, chemotherapy with Cisplatin/Pemetrexed and radiotherapy.* Lung Cancer, 2011. **71**(1): p. 75-81.
248. Yaziji, H., et al., *Evaluation of 12 antibodies for distinguishing epithelioid mesothelioma from adenocarcinoma: identification of a three-antibody immunohistochemical panel with maximal sensitivity and specificity.* Mod Pathol, 2006. **19**(4): p. 514-23.
249. Sekido, Y., *Molecular pathogenesis of malignant mesothelioma.* Carcinogenesis, 2013. **34**(7): p. 1413-9.
250. Barbieri, F., et al., *Receptor tyrosine kinase inhibitors and cytotoxic drugs affect pleural mesothelioma cell proliferation: insight into EGFR and ERK1/2 as antitumor targets.* Biochem Pharmacol, 2011. **82**(10): p. 1467-77.
251. Kindler, H.L., *Systemic treatments for mesothelioma: standard and novel.* Curr Treat Options Oncol, 2008. **9**(2-3): p. 171-9.
252. Morello, A., M. Sadelain, and P.S. Adusumilli, *Mesothelin-Targeted CARs: Driving T Cells to Solid Tumors.* Cancer Discov, 2016. **6**(2): p. 133-46.
253. Beatty, G.L., et al., *Mesothelin-specific chimeric antigen receptor mRNA-engineered T cells induce anti-tumor activity in solid malignancies.* Cancer Immunol Res, 2014. **2**(2): p. 112-20.
254. Hombach, A., et al., *Tumor-specific T cell activation by recombinant immunoreceptors: CD3 zeta signaling and CD28 costimulation are simultaneously required for efficient IL-2 secretion and can be integrated into one combined CD28/CD3 zeta signaling receptor molecule.* J Immunol, 2001. **167**(11): p. 6123-31.
255. Hombach, A., A.A. Hombach, and H. Abken, *Adoptive immunotherapy with genetically engineered T cells: modification of the IgG1 Fc 'spacer' domain in the extracellular moiety of chimeric antigen receptors avoids 'off-target' activation and unintended initiation of an innate immune response.* Gene Ther, 2010. **17**(10): p. 1206-13.
256. Burckhart, T., et al., *Tumor-specific crosslinking of GITR as costimulation for immunotherapy.* J Immunother, 2010. **33**(9): p. 925-34.
257. Weijtens, M.E., et al., *Chimeric scFv/gamma receptor-mediated T-cell lysis of tumor cells is coregulated by adhesion and accessory molecules.* Int J Cancer, 1998. **77**(2): p. 181-7.
258. Ferlazzo, G., et al., *The abundant NK cells in human secondary lymphoid tissues require activation to express killer cell Ig-like receptors and become cytolytic.* J Immunol, 2004. **172**(3): p. 1455-62.
259. Vignali, D.A., *Multiplexed particle-based flow cytometric assays.* J Immunol Methods, 2000. **243**(1-2): p. 243-55.

260. Leggett, R.M., et al., *Sequencing quality assessment tools to enable data-driven informatics for high throughput genomics.* Front Genet, 2013. **4**: p. 288.
261. Li, B. and C.N. Dewey, *RSEM: accurate transcript quantification from RNA-Seq data with or without a reference genome.* BMC Bioinformatics, 2011. **12**: p. 323.
262. Robinson, M.D. and A. Oshlack, *A scaling normalization method for differential expression analysis of RNA-seq data.* Genome Biol, 2010. **11**(3): p. R25.
263. Ritchie, M.E., et al., *limma powers differential expression analyses for RNA-sequencing and microarray studies.* Nucleic Acids Res, 2015. **43**(7): p. e47.
264. Wu, D. and G.K. Smyth, *Camera: a competitive gene set test accounting for inter-gene correlation.* Nucleic Acids Res, 2012. **40**(17): p. e133.
265. Strowig, T., et al., *Human NK cells of mice with reconstituted human immune system components require preactivation to acquire functional competence.* Blood, 2010. **116**(20): p. 4158-67.

Acknowledgements

Acknowledgements

First of all, I would like to thank my academic supervisor Christian Münz for providing me the opportunity to conduct my doctoral studies in his lab. Christian has always been tremendously supportive and helpful, exceedingly positively motivated and accommodative. His in depth knowledge of literature is overwhelming and I always enjoyed the outstanding intellectual exchange and prompt feedbacks from him.

A huge gratitude goes to my daily supervisor, Ulf Petrausch for his research insights, constant support, patience, motivation, optimism and eminent supervision. At several occasions, he has gone beyond his duties to fight my worries, concerns, and anxieties, and has continuously been working to instil great confidence in both myself and my work. Thank you, Ulf, for making me believe in myself and for bringing out the best in me.

I am forever indebted to Christoph Renner, who has been like a foundation stone for me. It is because of Christoph that I could come to Zurich at the first place. Thank you, Christoph, for offering your time, support and commitment throughout. Thank you for offering this PhD project to me and for staying with me during the thick and thins ☺ Now I realize that each problem had a distinct lesson attached to it and everything happens for a reason.

I would like to thank my lab-mate, Julia Rühl for her availability and tireless assistance during overnight animal sacrifices in the lab. Thank you, Julia, for your help at the bench and for a great company. I always enjoyed discussions with you and critical evaluation of our findings. More than that, I discovered my best lab-buddy in you and you were indeed a great emotional support to me ☺

I am equally thankful to all the current and former members of the Münz lab. I feel blessed to have had worked with such wonderful lab-mates. Thank you all for creating a friendly working environment, which was always conducive to discussions and collaboration. I would also like to thank the entire Institute of Experimental Immunology for their help and support whenever needed. A special praise to Christian, Petra and Bithi for making everyday life in the lab more exciting.

A huge breadth of relationships was drawn during my last 6 years in Zürich. I would like to thank my partner Abhilash Kannan for his unremitting encouragement. To put it simply, I have never met anyone who believes in me more. Thank you for making me more than I am. Thank you for making me persevere through the stress, isolation, loneliness, and emotional outbursts ☺

I also would like to thank my bestest buddy, Dorothea Greuter. She has been a sister, a friend and a mother to me. Her moral support helped me get through the ups and downs of my personal and professional life. Above all, I have always cherished her wisdom and our friendship. To Dora, without you, this journey would have been monotonous and lifeless. I hope to have you in my life forever and I look forward to spending more evening dates with you after your retirement in July ☺

In the end, I would like to thank my in-laws, my parents and friends who have always made a significant impact on my life and made sure that I had the proper work-life balance, thank you for being there and for helping me to get to where I am today.

Curriculum Vitae

PRATIKSHA GULATI

Research Fellow, Onco-Immunology

Home: Aprikosenstrasse 20, CH-8051 Zürich, Switzerland
Email: gulati@immunology.uzh.ch
Phone: +41 78 826 2685

Born: 18-01-1990 (Age 27)
Swiss Resident Permit -"B" (Familiennachzug mit Erwerbstätigkeit)

ABOUT ME

6+ years of research experience in **translational cancer research**. Skilled in **Chimeric Antigen Receptor (CAR)-T cell technology** and other personalized immunotherapeutic approaches for cancer. Proficient in several animal models of cancer including **humanized mouse models**. Contributed earnestly in initiation of **first phase-I clinical trial using CAR-T cells in Switzerland** to treat mesothelioma

CAREER OBJECTIVES

To work in healthcare services. Bringing 6+ years of translational research experience in public health and disease management.

EDUCATION

- Oct 2012 - July 2017 — PhD. Molecular Life Sciences
  Life Science Graduate School
  UZH and ETH Zurich, Switzerland
- Sep 2010 - Aug 2012 — MSc. Molecular Life Sciences
  Maastricht University
  The Netherlands
- Jun 2007 - May 2010 — BSc. Biotechnology
  Bharati Vidyapeeth University
  India

SKILLS (INTERPERSONAL)

- Considerable experience in managing several research projects together
- Maintaining strong work ethics - reliable and punctual
- Conducing friendly atmosphere with positive attitude
- Actively networking and collaborating!
- Robust in coping pressure and meeting deadlines.
- Flexibility to adapt to different working conditions
- Perceptive to constructive feedback
- Actively participating in and leading team activities

SKILLS (TECHNICAL)

- Monoclonal antibody technology, virology, recombinant DNA technology
- protein engineering, protein production,mammalian cell culture and other biochemical assays
- computational modelling of biological networks

PROFESSIONAL EXPERIENCE (RESEARCH)

- Since Oct 2012 — **Institute of Experimental Immunology, University of Zurich, Switzerland**
  Lab of Prof. Christian Münz

  PhD. Thesis: Optimization of co-stimulatory signal through Chimeric Antigen Receptor (CAR)-T cells combined with immune checkpoint (PD-1) blockade in humanized mice.

  Phase-I clinical trial (Department of Oncology, University Hospital Zurich): Re-directed T cells for treatment of Fibroblast Activation Protein (FAP) positive Malignant Pleural Mesothelioma **(Clinicaltrials.gov i.d. NCT01722149)**

- Oct 2011 - Jul 2012 — **Department of Oncology, University Hospital Zurich, Switzerland**
  Lab of Prof. Dr. med. Christoph Renner

  Master Thesis: Identifying role of Fibroblast Activation Protein (FAP) in extra-cellular matrix degradation and tumor cell migration.

- Jan 2011 - Jun 2011 — **Department of Toxicology (GRAT), Maastricht University, The Netherlands**
  Lab of Prof. Roland Chiu

  Research Internship: Investigating the effect of re-oxygenation on DNA repair mechanism and carcinogen Benzo-A-pyrene (BAP) metabolism in hypoxic tumors.

- Jan 2009 - Mar 2009 — **Rajiv Gandhi Institute of IT and Biotechnology, Bharati Vidyapeeth University, India**
  Lab of Prof. Bipinraj NK

  Research Internship: Purification and characterization of bacteriocin targeting *Clostridium botulinum*

- Dec 2009 - Feb 2010 — **Rajiv Gandhi Institute of IT and Biotechnology, Bharati Vidyapeeth University, India**
  Supervision of Late. Prof. R.L. Kothari

  Dissertation: Liver cirrhosis - causes, implications and remedies

CERTIFICATIONS IN CLINICAL RESEARCH

Nov 2016 3 weeks online course on **Good Clinical Practice guidelines (ICH-GCP)** by Elevate - online platform of Utrecht University and University Medical Center Utrecht

Jul 2016 1 week **Intensive Clinical Trials Administration training** organized at University Medical Center Utrecht in collaboration with University of California San Diego

Jun 2016 National Institute of Health (**NIH**) **Clinical Research training online course.**

OTHER CERTIFICATIONS

Transferrable skills

- Project management
- Business concept - how to initiate a startup
- Ethics in science
- Scientific writing

Microscopy

- Advanced microscopy and vital imaging
- Microscopy toolbox for immunologists

Computational / statistical

- Programming in biology using python
- Statistics for biologists
- R programming
- Data carpentry using R

Technical

- FACS Canto operator training at BD Biosciences
- Next generation sequencing
- Microarray Technologies

Specialized courses

- LTK module-I in Laboratory Animal Science (Switzerland)
- Laboratory Animal Science (article-9 Netherlands)
- Radionuclide Laboratory Course (article-5b Netherlands)
- Personalized medicine
- Advanced course in Flow Cytometry
- Systems Biology
- Mouse physiology and pathophysiology
- Safe microbiological techniques

HONORS AND AWARDS

- Nov 2013 Travel grant of €1000 awarded by Molecular Life Sciences PhD program for conference organized by Society of Immunotherapy for Cancer (SITC), USA
- Oct 2011 Faculty grant of €2000 awarded by Maastricht University and 10,000 CHF by University Hospital Zurich for master thesis internship
- Sep 2010 UM High Potential Scholarship covering €24000 tuition fee, monthly €800 for 24 months, relocation charges and health insurance for masters studies
- Apr 2010 Awarded Best ongoing Bachelor's student in Biotechnology batch 2007-2010
  Gold medal winner for being consistent top performer in three years of bachelors studies

INDUSTRIAL INTERNSHIPS

- May - Jun 2009 Arbro Pharmaceuticals Limited, New Delhi, India, Department of Molecular Biology
  Tasks: Testing release rate of capsules
- May - Jun 2008 Standard Analytical Laboratories Limited, New Delhi, India
  Department of Microbiology
  Tasks: Sterility testing of injectibles

PUBLICATIONS

- Optimization of co-stimulation through CAR-T cells combined with PD-1 blockade in humanized mice. **Gulati P**. et.al. 2017 (submitted to JCI).
- Treatment of malignant pleural mesothelioma by fibroblast aclvalon protein-specific re-directed T cells. Schuberth PC, Hagedorn C, Jensen SM, **Gulati P**. et. al. JTransl Med 2013

ORGANIZATIONS

- Initiator and organizor of SCORE (Students' Council of Education and Research) at Bharati Vidyapeeth University
- Committee member Indian Students' Association Maastricht (ISAM). Designation - Treasurer
- Member of Retreat organizing committee MLS PhD program. Organized annual PhD retreat in Aug 2014

REFERENCES

- Prof. Dr. med. Christoph Renner
  OnkoZentrum Klinik Hirslanden, Zurich, Switzerland
  christoph.renner@hirslanden.ch

- Prof. Dr. Christian Münz
  University of Zurich, Zurich, Switzerland
  muenzc@immunology.uzh.ch